MISCELLANEOUS PAPER DRP-92-1

US Army Corps of Engineers

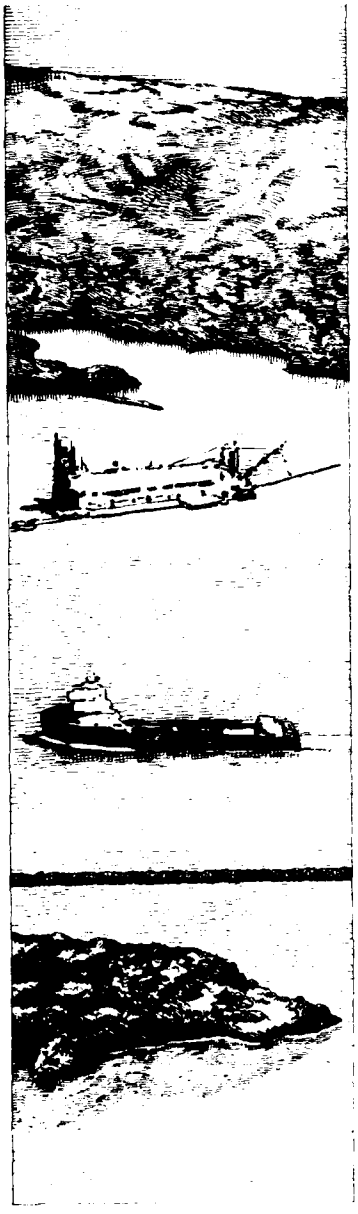

DISPERSION ANALYSIS OF HUMBOLDT BAY, CALIFORNIA, INTERIM OFFSHORE DISPOSAL SITE

by

Norman W. Scheffner

Coastal Engineering Research Center

DEPARTMENT OF THE ARMY
Waterways Experiment Station, Corps of Engineers
3909 Halls Ferry Road, Vicksburg, Mississippi 39180-6199

June 1992
Final Report

Prepared for DEPARTMENT OF THE ARMY
US Army Engineer District, San Francisco
San Francisco, California 94105-1905

and DEPARTMENT OF THE ARMY
US Army Corps of Engineers
Washington, DC 20314-1000

Under DRP Work Unit 32466

The Dredging Research Program (DRP) is a seven-year program of the US Army Corps of Engineers. DRP research is managed in these five technical areas:

Area 1 - Analysis of Dredged Material Placed in Open Water

Area 2 - Material Properties Related to Navigation and Dredging

Area 3 - Dredge Plant Equipment and Systems Processes

Area 4 - Vessel Positioning, Survey Controls, and Dredge Monitoring Systems

Area 5 - Management of Dredging Projects

The Dredging Research Program (DRP) is a seven-year program of the US Army Corps of Engineers. DRP research is managed in these five technical areas:

Area 1 - Analysis of Dredged Material Placed in Open Water

Area 2 - Material Properties Related to Navigation and Dredging

Area 3 - Dredge Plant Equipment and Systems Processes

Area 4 - Vessel Positioning, Survey Controls, and Dredge Monitoring Systems

Area 5 - Management of Dredging Projects

DEPARTMENT OF THE ARMY
WATERWAYS EXPERIMENT STATION, CORPS OF ENGINEERS
3909 HALLS FERRY ROAD
VICKSBURG, MISSISSIPPI 39180-6199

REPLY TO
ATTENTION OF

CEWES-CR-O

21 December 1992

Errata Sheet

No. 1

DISPERSION ANALYSIS OF HUMBOLDT BAY, CALIFORNIA, INTERIM OFFSHORE DISPOSAL SITE

Miscellaneous Paper DRP-92-1

June 1992

On pages 43, 44, 45, and 65 (or any page with reference to), concentrations of suspended sediment are erroneously reported in mg/ℓ. The reported values are actually nondimensional ratios of volume of solids to volume of solution. To convert these reported values to units of mg/ℓ, multiply by 2.6 (density, p. 37) $\times 10^{6}$. For example, the value of 5×10^{-8} mg/ℓ reported on p. 65 should read 1.3×10^{-1} mg/ℓ.

REPORT DOCUMENTATION PAGE

Form Approved
OMB No. 0704-0188

1. AGENCY USE ONLY (Leave blank)	2. REPORT DATE	3. REPORT TYPE AND DATES COVERED
	June 1992	Final report

4. TITLE AND SUBTITLE
Dispersion Analysis of Humboldt Bay, California
Interim Offshore Disposal Site

5. FUNDING NUMBERS

6. AUTHOR(S)

Norman W. Scheffner

7. PERFORMING ORGANIZATION NAME(S) AND ADDRESS(ES)

US Army Engineer Waterways Experiment Station
Coastal Engineering Research Center
3909 Halls Ferry Road, Vicksburg, MS 39180-6199

8. PERFORMING ORGANIZATION REPORT NUMBER

Miscellaneous Paper
DRP-92-1

9. SPONSORING/MONITORING AGENCY NAME(S) AND ADDRESS(ES)

US Army Engineer District, San Francisco
San Francisco, CA 94105-1905

10. SPONSORING/MONITORING AGENCY REPORT NUMBER

11. SUPPLEMENTARY NOTES

Available from National Technical Information Service, 5285 Port Royal Road, Springfield, VA 22161

12a. DISTRIBUTION/AVAILABILITY STATEMENT

Approved for public release; distribution is unlimited

12b. DISTRIBUTION CODE

13. ABSTRACT *(Maximum 200 words)*

The dispersive characteristics of an interim offshore dredged material disposal site located seaward of the entrance to Humboldt Bay, California, are investigated. These characteristics must be known to determine potential impact of the dredging operation on the local environment. Two phases of investigation were employed. A short-term analysis of the disposal operation was conducted to examine the immediate fate of material following release from the barge and subsequent descent to the ocean bottom. The second phase examined the long-term fate to determine whether local ocean currents are capable of eroding and transporting deposited material beyond the designated limits of the site. Results of this study indicate the site to be nondispersive, with little erosion and transport of material indicated under both normal and moderate storm conditions.

14. SUBJECT TERMS

Disposal site classification
Disposal site stability
Dredged material
Sediment fate
Sediment transport

15. NUMBER OF PAGES
84

16. PRICE CODE

17. SECURITY CLASSIFICATION OF REPORT	18. SECURITY CLASSIFICATION OF THIS PAGE	19. SECURITY CLASSIFICATION OF ABSTRACT	20. LIMITATION OF ABSTRACT
UNCLASSIFIED	UNCLASSIFIED		

PREFACE

The methodology used in this report was developed at the Coastal Engineering Research Center (CERC) and the Hydraulics Laboratory (HL), US Army Engineer Waterways Experiment Station (WES), under Dredging Research Program (DRP) Work Unit 32466, Numerical Simulation Techniques for Evaluating Long-Term Fate and Stability of Dredged Material Disposed in Open Water, of Technical Area 1 (TA1), Analysis of Dredged Materials Disposal in Open Water. Messrs. Robert H. Campbell and Glenn R. Drummond were DRP Chief and TA1 Technical Monitors, Headquarters, US Army Corps of Engineers, respectively. Mr. E. Clark McNair, Jr., CERC, was DRP Program Manager, Dr. Lyndell Z. Hales, CERC, was Assistant Program Manager, and Dr. Nicholas C. Kraus, Senior Scientist, Research Division (RD), CERC, was Technical Manager for DRP TA1.

This report describes a site designation study of the potential dispersion characteristics of an Interim Offshore Disposal Site located seaward of the entrance to Humboldt Bay, California. The study was conducted at WES by CERC at the request of the US Army Engineer District (USAED), San Francisco. Study data were collected by the EG&G Oceanographic Services for the US Department of the Interior's Minerals Management Service (MMS) as a component of the Northern California Coastal Circulation Study. Appreciation is extended to MMS for authorizing release of the data and to Dr. Bruce Magnell and Mr. Bruce Andrews, EG&G, for supplying the data to CERC. Appreciation is also extended to Mr. David Hodges, USAED, San Francisco, for providing information and insight crucial to the timely completion of this project. Both phases of the numerical investigation and the final report were prepared by Dr. Norman W. Scheffner, Coastal Processes Branch (CPB), RD, CERC.

General supervision was provided by Dr. James R. Houston and Mr. Charles C. Calhoun, Jr., Director and Assistant Director, respectively, CERC; direct supervision of the project was provided by Messrs. H. L. Butler, Chief, RD, and Bruce A. Ebersole, Chief, CPB.

During the publication of this report, Director of WES was Dr. Robert W. Whalin. COL Leonard G. Hassell, EN, was Commander and Deputy Director of WES.

For further information on this report or on the Dredging Research Program, please contact Dr. Nicholas C. Kraus at (601) 634-2018 or Mr. E. Clark McNair, Jr., Program Manager, at (601) 634-2070.

CONTENTS

	Page
PREFACE	1
LIST OF TABLES	3
LIST OF FIGURES	3
CONVERSION FACTORS, NON-SI TO SI (METRIC) UNITS OF MEASUREMENT	5
SUMMARY	6
PART I: INTRODUCTION	8
Background	8
Objective	10
PART II: WAVE AND CURRENT BOUNDARY CONDITIONS	12
Wave Height, Period, and Direction Time Series	12
Depth-Averaged Current Time Series	17
PART III: SHORT-TERM MODELING	32
General	32
Input Data Requirements	33
Short-Term Model Simulations	37
Fine-Grained Disposal Site Analysis	38
Coarse-Grained Disposal Site Analysis	47
PART IV: LONG-TERM MODELING	50
General	50
Input Data Requirement	51
Long-Term Model Simulations	55
Fine-Grained Disposal Site Analysis	59
Coarse-Grained Disposal Site Analysis	64
PART V: CONCLUSIONS	65
Fine-Grained Site	65
Coarse-Grained Site	66
Concluding Remarks	66
REFERENCES	68
APPENDIX A: RAW AND FILTERED VELOCITY DATA FROM MINERALS MANAGEMENT SERVICE GAGES E60 AND E90	A1

LIST OF TABLES

No.		Page
1	Comparison of Wave Statistics	20
2	Velocity Data Time Series Lengths	21
3	Summary Statistics of Velocity Time Series	23
4	Primary Astronomical Constituents for Gage E90/45	30
5	Capacities and Dimensions of Dredge "Yaquina"	34
6	Capacities and Dimensions of Dredge "Newport"	34
7	Model Input Parameters and Coefficients	36
8	Fine-Grained Sediment Composition and Characteristics	37
9	Coarse-Grained Sediment Composition and Characteristics	37
10	Summary of Computed Maximum Suspended Sand Concentration	45
11	Summary of Computed Maximum Suspended Silt-Clay Concentration	45

LIST OF FIGURES

No.		Page
1	Humboldt Bay interim offshore disposal site location	9
2	WIS hindcast data station location	13
3	Simulated 1-year time series of wave height, period, and direction	14
4	WIS Station 69 time series for 1956	15
5	WIS Station 69 time series for 1964	16
6	Probability histograms for simulated wave and 1956 WIS data	18
7	Probability histograms for simulated wave and 1964 WIS data	19
8	Thirty-three-Hour low-pass filtered currents (EG&G 1990)	22
9	Period 2 Velocity components for Gage E60/10	25
10	Period 2 Velocity components for Gage E90/10	26
11	Auto- and cross-correlation functions for U velocity component for Gages E60/10 and E90/10	27
12	Auto- and cross-correlation functions for V velocity component for Gages E60/10 and E90/10	27
13	Velocity components for Gage E90/45	29
14	Synthesized tidal series for interim site	31
15	Computational phases of DIFID model (from Brandsma and Divoky 1976)	33
16	Suspended sediment cloud at 120 ft deep, 900 sec after disposal	39
17	Suspended sediment cloud at 120 ft deep, 1,800 sec after disposal	40
18	Suspended sediment cloud at 120 ft deep, 2,700 sec after disposal	41
19	Suspended sediment cloud at 120 ft deep, 3,600 sec after disposal	42
20	Sand concentration evolution relationships, fine-grained site	43
21	Silt-clay concentration evolution relationships, fine-grained site	44
22	Total deposition pattern for fine-grained site	46
23	Three-dimensional view of fine-grained site deposition pattern	46
24	Contour plot of fine-grained site deposition pattern	47
25	Total deposition pattern for coarse-grained site	48
26	Three-dimensional, coarse-grained site deposition pattern	48
27	Contour plot of coarse-grained site deposition pattern	49
28	Sediment transport-velocity relationships for D_{50} = 0.277 mm	52
29	Sediment transport-velocity relationships for D_{50} = 0.0384 mm	53

LIST OF FIGURES (Continued)

No.		Page
30	Sediment transport-velocity relationships for D_{50} = 0.0625 mm	54
31	Idealized disposal mound perspective view	56
32	Idealized disposal mound contour map	56
33	Simulated storm surge time series	57
34	Long-term simulation contour of fine-grained site	60
35	Long-term simulation mound axis migration history	61
36	Storm event simulation contour of fine-grained site	62
37	Storm event simulation mound axis migration history for fine-grained site	63
A1	Meter E60/15 current data - Period 1	A3
A2	Meter E90/15 current data - Period 1	A4
A3	Meter E90/75 current data - Period 1	A5
A4	Meter E60/10 current data - Period 2	A6
A5	Meter E90/10 current data - Period 2	A7
A6	Meter E90/75 current data - Period 2	A8
A7	Meter E90/10 current data - Period 3	A9
A8	Meter E90/45 current data - Period 3	A10
A9	Meter E60/10 current data - Period 4	A11
A1	Meter E90/10 current data - Period 4	A12
A1	Meter E90/45 current data - Period 4	A13
A1	Meter E90/75 current data - Period 4	A14

CONVERSION FACTORS, NON-SI TO SI (METRIC)
UNITS OF MEASUREMENT

Non-SI units of measurement used in this report can be converted to SI (metric) units as follows:

Multiply	By	To Obtain
cubic feet	0.02831685	cubic metres
cubic yards	0.7645549	cubic metres
degrees (angle)	0.01745329	radians
feet	0.3048	metres
miles (US nautical)	1.852	kilometres
miles (US statute)	1.609347	kilometres
square miles	2.58998	square kilometres

SUMMARY

In this report the dispersion characteristics of dredged material placement operations at the Interim Offshore Site located seaward of the entrance of Humboldt Bay, California, are investigated. The characteristics are required to determine the impact of the disposal operation on the local environment. This study was conducted at the request of the US Army Engineer District, San Francisco.

A disposal site can be classified as dispersive or nondispersive depending on whether sediment is transported out of or remains within the designated limits of the site. The dredged material dispersion characteristics of the Humboldt Bay Site were investigated in two phases, a short-term and a long-term phase. In the short-term phase the potential impact of the actual barge disposal operation on the local environment was investigated. This phase of the study represents the initial minutes to hours following the disposal operation during which time the material is entrained and dispersed as it descends through the water column to be deposited on the ocean floor. Efforts were focused on modeling the time rate of change of suspended sediment concentration and the total sediment deposition pattern on the ocean bottom. In the second phase, the long-term analysis focuses on the extent and probable direction in which local waves and currents erode and transport the dredged material mound. The methodologies used to accomplish these goals are thoroughly discussed in the report.

Short-term numerical simulations were performed for worst-case wave and current conditions. Results include the water column spatial distribution of the sand and silt-clay components of the sediment load in the form of sediment concentration (ppb) above the background level. Computational results indicate that a significant fraction of the sand and silt-clay materials fall rapidly to the ocean floor and do not impact regions beyond a 0.3-mile radius of the point of disposal. However, a small amount of silt-clay material (concentrations above background approximately 1 ppb) remained suspended in the water column for 1 hour after the disposal operation. This cloud of suspended material is transported about 1 mile from the disposal point. The maximum thickness of the final simulated deposition was approximately 0.06 ft at approximately 300 ft from the disposal point. The minimal impact outside the immediate disposal area is due to the low ambient currents in the vicinity of the disposal site.

Results of the long-term simulation indicate that the mound is nondispersive with respect to normal wave and tidal/circulation currents; however, storm events initiated some mound movement. The simulation of a storm event with an 8-day duration showed the mound migration to be approximately 3.0 ft for coarse sediments and 30.0 ft for fine sediments.

Based on the findings of this report, it is concluded that both proposed sites are basically nondispersive. These results are based on both short- and long-term simulations of sediment transport.

DISPERSION ANALYSIS OF HUMBOLDT BAY, CALIFORNIA INTERIM OFFSHORE DISPOSAL SITE

PART I: INTRODUCTION

Background

1. The US Army Engineer District, San Francisco, was scheduled to begin dredging activities in the vicinity of Humboldt Bay, California, in early September and November of 1990. It was proposed that the Interim Offshore Disposal Site, located approximately 3 nautical miles* northwest of the entrance to Humboldt Bay and shown in Figure 1,** be used for the placement of the dredged material. The objective of this report is to evaluate the probable impact of this disposal site on the local environment.

2. The proposed disposal site is 1 square nautical mile in dimension with the corners located at the coordinates indicated in Figure 1. The nearshore limits of the site are located approximately 3 nautical miles from shore. The offshore boundary of the site is located in 55 m of water, while the nearshore boundary is in 49 m of water. Laboratory analyses of sediment samples** collected at the corners of the disposal site indicate that native ocean floor materials range from fine to medium sand at the nearshore boundary (D_{50} = 0.092 - 0.72 mm) and from silts to fine sands (D_{50} = 0.040 - 0.044 mm) at the outer boundary.

3. The proposed disposal site will be used for disposal of both fine-grained sediment dredged from the interior channel areas during the spring and coarse-grained materials dredged from the general proximity of the entrance channel during the fall months. It is anticipated that the fine-grained material will be disposed near the outer boundaries of the site, while the coarse-grained materials will be placed near the shoreward boundary.** The objective of this report is to evaluate the dispersive or nondispersive nature of the proposed disposal site.

---

* A table of factors for converting non-SI units of measurement to SI (metric) units is presented on page 5.

** Personal Communication, June 1990, David Hodges, USACE, San Francisco, CA.

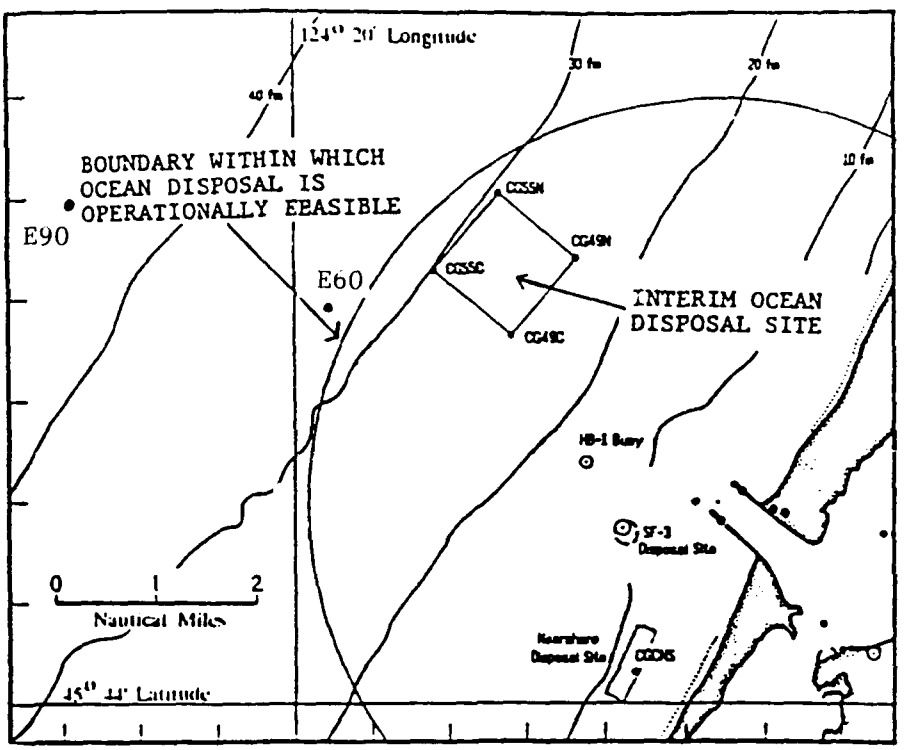

a. Location map

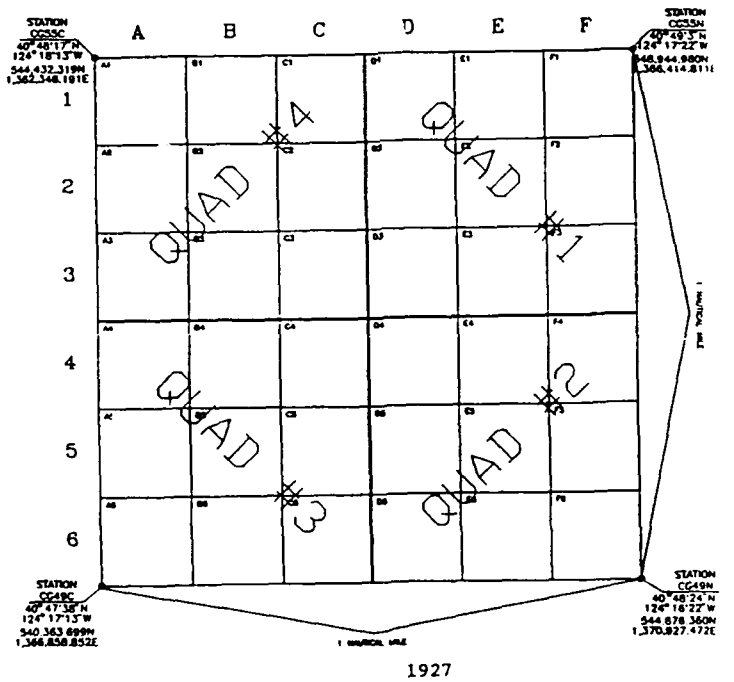

b. Quadratic grid of area

Figure 1. Humboldt Bay interim offshore disposal site location

Objective

4. The objective of this study is to determine the dispersive characteristics of the proposed site by investigating whether material can effectively be deposited within the designated limits of the site and remain within those limits over time. This site analysis is evaluated in a two-phase approach. First, the short-term effects of the dredging operation are investigated to determine whether material will be carried from the site by ambient currents as it descends from the barge to the ocean bottom. The modeling of this short-term phase of the operation is performed by the disposal from an instantaneous dump (DIFID) numerical model (Johnson in preparation). This model computes the convective descent and dynamic collapse of the sediment following its release from the barge. Results of the simulations are presented in the form of time rate of change of suspended sediment in the water column immediately following the disposal and the final configuration of the material on the ocean floor.

5. The second phase of the investigation examines the behavior of the sediment mound over long periods of time. This long-term analysis focuses on whether the local wave and current climate are sufficient to erode and transport deposited material outside the designated limits of the site. These simulations are performed with a coupled hydrodynamic, sediment transport, and bathymetry change model (Scheffner in preparation) that computes mound stability as a function of mound composition and environmental forcings. Both modeling efforts require site specific information, including waves, currents, bathymetry, sediment types, and disposal methods.

6. A realistic analysis of the dispersion characteristics of the candidate disposal site can be made only if the prediction is based on site specific wave and current information. This investigation is fortunate in that current data for several sites near the disposal site are available. Current measurements were collected for the US Department of the Interior's Minerals Management Service (MMS) as a component of the Northern California Coastal Circulation Study (MMS 1989). These data were collected for the MMS by EG&G Oceanographic Services and were made available to the Coastal Engineering Research Center (CERC) of the US Army Engineer Waterways Experiment Station for subsequent analysis and use in this study.

7. This report concentrates on the three primary components of the study: boundary condition development and short- and long-term modeling. The

most important component of the three is the development of realistic boundary conditions at the site. The accuracy and credibility of the numerical modeling results are dependent on the realistic approximation of waves and currents at the disposal site. The importance of this aspect of the study has been stressed in similar site designation studies (Scheffner in preparation; Scheffner and Swain in preparation) and will be the subject of Part II of this report.

PART II: WAVE AND CURRENT BOUNDARY CONDITIONS

8. Both short- and long-term modeling phases of this investigation require specification of local waves and currents. This specification is not as critical for the short-term analysis as it is in the long-term modeling, since the DIFID model applies only to the time immediately following disposal. This time is normally on the order of a few minutes to an hour. A single value, depth-averaged velocity is adequate for this purpose. The long-term modeling phase, however, requires a more precise and accurate definition of local waves and currents since the modeling approach investigates the behavior of the mound over long periods of time, on the order of months. As such, a realistic representation of the local wave and current time series is required for the site; otherwise, realistic predictions of mound stability cannot be made. The following two sections will concentrate on defining the wave and current time series for input to the long-term sediment model.

Wave Height, Period, and Direction Time Series

9. The long-term transport model computes sediment transport as a function of a time series of both waves and currents. The wave time series component of the input is specified as a statistical simulation of the 20-year hindcast data base of the Wave Information Study (WIS), Phase III, Station 69 "sea" conditions. The location of Station 69 is shown in Figure 2. The statistical approach to defining time series of wave height, period, and direction for a specific WIS station is reported in detail by Borgman and Scheffner (1991). The approach allows the user to simulate wave sequences that preserve the statistical qualities of the entire 20-year data base, including seasonality and wave sequencing. The statistically based time series provides a site specific wave climate that is ideal for the long-term simulation.

10. A 1-year time series of waves was generated as input for the long-term model. Plots of the simulated sequence of wave height, period, and direction are shown in Figure 3. To demonstrate the similarity between the simulated wave field and actual hindcast data, Figures 4 and 5 represent 1-year time series of WIS data for the years 1956 and 1964. All plots begin on 1 January and extend through 31 December. The similarity in patterns of increased winter activity with a decrease in intensity during the summer

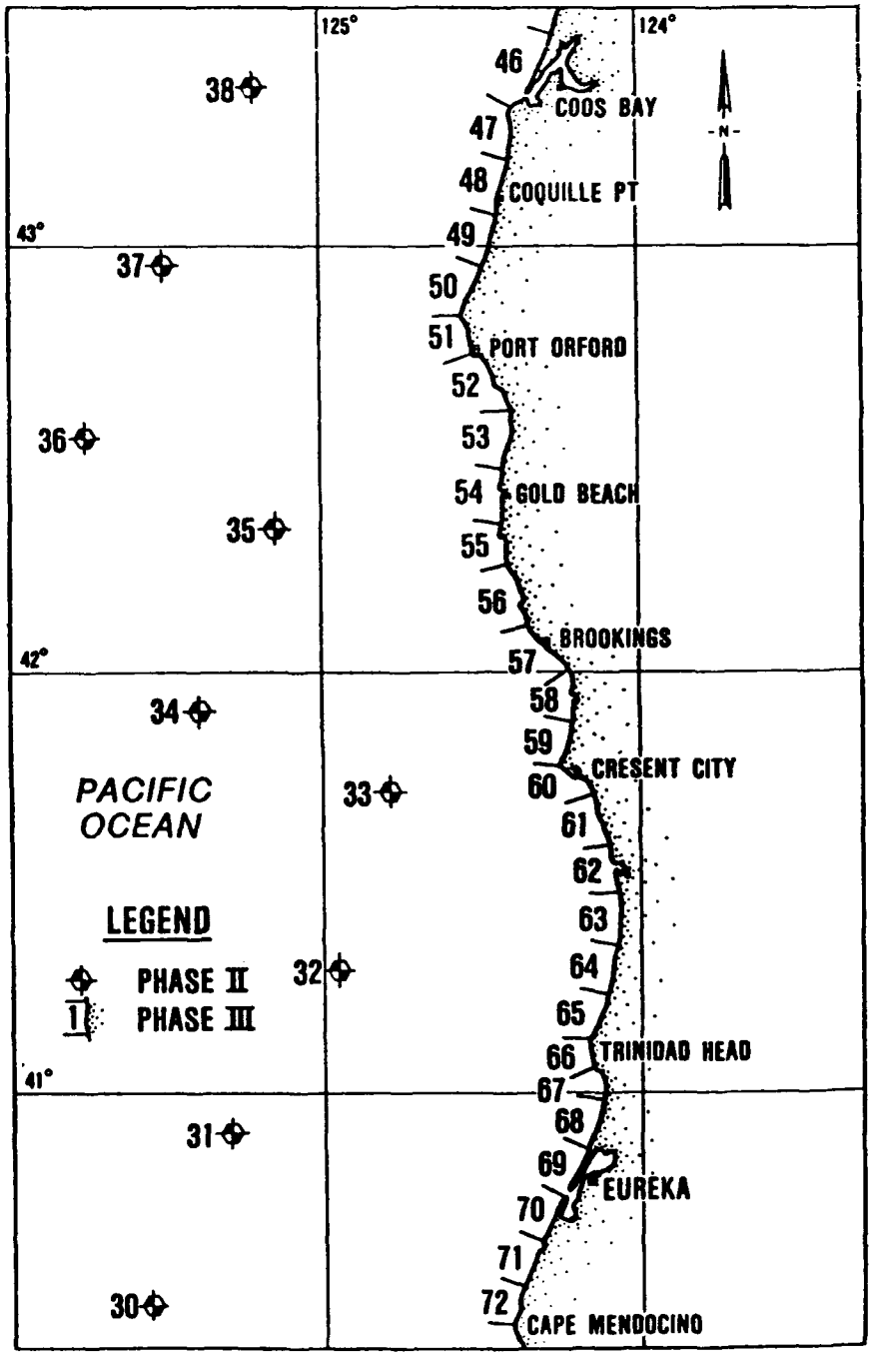

Figure 2. WIS hindcast data station location

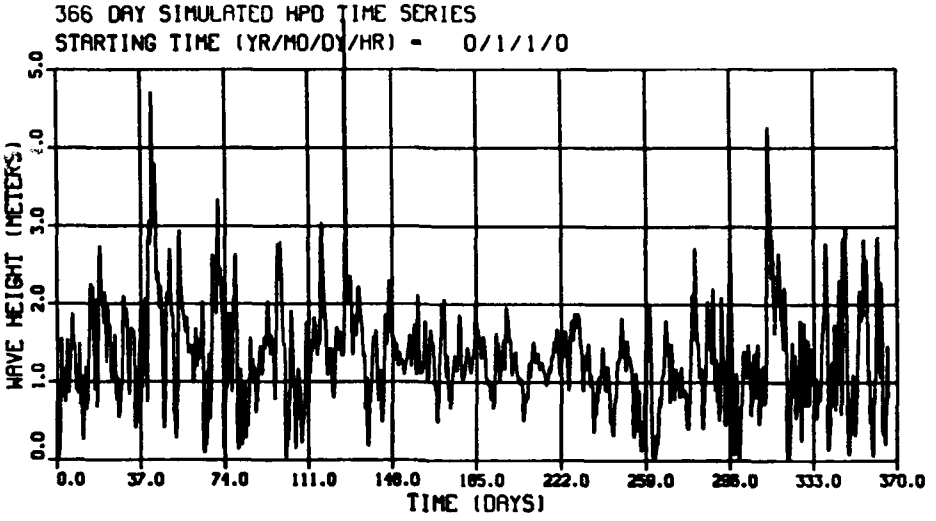

a. Wave height

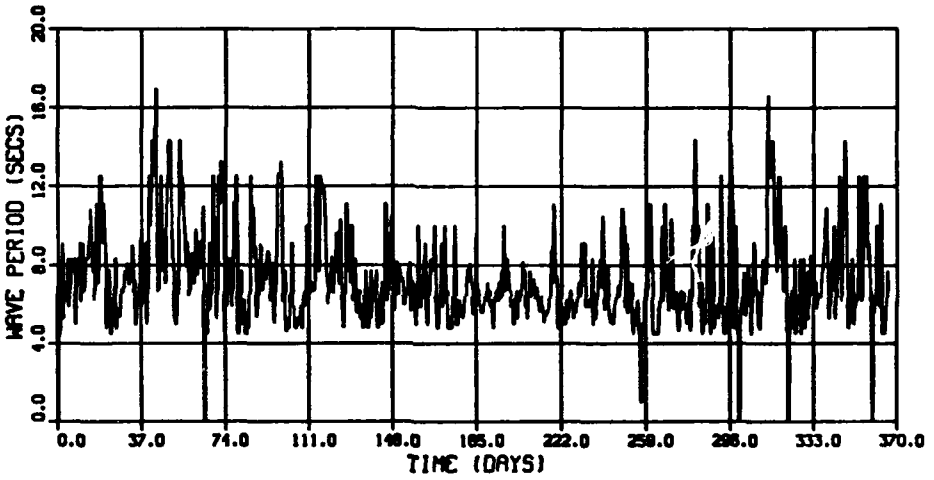

b. Wave period

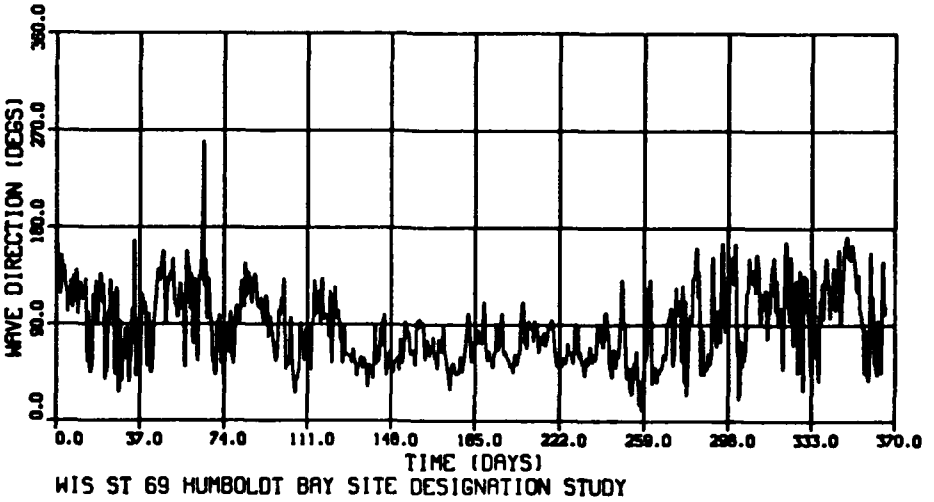

c. Wave direction

Figure 3. Simulated 1-year time series of wave height, period, and direction

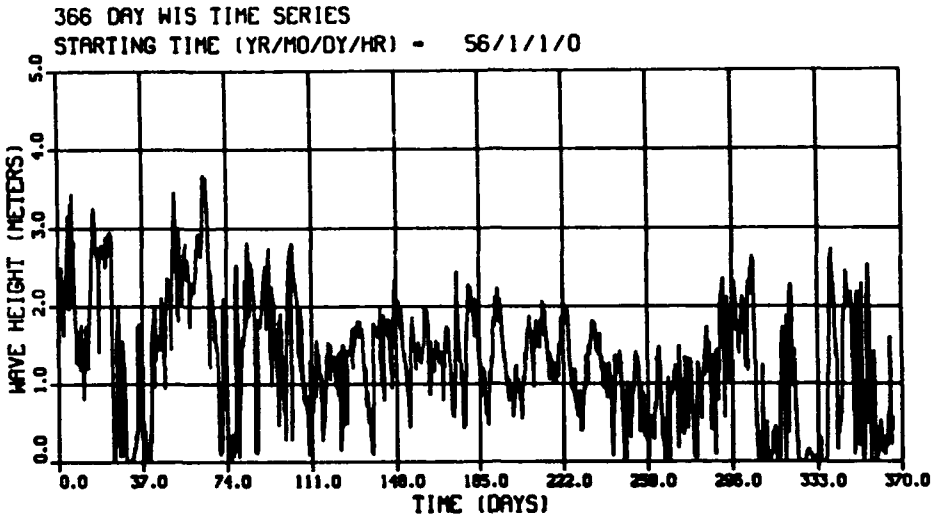

a. Wave height

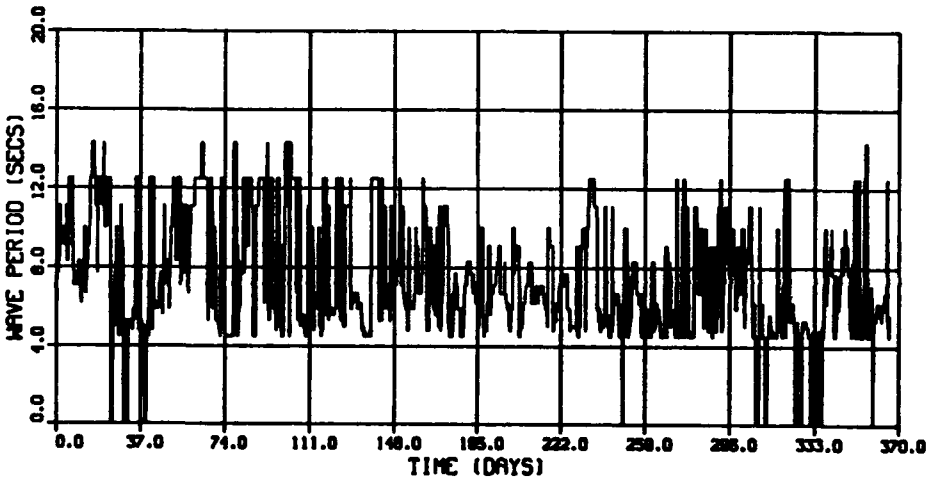

b. Wave period

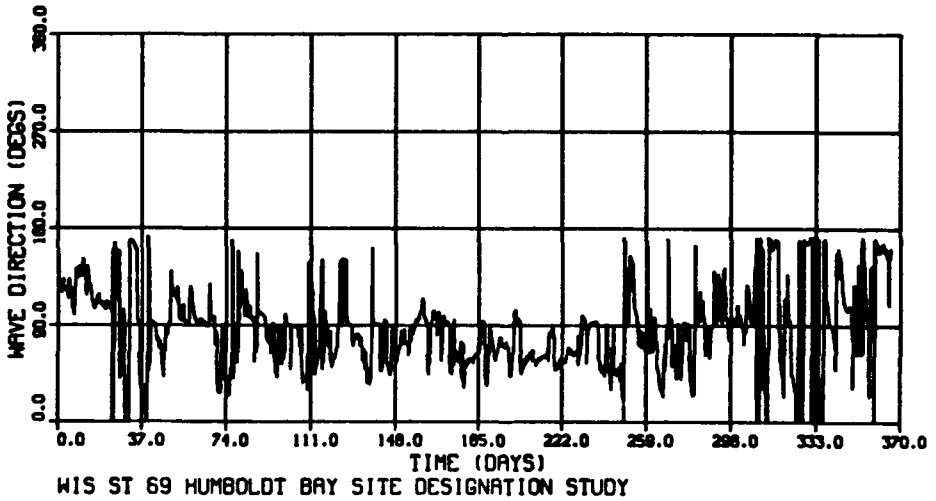

c. Wave direction

Figure 4. WIS Station 69 time series for 1956

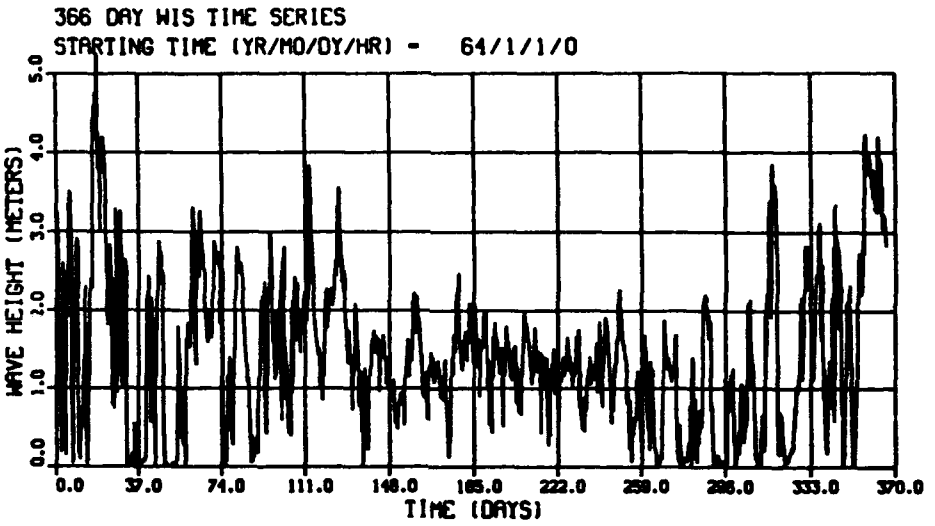

a. Wave height

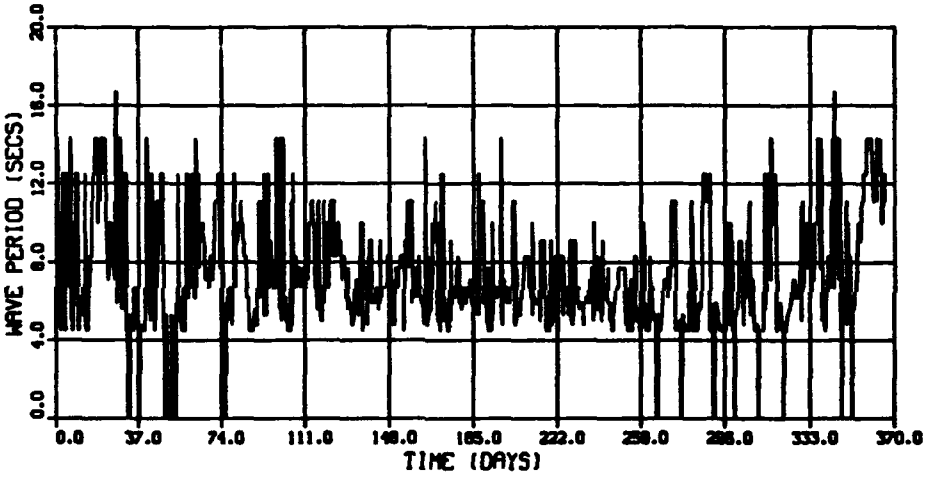

b. Wave period

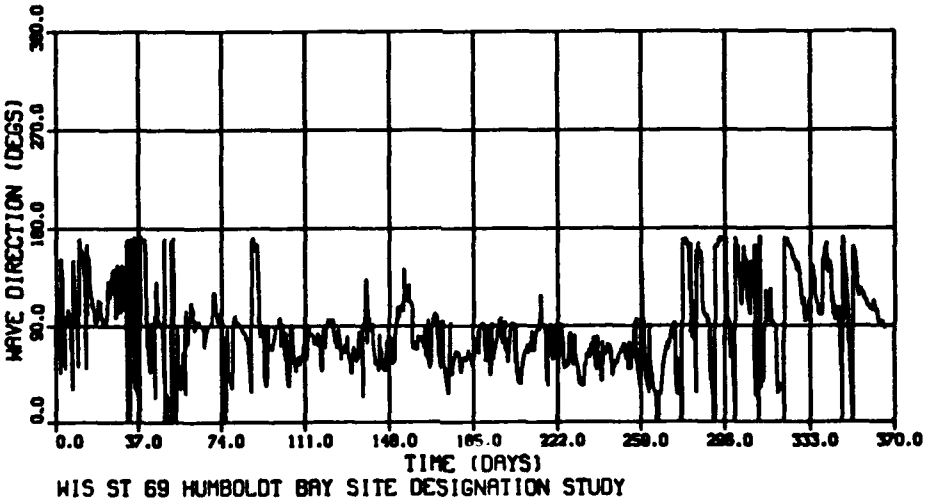

c. Wave direction

Figure 5. WIS Station 69 time series for 1964

months can be seen in all plots. A more quantitative comparison of the data can be seen in the percent probability histogram plots in which the probability statistics of the simulated waves are overlaid with those of the WIS data. Comparisons of the simulated and the 1956 data are shown in Figure 6, while Figure 7 corresponds to 1964. A comparison of computed maximum, minimum, average, and standard deviation for the three series (shown in Table 1) also demonstrates the similarity of the simulated and hindcast data.

11. Station 69 represents a Phase III WIS hindcast station, and the hindcast is developed for 10 m of water. The following relationships were used to transform the wave height from 10 m to deep water and then to shoal the wave from deep water to the disposal site (Ebersole, Cialone, and Prater 1986):

$$H = H_0 \, k_s \tag{1}$$

where H_0 is the deepwater wave height and the shoaling coefficient k_s is defined as

$$k_s = \left\{ \frac{1}{\left[1 + \frac{2kh}{\sinh(2kh)} \right] \tanh(kh)} \right\}^{1/2} \tag{2}$$

12. The parameters h and k represent the local depth and the wave number, respectively.

Depth-Averaged Current Time Series

13. The current information obtained from EG&G Oceanographic Services was measured at two mooring sites, Station E60 at a depth of 60 m and Station E90 at a depth of 90 m of water. The location of both stations are indicated in Figure 1. The current meters were deployed during the four time periods shown in Table 2. Station E60 consisted of one current meter at a depth of 10 m for three of the deployments and 15 m for the other. Station E90 consisted of three current meters, at depths of 10 or 15, 45, and 75 m. The data were provided in the form of hourly averages, as requested by CERC.

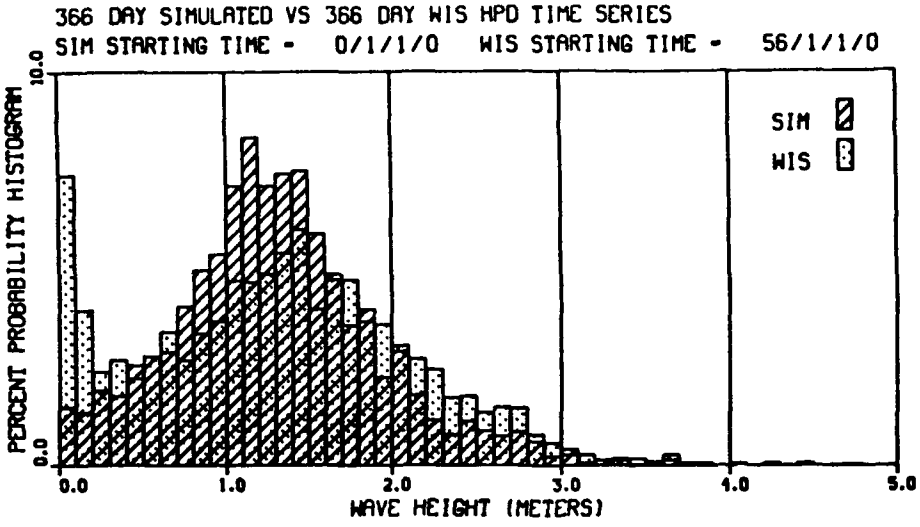

a. Wave height

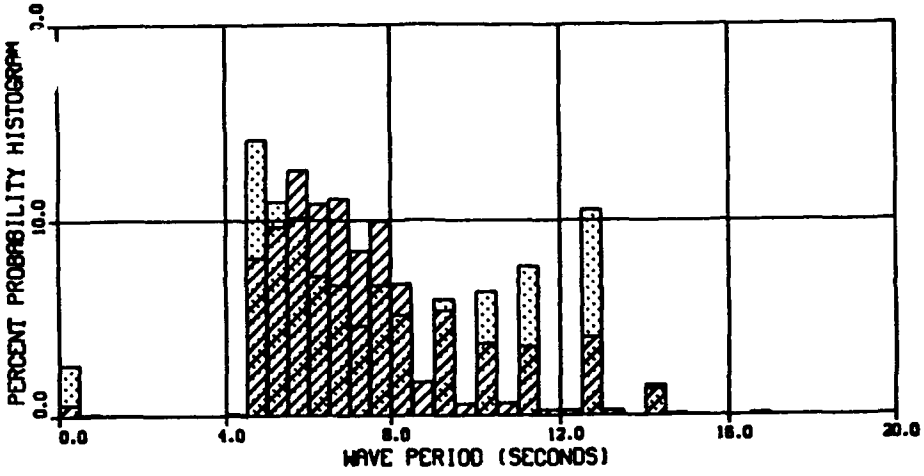

b. Wave period

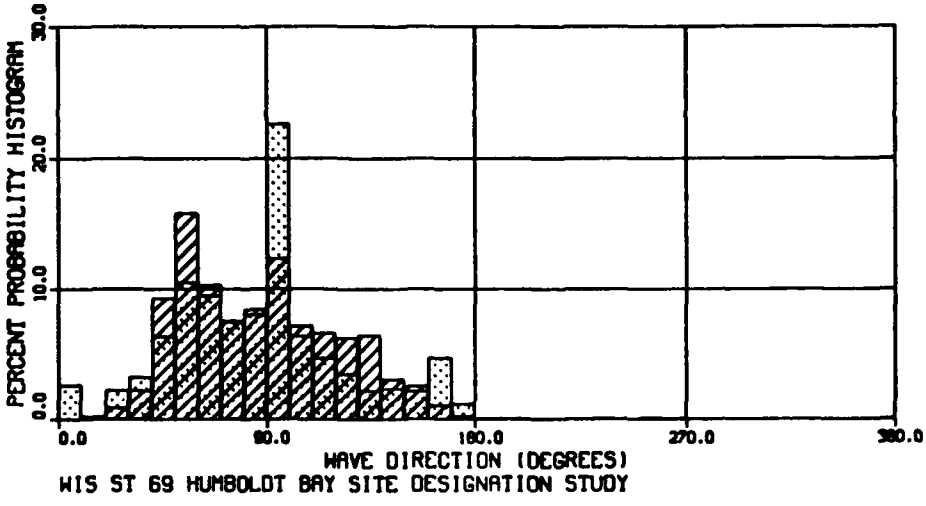

c. Wave direction

Figure 6. Probability histograms for simulated wave and 1956 WIS data

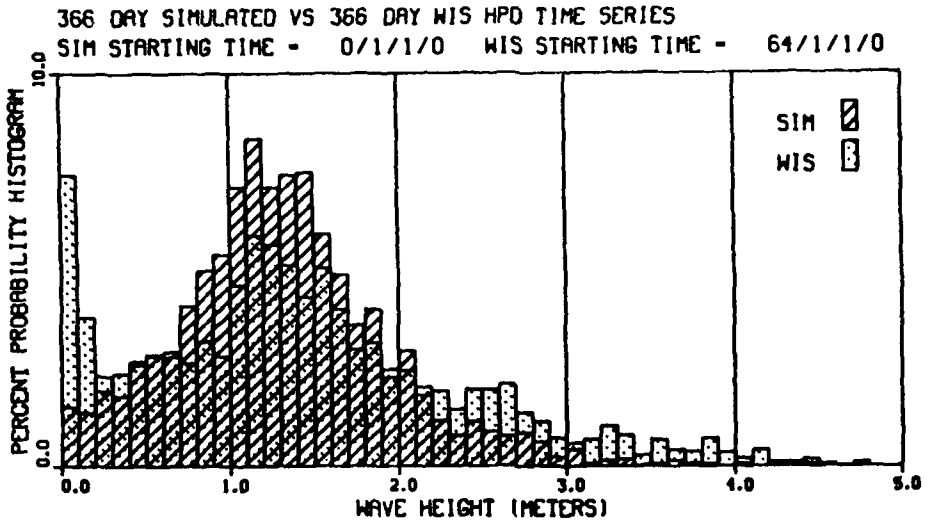

a. Wave height

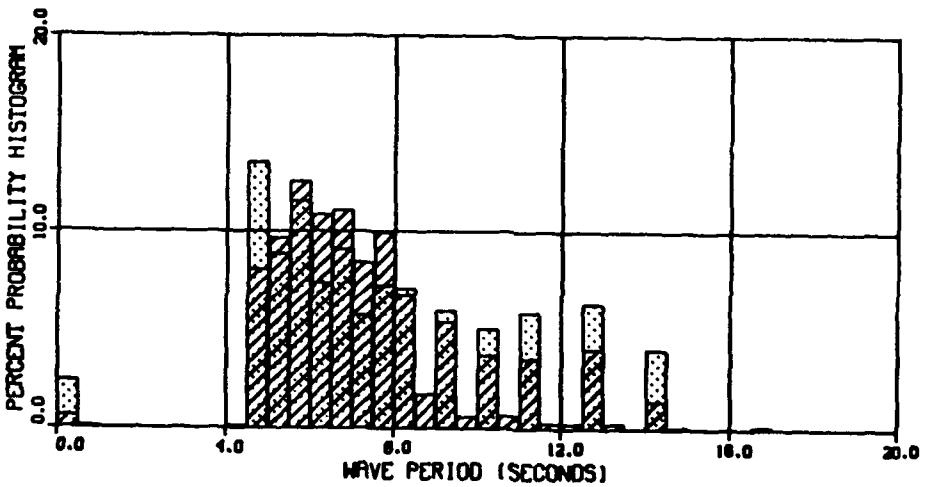

b. Wave period

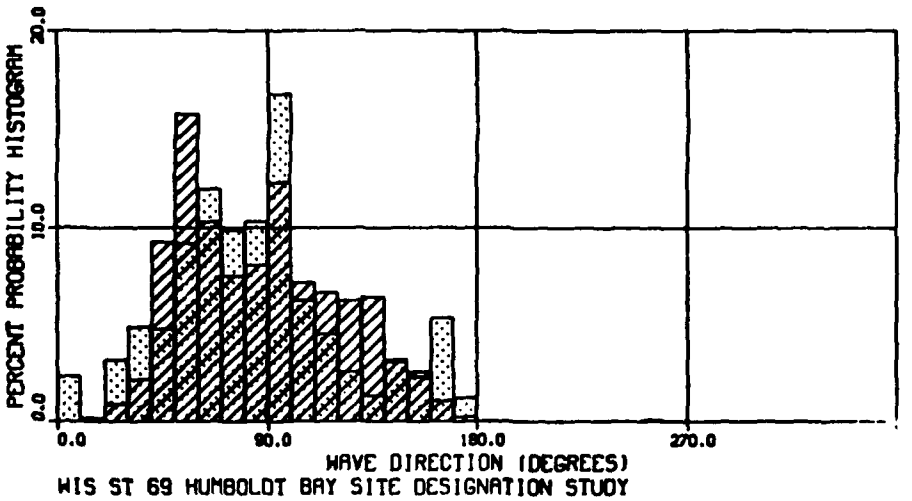

c. Wave direction

Figure 7. Probability histograms for simulated wave and 1964 WIS data

Table 1

Comparison of Wave Statistics

Parameters	Simulated	WIS 1956	WIS 1964
Maximum wave height, m	5.90	3.68	5.26
Minimum wave height, m	0.00	0.00	0.00
Average wave height, m	1.32	1.30	1.43
Standard deviation, m	0.65	0.78	0.96
Maximum wave period, sec	16.95	14.30	16.70
Minimum wave period, sec	0.00	0.00	0.00
Average wave period, sec	7.32	7.51	7.44
Standard deviation, sec	2.27	2.95	2.88

Additional background data were also provided and included wind velocities, temperatures, and pressure gage information. Summary plots of the data provided to CERC by EG&G included 33-hr low-pass filter plots for the current meter data to indicate nontidal trends and magnitudes of the data. The summary plots of the four-velocity record time periods are shown in Figure 8. The current vectors shown in the figure are oriented up-/down-coast with upcoast as positive.

14. The raw (unfiltered) data for each of the time series of Table 2 were obtained in the form of a northerly (+U) and easterly (+V) component. Separate analyses of each data series were performed to determine the average value and magnitude, defined as the square root of the sum of the squared U and V components. Since sediment is primarily transported by local currents, this computed total magnitude of local currents provides an indication of maximum anticipated erosion rate. The computed average values of the separate components, however, provide a measure of net movement. For example, although the velocity magnitude may be sufficient to transport material, the net transport effect may be zero if the magnitudes first flood then ebb in equal magnitudes but opposite directions. Summary computations of U and V averages, velocity magnitudes (Mag), standard deviation (St. Dev.), and percent magnitudes above 50 cm/sec are shown in Table 3.

15. In addition to the computations in Table 3, a 40-hr low-pass filter was applied to velocity magnitude time series to determine the tidal

Table 2

Velocity Data Time Series Lengths

Meter	Beginning yr-mo-day @hr	Ending yr-mo-day @hr	Length, days
		Period 1	
E-60/15	87-03-13 @2300	87-04-11 @0600	28.3
E-90/15	87-03-19 @2000	87-08-08 @1400	141.8
E-90/45	-	-	-
E-90/75	87-03-20 @0000	87-08-11 @0500	141.2
		Period 2	
E-60/10	88-03-15 @1000	88-08-30 @1800	168.4
E-90/10	88-03-15 @0600	88-08-30 @1600	168.5
E-90/45	-	-	-
E-90/75	88-03-15 @0600	88-08-30 @1600	168.5
		Period 3	
E-60/10	-	-	-
E-90/10	88-08-30 @1900	89-03-07 @0300	188.4
E-90/45	88-08-30 @1900	88-12-09 @2000	101.2
E-90/75	-	-	-
		Period 4	
E-60/10	89-03-06 @2100	89-05-11-@2100	66.0
E-90/10	89-03-06 @2300	89-10-31-@1500	238.7
E-90/45	89-03-06 @2100	89-10-31-@1500	238.7
E-90/75	89-03-06 @2100	89-10-31-@1500	238.7

contribution to the total current. This filtering technique effectively separates the diurnal and semidiurnal high frequencies (period less than 40 hr) from the time series so that low-frequency nonperiodic events (e.g. storm or residual currents) can be identified in the time series. This separation can be seen for each time series in Appendix A in which the upper diagram represents the velocity magnitude, the middle diagram shows the high- and low-frequency components, and the lower diagram represents the computed angle of direction of the velocity magnitude. The general trends of the data can be seen in the plots of Appendix A and in Table 3. Average surface velocities are on the order of 25 cm/sec, middepth of 20 cm/sec, and bottom velocities of

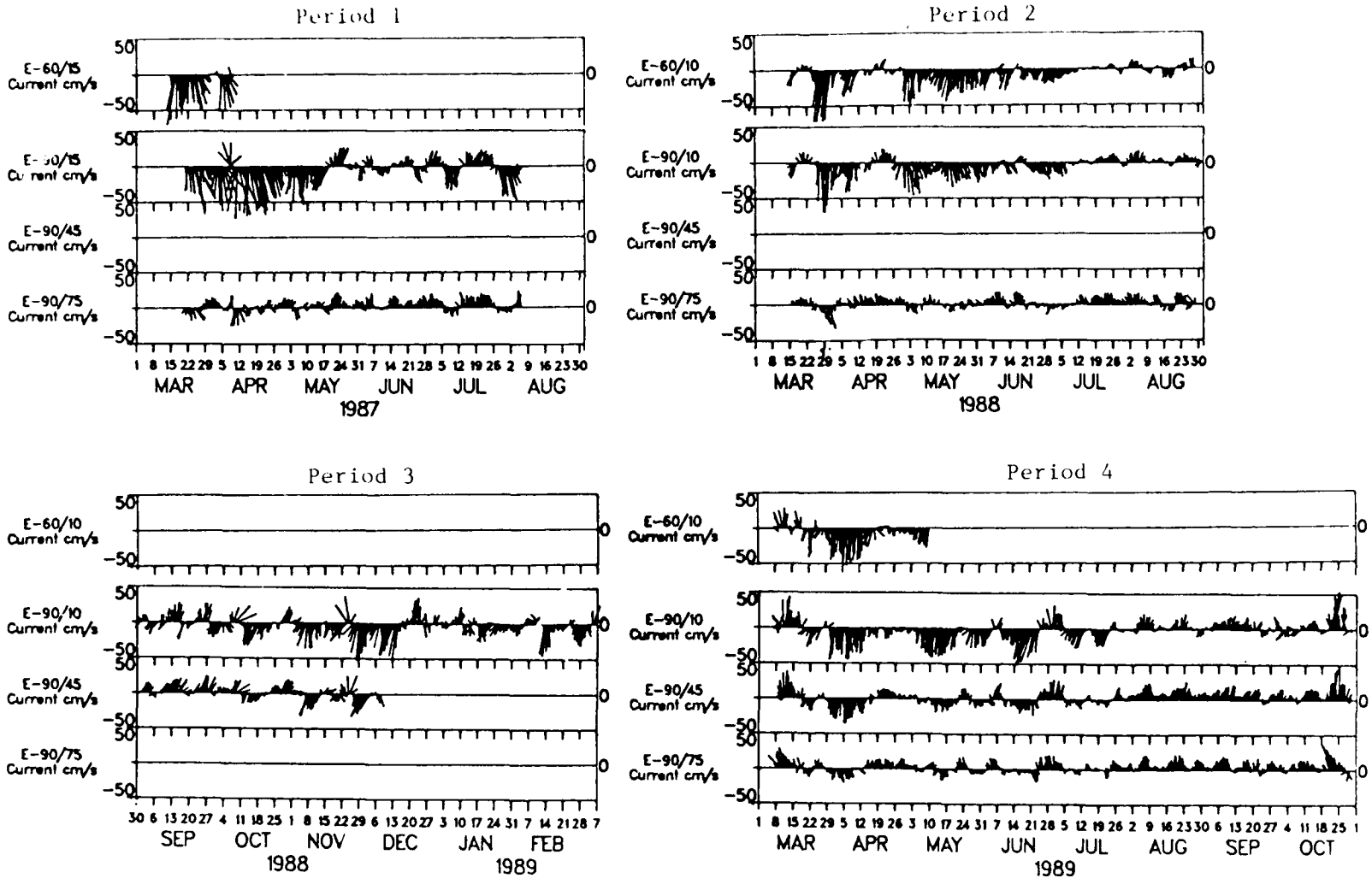

Figure 8. 33-hour low-pass filtered currents

Table 3

Summary Statistics of Velocity Time Series

Meter	Ave U cm/sec	Ave V cm/sec	Ave Mag cm/sec	Mag St Dev cm/sec	% Exceeding 50 cm/sec
			Period 1		
E-60/15	-1.90	-4.36	30.51	17.63	15.29
E-90/15	-5.37	14.08	27.12	17.03	11.08
E-90/45					
E-90/75	2.46	3.52	15.54	8.28	0.00
			Period 2		
E-60/10	-6.70	-8.40	17.82	14.45	3.79
E-90/10	-2.88	-6.81	17.63	13.51	3.24
E-90/45					
E-90/75	0.41	4.06	14.90	8.06	0.10
			Period 3		
E-60/10					
E-90/10	-4.49	-5.48	22.12	12.71	3.25
E-90/45	1.89	-0.44	16.65	10.23	0.45
E-90/75					
			Period 4		
E-60/10	-7.82	-12.23	24.79	13.96	4.42
E-90/10	-3.74	-3.68	20.60	13.12	3.26
E-90/45	2.47	1.91	14.80	9.46	0.58
E-90/75	1.11	3.93	15.79	8.79	0.17

15 cm/sec. Elevated surface, standard deviation values are probably due to the effect of local winds.

16. The sediment transport formulation used in this analysis requires a depth-averaged velocity distribution for input to the transport computations. The selection of an appropriate depth-averaged velocity distribution from the limited data shown in Table 2 is made as follows. Unfortunately, middepth data are not available for the gage at Site E60, located nearest the disposal site. However, if it can be shown that the surface data for gages at Sites E60/10 and E90/10 are well correlated, it is reasonable to assume that the middepth velocity at the gage located at Site E60 would be equally

correlated with that at Site E90. If this correlation between the two gages for Periods 2 and 4 can be demonstrated, then data from the gage at Site E90/45 from sampling Period 4 can be selected as representative of the currents to be anticipated at the candidate disposal site. The development of this correlation follows.

17. The general similarity in magnitude and distribution of velocity data from Gages E60/10 and E90/10 can be seen from the Table 3 statistics and from the time series plots in Appendix A. A comparison of the Period 2 U and V components for Gage E60/10 in Figure 9 and E90/10 in Figure 10 also exhibit this similarity. Auto- and cross-correlation functions were computed for each time series to quantify the similarity in data from the two gage locations. Auto- and cross-correlation functions of the U and V time series are defined as follows (Burington and May 1958):

Auto-correlation

$$f(k) = \frac{1}{(2N + 1)} \sum_{j=1}^{N} \frac{U60}{10(j+k)} \frac{U60}{10(j)} \tag{3}$$

Cross-correlation

$$f(k) = \frac{1}{(2N + 1)} \sum_{j=1}^{N} \frac{U90}{10(j+k)} \frac{U60}{10(j)} \tag{4}$$

where the time lag k was computed for 0 to 480 hr. The auto- and cross-correlation function plots are shown in Figures 11 and 12. Both curves are normalized to the computed zero lag auto-correlation value for Gage E60/10.

18. The auto-correlation function shows periodicities in the data by performing a self correlation with an increasing time shift in the data. At a zero time shift, the perfect correlation of 1.0 is shown. As the time lag of the data increases to span tidal periods, the tidal peaks of the two series come in phases producing a characteristic peak in the correlation function. These peaks, clearly visible in Figures 11 and 12, show both the diurnal and semidiurnal tidal signal. If the cross-correlation function is identical to the auto-correlation, then the two signals are identical. A time lag between

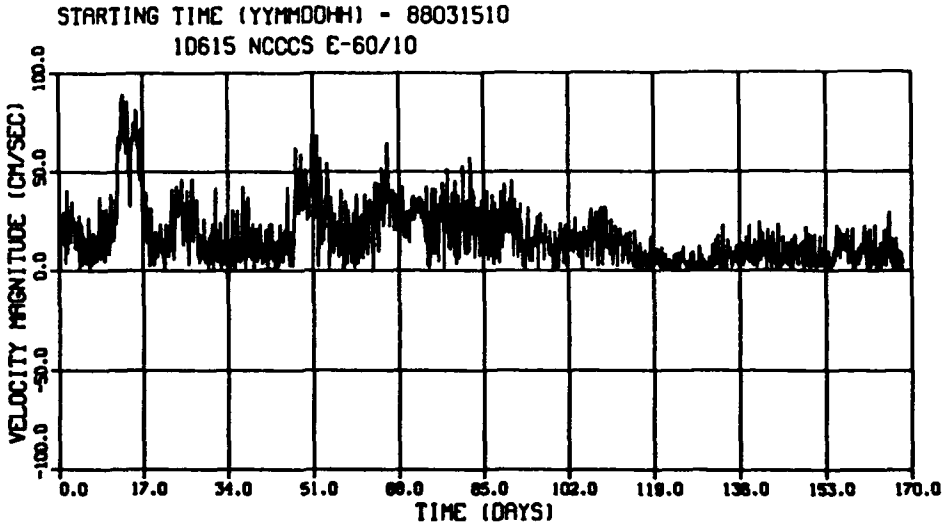

a. Velocity magnitude

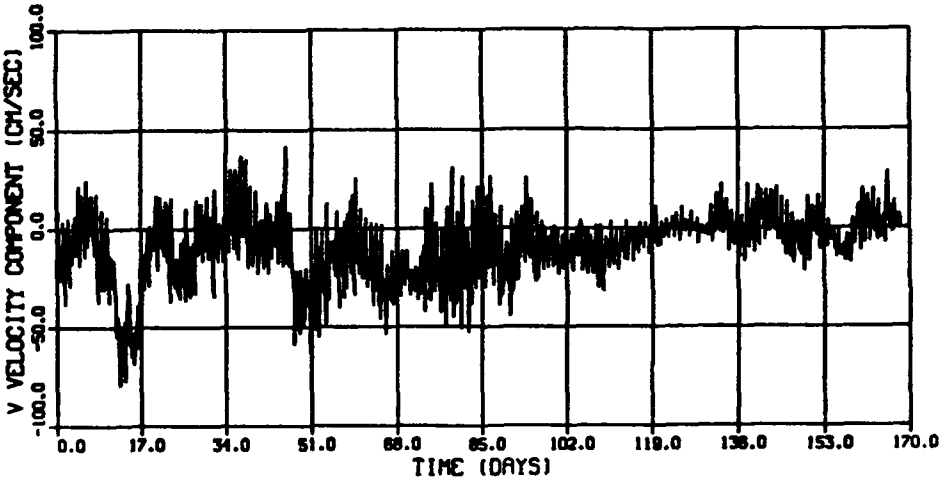

b. Velocity component

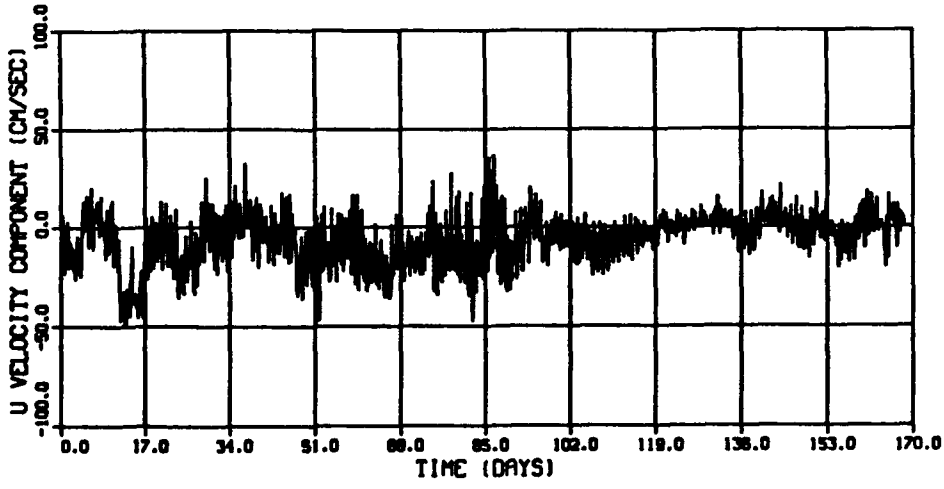

c. Velocity component

Figure 9. Period 2 Velocity components for Gage E60/10

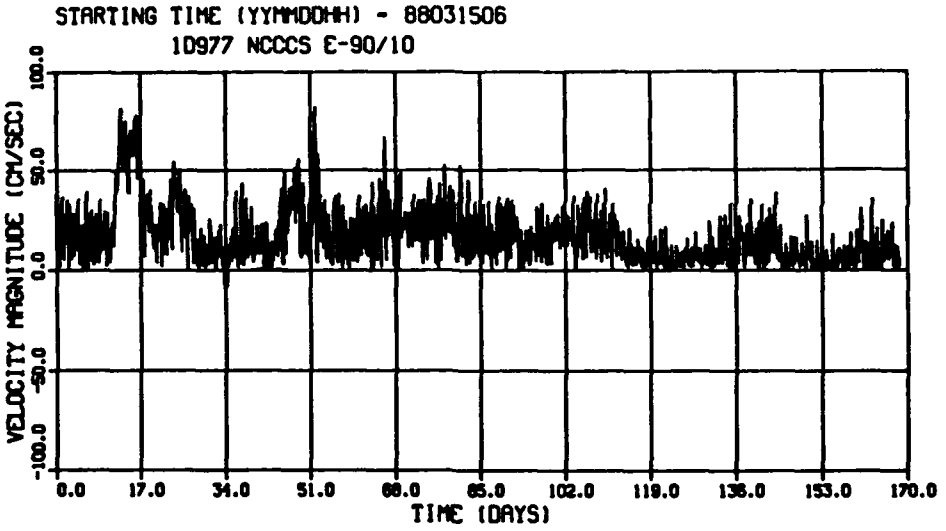

a. Velocity magnitude

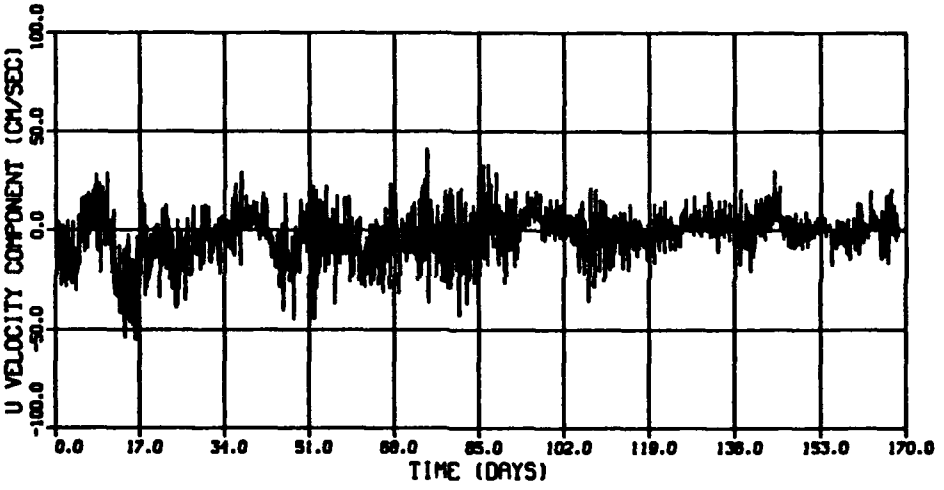

b. Velocity component

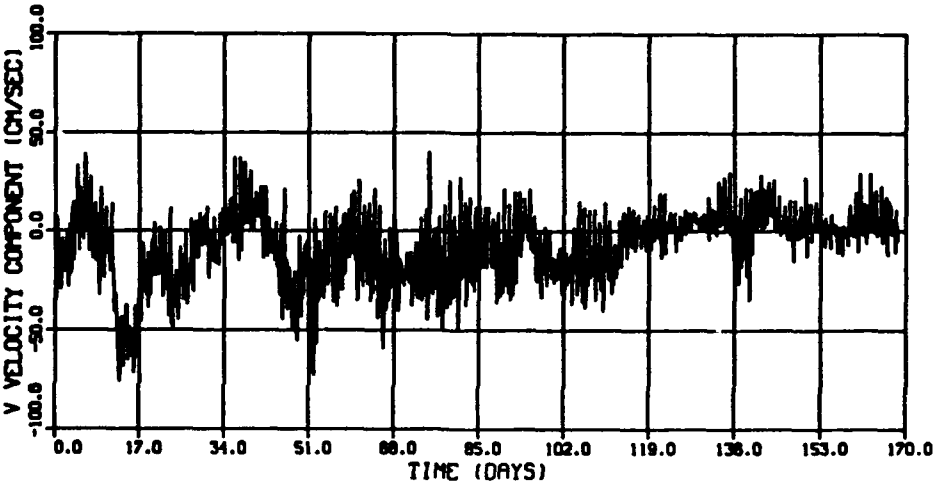

c. Velocity component

Figure 10. Period 2 Velocity components for Gage E90/10

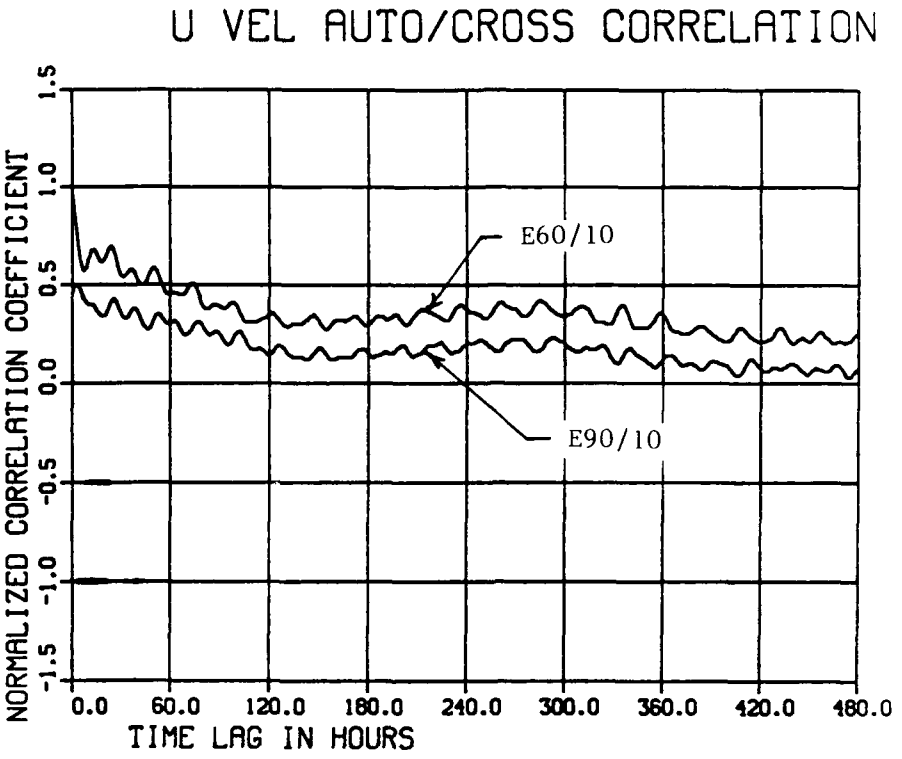

Figure 11. Auto- and cross-correlation functions for U velocity component for Gages E60/10 and E90/10

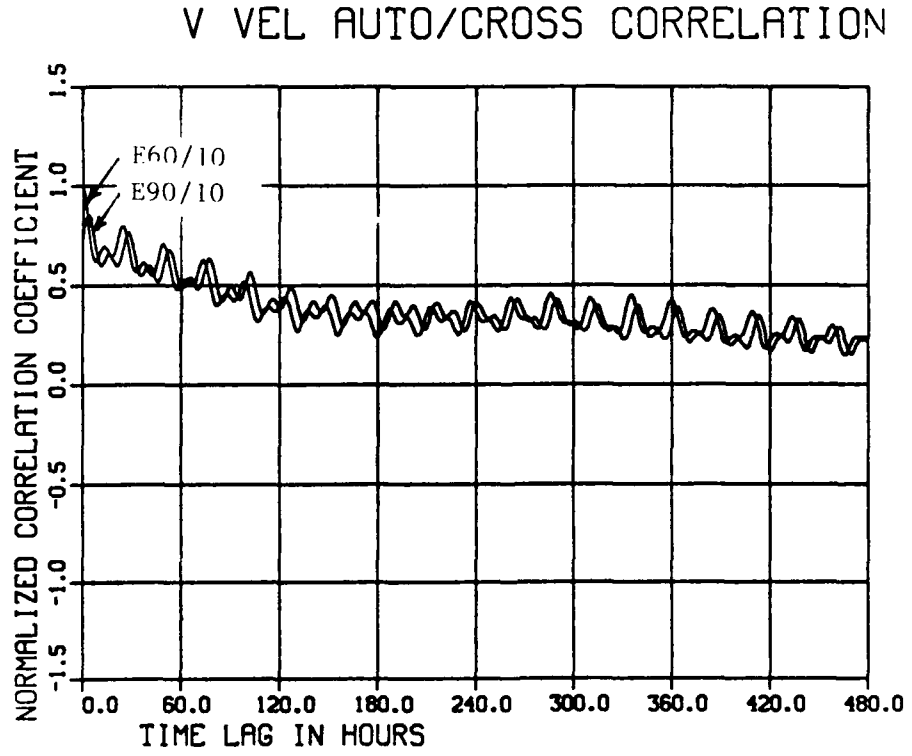

Figure 12. Auto- and cross-correlation functions for V velocity component for Gages E60/10 and E90/10

the signals is indicated when the signals are shifted horizontally. This phase shift is a measure of the difference in arrival time of the same signal at different locations. The shift in the functions shown in Figures 11 and 12 indicates an approximate lag of 4.5 hr between the two signals.

19. A vertical offset in the two signals can indicate a lower mean value for the second data set. For example, the vertical offset in the auto-correlation function of Figure 11 is indicative of the fact that the mean U magnitude for Gage E60/10 is larger (-6.7 cm/sec) than that of the mean U magnitude for Gage E90/10 (-2.9 cm/sec). Less offset is shown in Figure 12, reflecting the fact that the V data averages are closer in value, -8.4 cm/sec for E60/10 and -6.8 cm/sec for E90/10. A similarity in shape demonstrates a similarity in data. Results shown in Figures 11 and 12 demonstrate a sufficiently strong correlation to justify the selection of the middepth E90/45 data as representative of the interim site.

20. The long-term modeling goal is to generate a data base of simulated current data that is realistically representative of currents at the disposal site. In the same manner that the wave fields were simulated to reflect the same statistical distribution as the WIS data, the 240-day time series for Period 4 of Gage E90/45 is used to compute harmonic constituents that can be used to simulate prototype velocity time series. Plots of the velocity magnitude and the U and V components of the E90/45 time series are shown in Figure 13. A 16-constituent harmonic analysis was performed on each component of the time series. Although the data are not of sufficient length for a reliable harmonic analysis, the procedure provides an approximate estimate of tidal influence. Results show that approximately 28 percent of the U and 20 percent of the V velocity time series are tide related. These results are not surprising in view of the relative magnitudes of the low- and high-frequency components of the data shown in the figures of Appendix A. Even though the tidal energy is small in comparison with the total signal, the primary astronomical constituents were extracted from the time series and are shown in Table 4.

21. Average current values for Period 4 for the U and V components of Gage E90/45 were 2.47 and 1.91 cm/sec respectively, indicating a mean current direction to the northeast. This directionality is in contrast to the mean surface direction to the southwest, indicated by the mean value data for Gages E60/10 and E90/10. Inspection of the low- and high-frequency portions of the velocity magnitude as well as the actual U and V components of the

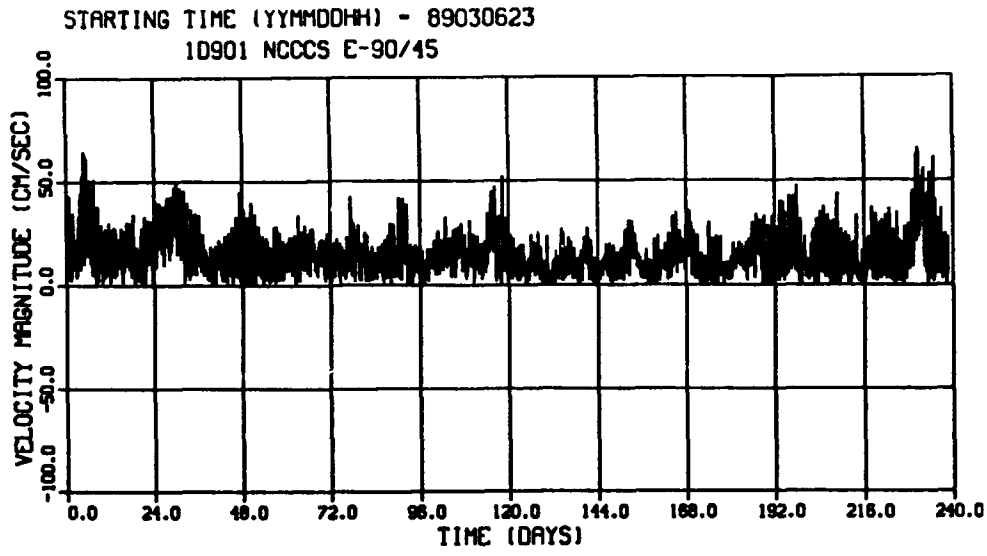

a. Velocity magnitude

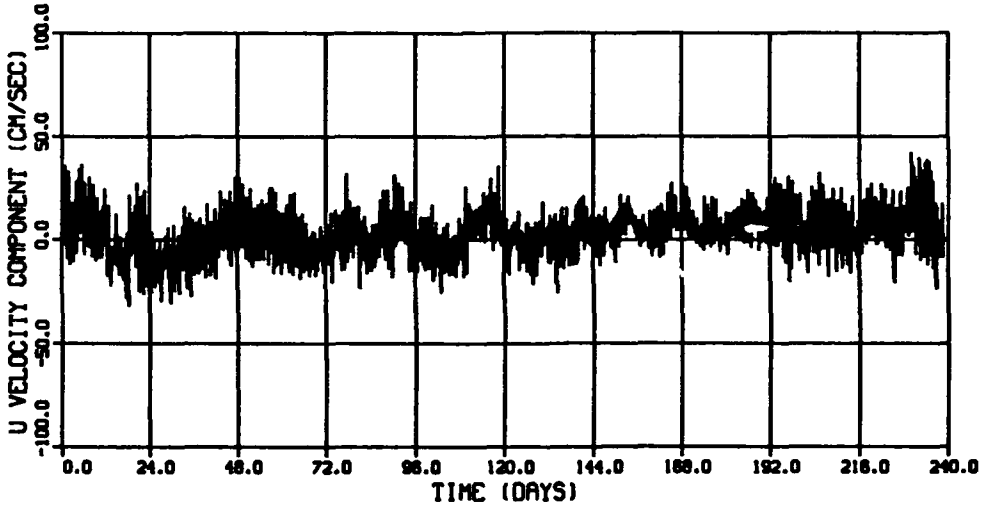

b. Velocity component

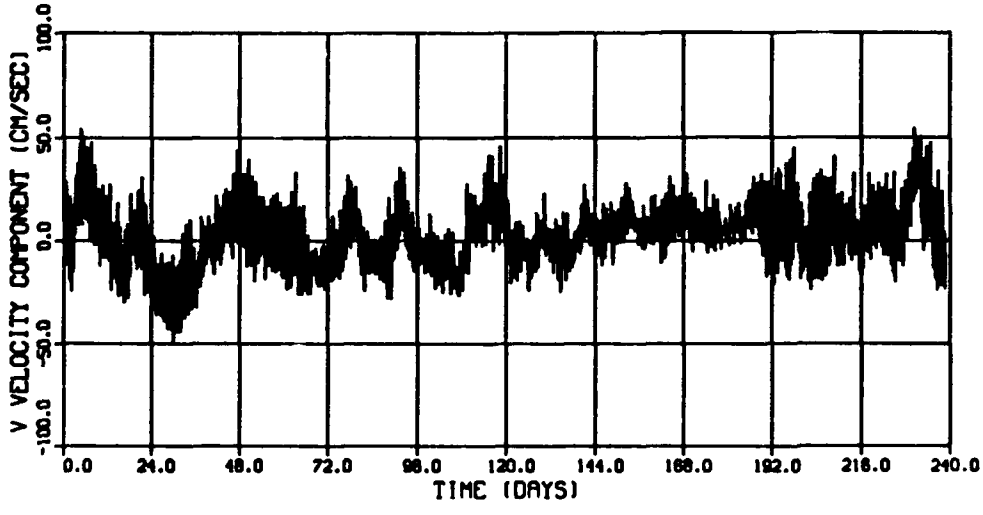

c. Velocity component

Figure 13. Period 4 Velocity components for Gage E90/45

Table 4

Primary Astronomical Constituents for Gage E90/45

Const	Speed-deg/hr	Vel. U		Vel. V	
		AMP-cm/sec	Phase-deg	AMP-cm/sec	Phase-deg
O_1	13.943036	3.3	337.0	2.1	54.0
K_1	15.041069	5.6	221.0	3.4	293.0
M_2	28.984104	5.4	186.0	2.5	218.0
S_2	30.000000	2.7	222.0	1.2	310.0
M_n	0.544400	1.9	118.0	2.0	76.0
M_{sf}	1.105900	1.5	165.0	0.6	146.0

data shown in Figure 13 suggest that the addition of a long period, large amplitude component to the tidal signal would produce fluctuations in the simulated current time series that would be representative of prototype conditions. Therefore, a synthetic tidal component with an amplitude of 30 cm/sec and a period of 48 days was added to the constituent list shown in Table 4. The resulting tidal signal is shown in Figure 14. Note that the maximum magnitude approaches 50 cm/sec approximately six times in the 240-day simulation. Prototype data also approach (or slightly exceed) this value about the same number of times. As such, the tidal constituents listed in Table 4 and the 48-hr component are used to simulate tidal height and current fluctuation in the long-term modeling effort. A residual current of 5 cm/sec was imposed on the computed V component of the tidal signal.

22. A single velocity value is specified for the short-term modeling effort since the model simulations are made only for a total of 1 hr. In view of the magnitudes shown in Figure 13, a sustained depth-averaged value of 45.7 cm/sec was used for both the fine-grained and coarse-grained computations. As shown in Table 3, this value is more representative of extreme conditions than of average conditions; however, it was selected to produce an "upper envelope" dispersion pattern. A description of both the short- and long-term simulations follow.

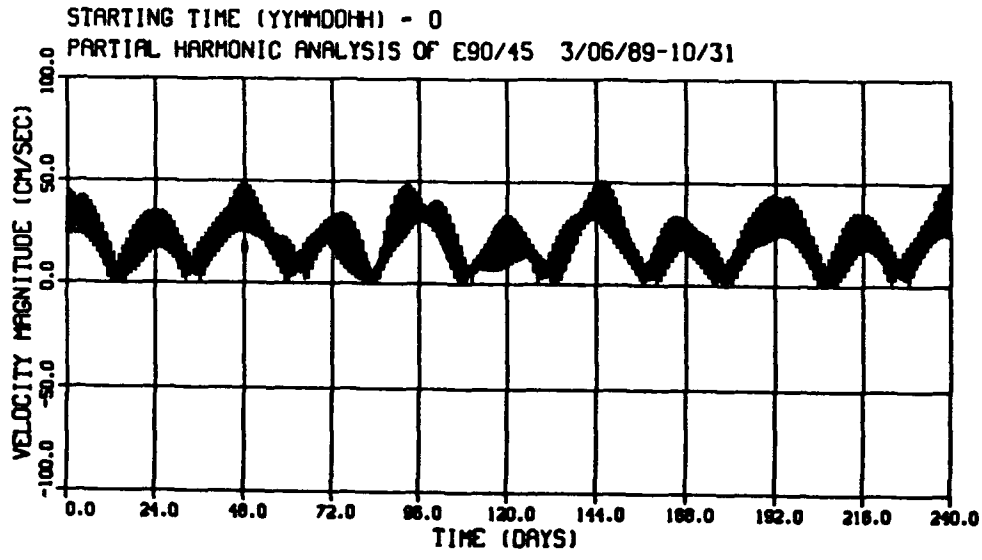

a. Velocity magnitude

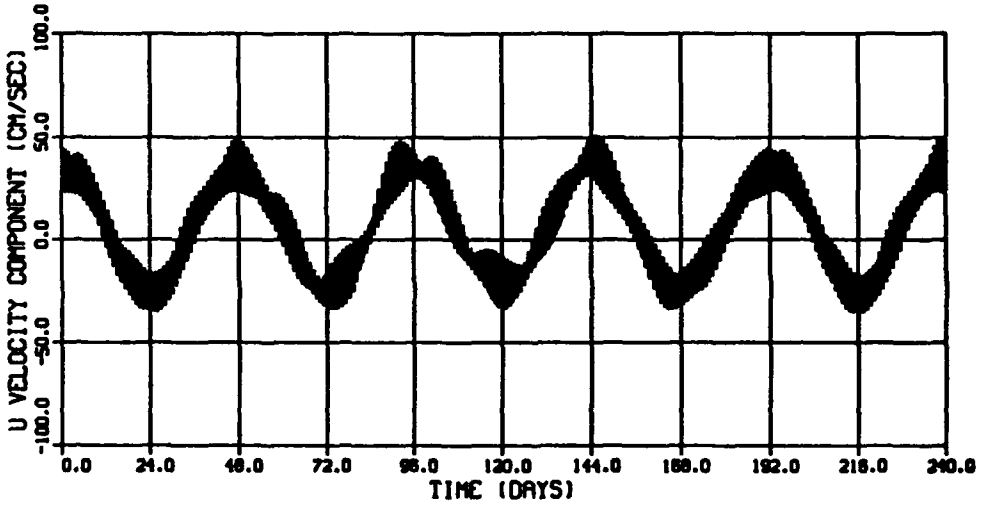

b. Velocity component

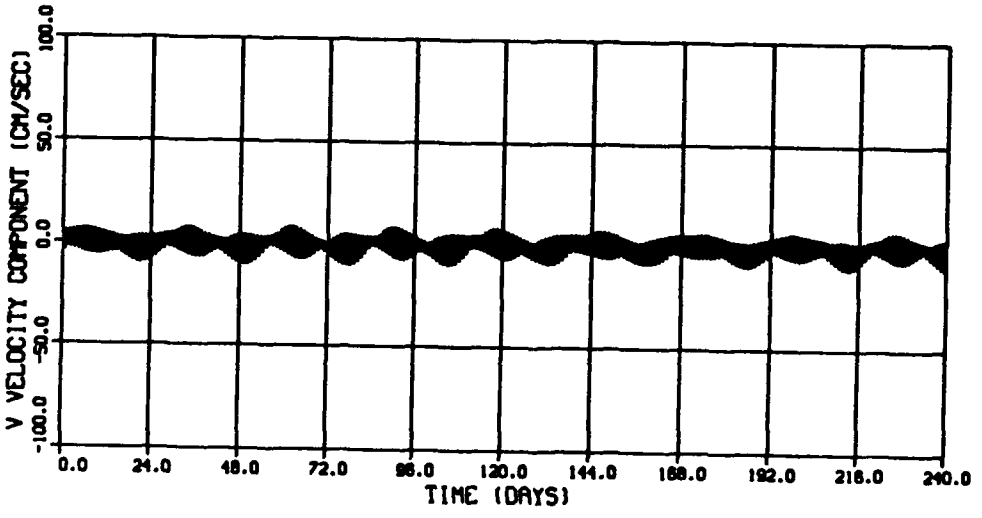

c. Velocity component

Figure 14. Synthesized tidal series for interim site

PART III: SHORT-TERM MODELING

General

23. The short-term modeling component of this investigation examines the immediate impact of the actual disposal operation on the surrounding area. Numerical simulations of the discharge are used to determine whether the combined effects of the local topography at the site and the depth-averaged velocity field adversely impact the effectiveness of the dredged material disposal operation. Can the material be physically placed within the limits of the designated site as the material descends through the water column to the ocean floor, or are the local currents of sufficient magnitude to transport material out of the site before deposition?

24. The short-term site evaluation phase is made by numerically modeling the disposal operation using the DIFID numerical model. Theory and background of the model are reported in Johnson and Holliday (1978), Johnson (in preparation), and Johnson, Trawle, and Ademec (1988). Applications of the model are reported in Trawle and Johnson (1986), Scheffner (in preparation), and Scheffner and Swain (in preparation). The model computes the time history of a single disposal operation from the time the dredged material is released from the barge until it reaches equilibrium on the ocean floor. The DIFID model separates the dumping operation into three distinct phases. In the first phase, material released from the bin is assumed to form a hemispherically shaped cloud that descends through the water column under the influence of gravity. This phase is called the convective descent phase.

25. The convective descent phase continues until the cloud of material impacts the bottom or reaches a stable point of neutral buoyancy. In either case, horizontal spreading of material marks the beginning of the dynamic collapse phase in which the material spreads horizontally. When the rate of spreading becomes less than spreading due to turbulent diffusion, the final phase of transport begins, the transport-diffusion phase. The termination of this phase marks the end of the short-term investigation and initializes the boundary conditions for the long-term transport computations to be described in Part IV. An idealization of all three phases of the short-term disposal are shown in Figure 15.

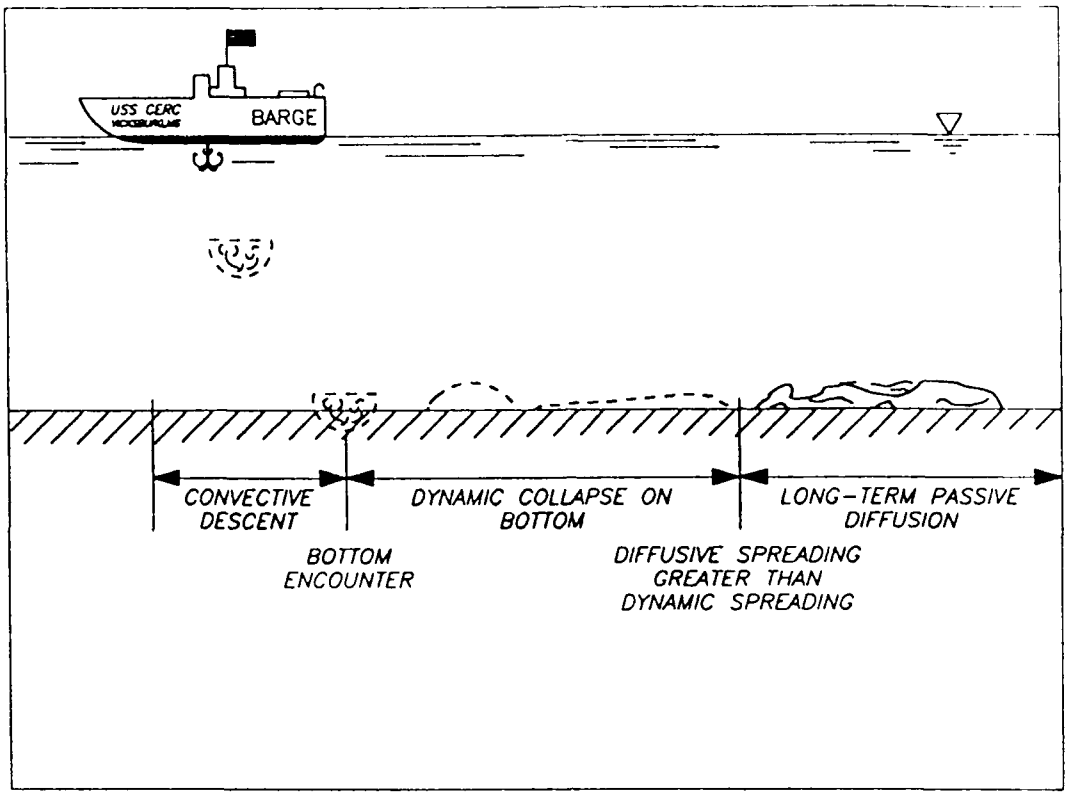

Figure 15. Computational phases of DIFID model (from Brandsma and Divoky 1976)

Input Data Requirements

26. The DIFID model requires site-specific input data to quantitatively predict the short-term sediment fate of a disposal operation. These data include the physical dimensions of the dredge, a description of the local environment (local depth and velocity field), and a knowledge of the composition and characteristics of the dredged material in the dredge. In addition, numerous modeling parameters and coefficients must be specified. Since the input parameters are dependent on the specific disposal operation, two simulations are performed to effectively analyze the dispersive characteristics of the interim site, one for the placement of fine-grained material and one for the coarse-grained material.

27. Model input requires the specification of the size and capacity of the dredge. It is anticipated that the dredge "Yaquina," or one of similar dimensions, will be used for the spring disposal of fine-grained material. The "Yaquina" is a single hopper-type dredge that will deposit material at the

outer boundary of the interim site in 55 m of water. Capacities and dimension of the "Yaquina" are given in Table 5.

Table 5

Capacities and Dimensions of Dredge "Yaquina"

Capacities	Dimensions
Overall length	200 ft
Width	58 ft
Depth	17 ft
Unloaded draft	8 ft
Loaded draft of vessel	13 ft
Volume	500 cu yd

28. dredge "Newport," or a dredge of similar capacity, is anticipated for use in the fall disposal of coarse-grained material. The disposal operation will operate near the shoreward boundary of the interim site in a depth of approximately 49 m of water. Capacities and dimension of the "Newport" are given in Table 6.

Table 6

Capacities and Dimensions of Dredge "Newport"

Capacities	Dimensions
Overall length	260 ft
Width	60 ft
Depth	22 ft
Unloaded draft	9-10 ft
Loaded draft of vessel	18-19 ft
Volume	2,500 cu yd

29. Additional site-specific parameters include specification of grid resolution, total simulation duration, and time-step parameters to best represent the disposal operation. The bottom slope was computed from the location map shown in Figure 1. Values for the internal model coefficients were based on recommendations and applications reported by Johnson (in preparation) and

Johnson and Holliday (1978). The parameters and coefficients used in both simulations are shown in Table 7.

30. Final input to the DIFID model is the specification of the composition of the solid material in the dredge according to percent volume of sand, clay and silt, clumps, rocks, etc. Each component must be defined according to its respective density, concentration by volume, fall velocity, and voids ratio. Sediment composition for the fine and coarse sites were based on sediment gradation curves corresponding to sediment samples collected from 20 locations within the Humboldt Bay navigation channel complex.* The median sediment diameter (D_{50}) was extracted from each gradation curve, and the respective sample was defined as coarse if this value was greater than 0.075 mm. Those samples with a D_{50} value below 0.075 mm were defined as fine. Based on this criterion, 13 of the 20 samples were coarse-grained for deposition in the 49-m site and 7 of the 20 samples were fine-grained for deposition at the 55-m site.

31. The percent distribution of sediments within each category (coarse or fine) was made by first tabulating the percent distribution above and below 0.075 mm for each distribution of sediments within the sample and then averaging the total percent distributions. Results indicate the coarse sediments to contain a 93-percent/7-percent distribution of sand/silt-clay whereas the fine sediments contained a 25-percent/75-percent distribution of sand/silt-clay. These percentages represent only the solids portion of the material. The total fluid composition of each sample was based on a separate percent distribution computation for the water content of the sand portion and the silt-clay portion. Results show the coarse materials to be 72-percent solids, of which 93 percent is sand and 7 percent is silt-clay. The fine-grained samples were 33.3 percent solid, with 25 percent sand and 75 percent silt-clay. Final results of the computations are shown in Table 7 for the fine-grained material and Table 8 for the coarse-grained material.

32. The data in Tables 8 and 9 were input to the DIFID model. Results of the computations are presented in the following section.

---

* Personal Communication, June 1990, D. Hodges, USACE, San Francisco, CA.

Table 7

Model Input Parameters and Coefficients

Variables	Values
Grid size, ft	100
Number of cells:	
Cross-shore direction	105
Alongshore direction	28
Time-step, sec	100
Duration of simulation, sec	3,600 (fine-grained site)
	400 (coarse-grained site)
Ambient velocity, ft/sec	1.50
Local depth, m	55.0 (fine-grained site)
	49.0 (coarse-grained site)
X-Direction (on-offshore) bottom slope, deg	0.315
Y-Direction (alongshore) bottom slope, deg	0.0
Ambient density, g/cc	1.018
DINCR1	1.0
DINCR2	1.0
Entrainment coefficient ALAPHO	0.235
BETA	0.0
CM	1.0
Drag coefficient for sphere, CD	0.5
GAMA	0.25
Drag coefficient for elliptic cylinder, CDRAG	1.0
CFRIC	0.01
CD3	0.10
CD4	1.00
ALPHAC	0.0010
Bottom friction, FRICTN	0.0100
FI	0.10
ALAMDA	0.005
AKYO	0.05

Table 8

Fine-Grained Sediment Composition and Characteristics

Description	Density g/cc	Concentration percent	Fall Velocity ft/sec	Voids Ratio	Cohesive? (1 or 0)
Sand	2.600	0.0830	0.06500	0.80	0
Silt-clay	2.600	0.2500	0.02560	0.80	1
Water	1.018	0.6670	0.00		

Table 9

Coarse-Grained Sediment Composition and Characteristics

Description	Density g/cc	Concentration percent	Fall Velocity ft/sec	Voids Ratio	Cohesive? (1 or 0)
Sand	2.600	0.6700	0.06500	0.80	0
Silt-clay	2.600	0.0500	0.02560	0.80	1
Water	1.018	0.2800	0.00		

Short-Term Model Simulations

33. The objective of the short-term simulations is to determine whether dredged material can be effectively placed within the limits of the designated disposal sites under the action of a realistic, localized velocity field. Two measures of impact can be addressed by the model. The first measure of impact is the calculation of the movement and concentration distribution of the suspended sediment as it descends to the bottom. During the descent and collapse phases, the sediment cloud grows larger (diffuses) and becomes less concentrated. Calculations during this phase can be used to estimate the time change in sediment concentration with depth and distance from the barge. Model results also provide an estimation of the spatial extent of the deposited material on the ocean floor with respect to the initial release site. Both concentration distribution and total deposition results are presented separately for the fine- and coarse-grained sites.

Fine-Grained Disposal Site Analysis

34. The coefficients presented above for the 55-m-deep fine-grained deposition site were input to the numerical model. Model results include the spatial distribution of each component (sand and silt-clay) of the sediment load in the form of sediment concentration in parts per million (ppm) above background level. An example of transport and diffusion of the sediment cloud is shown in Figures 16 through 19, in which the horizontal distribution of the suspended sediment concentration of the silt-clay cloud is shown at the 120-ft depth (below the surface) for the quarter-point times of 900, 1,800, 2,700, and 3,600 sec. These concentration snapshots show the increase in size and corresponding decrease in concentration of the settling cloud as it is dispersed and diffused from the point of disposal.

35. Results of the concentration computation are used to produce a concentration-versus-distance relationship along the central axis of the grid at five discrete depths for four specified time periods (i.e., along the axis of symmetry at grid 14 of Figures 16 through 19). Quarter-point times were selected to show results at the 1/4, 1/2, 3/4, and termination times following the initial release of material from the barge. These plots were prepared for both the sand and silt-clay components of the disposed material. Figure 20 presents the concentration history plots for sand, whereas Figure 21 presents the plot corresponding to the silt-clay.

36. The results shown in Figures 20 and 21 represent time-concentration histories along the suspended sediment cloud axis. The four concentration profiles shown at the 120-ft level of Figure 21 correspond to the central axis of Figures 16 through 19. The five depths of 30, 60, 90, 120, and 150 ft were used to demonstrate the sediment distribution through the water column. For example, simulations of the disposal operation in depths of 180 ft indicate essentially no suspended sediment, sand or silt-clay, in the upper 60 ft of the water column 900 sec after the initial dump; i.e., the material has passed through that depth. Results demonstrate that the descent phase of the hemispherically shaped cloud passes through the water rapidly leaving little sediment in the upper water column. The examples presented in Figures 20 and 21 indicate that the maximum sand concentration is located near the bottom, whereas the point of maximum silt-clay concentration stabilizes at approximately middepth, and that a concentration decrease is seen both above and below this point. This relationship of maximum concentration at the 90-ft

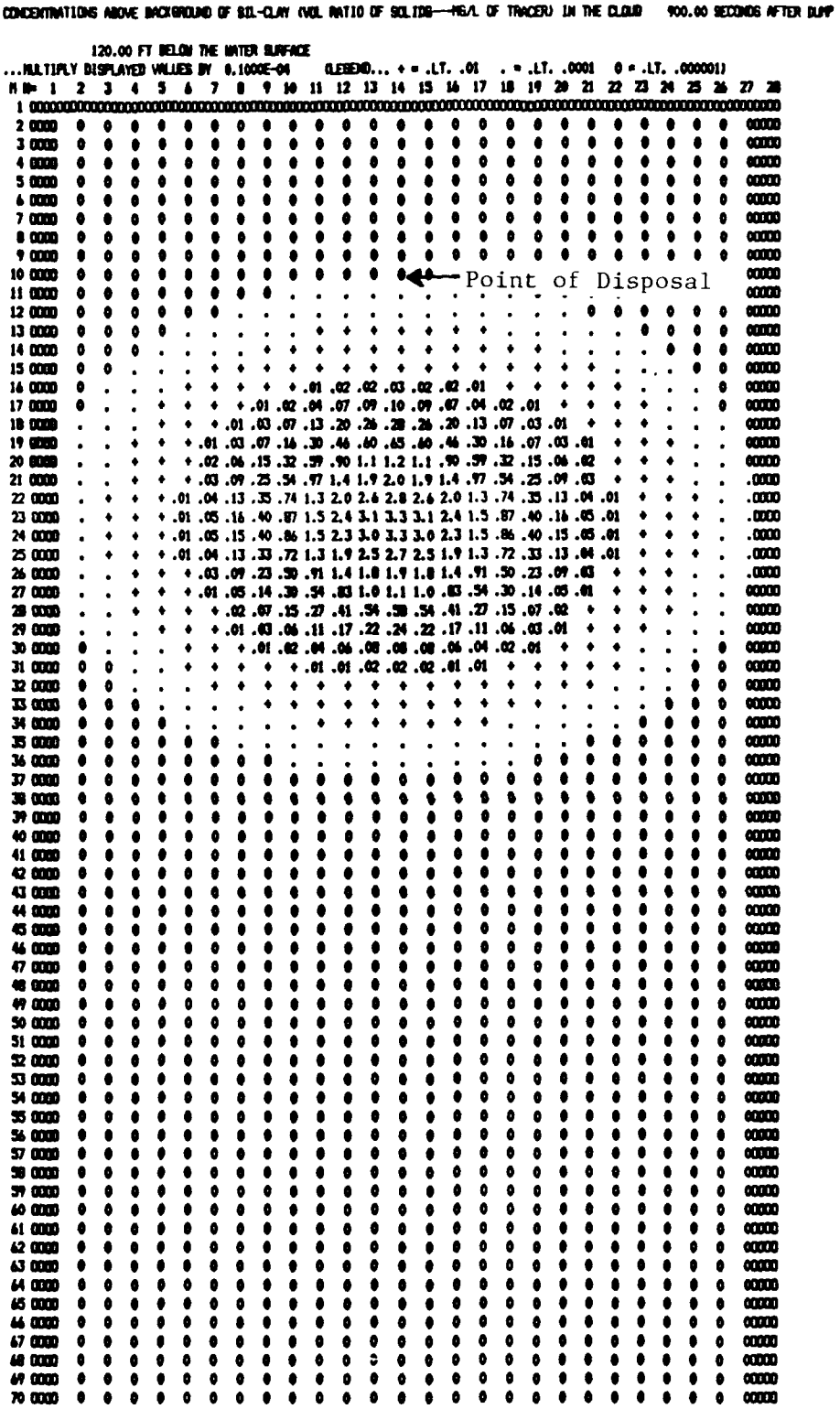

Figure 16. Suspended sediment cloud at 120 ft deep at 900 sec after disposal

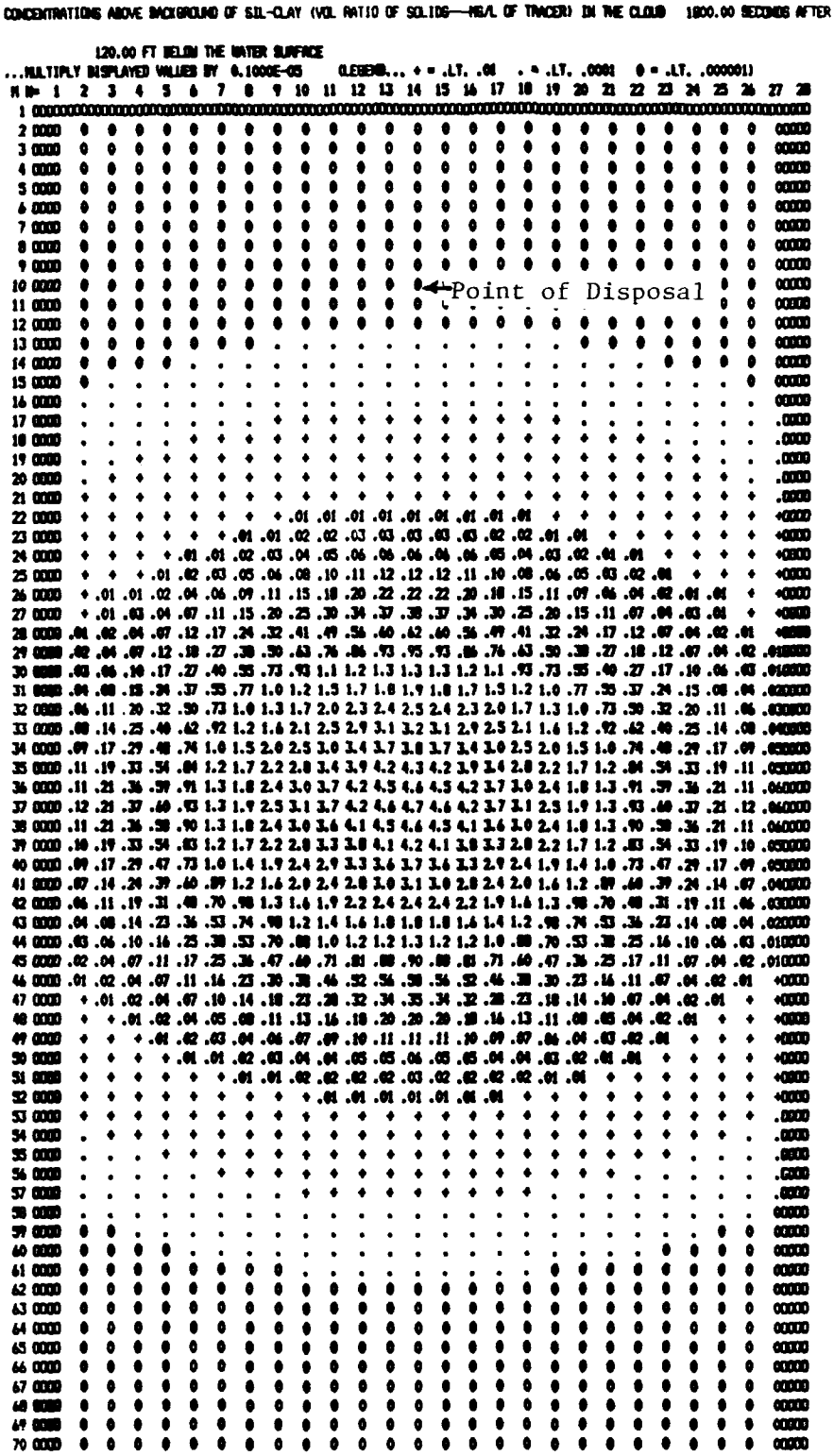

Figure 17. Suspended sediment cloud at 120 ft deep at 1,800 sec after disposal

CONCENTRATIONS ABOVE BACKGROUND OF SIL-CLAY (VOL RATIO OF SOLIDS—MG/L OF TRACER) IN THE CLOUD 2700.00 SECONDS AFTER DUMP

120.00 FT BELOW THE WATER SURFACE

...MULTIPLY DISPLAYED VALUES BY 0.1000E-05 LEGEND... + = .LT. .01 . = .LT. .0001 0 = .LT. .000001)

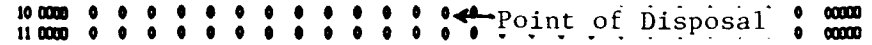

N I=	1	2	3	4	5	6	7	8	9	10	11	12	13	14	15	16	17	18	19	20	21	22	23	24	25	26	27	28
1	0	0	0	0	0	0	0	0	0	0	0	0	0	0	0	0	0	0	0	0	0	0	0	0	0	0	0	0
2	0	0	0	0	0	0	0	0	0	0	0	0	0	0	0	0	0	0	0	0	0	0	0	0	0	0	0	0
3	0	0	0	0	0	0	0	0	0	0	0	0	0	0	0	0	0	0	0	0	0	0	0	0	0	0	0	0
4	0	0	0	0	0	0	0	0	0	0	0	0	0	0	0	0	0	0	0	0	0	0	0	0	0	0	0	0
5	0	0	0	0	0	0	0	0	0	0	0	0	0	0	0	0	0	0	0	0	0	0	0	0	0	0	0	0
6	0	0	0	0	0	0	0	0	0	0	0	0	0	0	0	0	0	0	0	0	0	0	0	0	0	0	0	0
7	0	0	0	0	0	0	0	0	0	0	0	0	0	0	0	0	0	0	0	0	0	0	0	0	0	0	0	0
8	0	0	0	0	0	0	0	0	0	0	0	0	0	0	0	0	0	0	0	0	0	0	0	0	0	0	0	0
9	0	0	0	0	0	0	0	0	0	0	0	0	0	0	0	0	0	0	0	0	0	0	0	0	0	0	0	0
10	0	0	0	0	0	0	0	0	0	0	0	0	0	0	0	0	0	0	0	0	0	0	0	0	0	0	0	0
11	0	0	0	0	0	0	0	0	0	0	0	0	0	0	0	0	0	0	0	0	0	0	0	0	0	0	0	0
12	0	0	0	0	0	0	0	0	0	0	0	0	0	0	0	0	0	0	0	0	0	0	0	0	0	0	0	0
13	0	0	0	0	0	0	0	0	0	0	0	0	0	0	0	0	0	0	0	0	0	0	0	0	0	0	0	0
14	0	0	0	0	0	0	0	0	0	0	.	.	.	.	.	.	0	0	0	0	0	0	0	0	0	0	0	0
15	0	0	0	0	.	.	.	.	.	.	.	.	.	.	.	.	.	.	.	.	.	.	0	0	0	0	0	0
16	.	.	.	.	.	.	.	.	.	.	.	.	.	.	.	.	.	.	.	.	.	.	.	.	.	.	.	0
17	.	.	.	.	.	.	.	.	.	.	.	.	.	.	.	.	.	.	.	.	.	.	.	.	.	.	.	.
18	.	.	.	.	.	.	.	.	.	.	.	.	.	.	.	.	.	.	.	.	.	.	.	.	.	.	.	.
19	.	.	.	.	.	.	.	.	.	.	.	.	.	.	.	.	.	.	.	.	.	.	.	.	.	.	.	.
20	.	.	.	.	.	.	.	.	.	.	.	.	.	.	.	.	.	.	.	.	.	.	.	.	.	.	.	.
21	.	.	.	.	.	.	+	+	+	+	+	+	+	+	+	+	+	+	+	+	.	.	.	.	.	.	.	.
22	.	.	+	+	+	+	+	+	+	+	+	+	+	+	+	+	+	+	+	+	+	+	+	+	.	.	.	.
23	+	+	+	+	+	+	+	+	+	+	+	+	+	+	+	+	+	+	+	+	+	+	+	+	+	+	+	+
24	+	+	+	+	+	+	+	+	+	+	+	+	+	+	+	+	+	+	+	+	+	+	+	+	+	+	+	+
25	+	+	+	+	+	+	+	+	+	+	+	+	+	+	+	+	+	+	+	+	+	+	+	+	+	+	+	+
26	+	+	+	+	+	+	+	+	+	+	+	+	+	+	+	+	+	+	+	+	+	+	+	+	+	+	+	+
27	+	+	+	+	+	+	+	+	+	+	+	+	+	+	+	+	+	+	+	+	+	+	+	+	+	+	+	+
28	+	+	+	+	+	+	+	+	+	+	+	+	+	+	+	+	+	+	+	+	+	+	+	+	+	+	+	+
29	+	+	+	+	+	+	+	.01	.01	.01	.01	.01	.01	.01	.01	.01	.01	.01	.01	+	+	+	+	+	+	+	+	+
30	+	+	+	+	.01	.01	.01	.01	.01	.01	.02	.02	.02	.02	.02	.02	.01	.01	.01	.01	.01	.01	+	+	+	+	+	+
31	+	+	.01	.01	.01	.01	.02	.02	.02	.02	.03	.03	.03	.03	.03	.02	.02	.02	.02	.01	.01	.01	.01	+	+	+	+	+
32	.01	.01	.01	.02	.02	.02	.03	.03	.04	.04	.04	.04	.04	.04	.04	.04	.04	.03	.03	.02	.02	.02	.01	.01	.01	+	+	+
33	.01	.01	.02	.03	.03	.04	.04	.05	.06	.06	.07	.07	.07	.07	.07	.06	.06	.05	.04	.04	.03	.03	.02	.01	.01	.01	+	+
34	.02	.02	.03	.04	.05	.06	.07	.08	.08	.09	.10	.10	.10	.10	.10	.09	.08	.08	.07	.06	.05	.04	.03	.02	.02	.01	+	+
35	.03	.04	.05	.06	.07	.08	.10	.11	.12	.13	.14	.14	.14	.14	.14	.13	.12	.11	.10	.08	.07	.06	.05	.04	.03	.02	+	+
36	.04	.05	.06	.08	.10	.12	.14	.15	.17	.18	.19	.20	.20	.20	.19	.18	.17	.15	.14	.12	.10	.08	.06	.05	.04	.03	+	+
37	.05	.07	.09	.11	.14	.16	.18	.21	.23	.25	.26	.27	.28	.27	.26	.25	.23	.21	.18	.16	.14	.11	.09	.07	.05	.04	+	+
38	.07	.09	.12	.15	.18	.21	.25	.28	.31	.33	.35	.36	.37	.36	.35	.33	.31	.28	.25	.21	.18	.15	.12	.09	.07	.05	+	+
39	.10	.12	.16	.19	.24	.28	.32	.36	.40	.43	.46	.47	.48	.47	.46	.43	.40	.36	.32	.28	.24	.19	.16	.12	.10	.07	+	+
40	.12	.16	.20	.25	.30	.35	.41	.46	.51	.55	.58	.60	.61	.60	.58	.55	.51	.46	.41	.35	.30	.25	.20	.16	.12	.09	+	+
41	.15	.20	.25	.31	.37	.44	.51	.57	.63	.68	.72	.74	.75	.74	.72	.68	.63	.57	.51	.44	.37	.31	.25	.20	.15	.12	+	+
42	.19	.24	.31	.38	.45	.53	.62	.70	.77	.83	.88	.90	.91	.90	.88	.83	.77	.70	.62	.53	.45	.38	.31	.24	.19	.14	+	+
43	.22	.29	.36	.45	.54	.64	.73	.83	.91	.99	1.0	1.0	1.0	1.0	1.0	.99	.91	.83	.73	.64	.54	.45	.36	.29	.22	.17	+	+
44	.26	.34	.42	.52	.63	.74	.85	.96	1.0	1.1	1.2	1.2	1.2	1.2	1.2	1.1	1.0	.96	.85	.74	.63	.52	.42	.34	.26	.20	+	+
45	.30	.38	.48	.59	.72	.84	.97	1.1	1.2	1.3	1.3	1.4	1.4	1.4	1.3	1.3	1.2	1.1	.97	.84	.72	.59	.48	.38	.30	.23	+	+
46	.33	.43	.54	.66	.80	.94	1.0	1.2	1.3	1.4	1.5	1.5	1.6	1.5	1.5	1.4	1.3	1.2	1.0	.94	.80	.66	.54	.43	.33	.25	+	+
47	.36	.47	.59	.72	.87	1.0	1.1	1.3	1.4	1.5	1.6	1.7	1.7	1.7	1.6	1.5	1.4	1.3	1.1	1.0	.87	.72	.59	.47	.36	.27	+	+
48	.39	.50	.62	.77	.93	1.0	1.2	1.4	1.5	1.6	1.7	1.8	1.8	1.8	1.7	1.6	1.5	1.4	1.2	1.0	.93	.77	.62	.50	.39	.29	+	+
49	.40	.52	.65	.80	.97	1.1	1.3	1.4	1.6	1.7	1.8	1.9	1.9	1.9	1.8	1.7	1.6	1.4	1.3	1.1	.97	.80	.65	.52	.40	.31	+	+
50	.41	.53	.66	.82	.99	1.1	1.3	1.5	1.6	1.7	1.8	1.9	1.9	1.9	1.8	1.7	1.6	1.5	1.3	1.1	.99	.82	.66	.53	.41	.31	+	+
51	.41	.53	.66	.82	.98	1.1	1.3	1.5	1.6	1.7	1.8	1.9	1.9	1.9	1.8	1.7	1.6	1.5	1.3	1.1	.98	.82	.66	.53	.41	.31	+	+
52	.40	.52	.65	.80	.96	1.1	1.3	1.4	1.6	1.7	1.8	1.9	1.9	1.9	1.8	1.7	1.6	1.4	1.3	1.1	.96	.80	.65	.52	.40	.30	+	+
53	.38	.49	.62	.76	.92	1.0	1.2	1.4	1.5	1.6	1.7	1.8	1.8	1.8	1.7	1.6	1.5	1.4	1.2	1.0	.92	.76	.62	.49	.38	.29	+	+
54	.36	.46	.58	.71	.86	1.0	1.1	1.3	1.4	1.5	1.6	1.7	1.7	1.7	1.6	1.5	1.4	1.3	1.1	1.0	.86	.71	.58	.46	.36	.27	+	+
55	.33	.42	.53	.65	.79	.93	1.0	1.2	1.3	1.4	1.5	1.5	1.5	1.5	1.5	1.4	1.3	1.2	1.0	.93	.79	.65	.53	.42	.33	.25	+	+
56	.29	.38	.47	.58	.70	.83	.95	1.0	1.1	1.2	1.3	1.4	1.4	1.4	1.3	1.2	1.1	1.0	.95	.83	.70	.58	.47	.38	.29	.22	+	+
57	.26	.33	.41	.51	.62	.73	.84	.94	1.0	1.1	1.1	1.2	1.2	1.2	1.1	1.1	1.0	.94	.84	.73	.62	.51	.41	.33	.26	.19	+	+
58	.22	.28	.36	.44	.53	.62	.72	.81	.89	.96	1.0	1.0	1.0	1.0	1.0	.96	.89	.81	.72	.62	.53	.44	.36	.28	.22	.17	+	+
59	.18	.24	.30	.37	.44	.52	.60	.68	.75	.81	.85	.88	.89	.88	.85	.81	.75	.68	.60	.52	.44	.37	.30	.24	.18	.14	+	+
60	.15	.19	.24	.30	.36	.43	.49	.56	.61	.66	.70	.72	.73	.72	.70	.66	.61	.56	.49	.43	.36	.30	.24	.19	.15	.11	+	+
61	.12	.15	.19	.24	.29	.34	.39	.45	.49	.53	.56	.58	.59	.58	.56	.53	.49	.45	.39	.34	.29	.24	.19	.15	.12	.09	+	+
62	.09	.12	.15	.19	.23	.27	.31	.35	.39	.42	.44	.45	.46	.45	.44	.42	.39	.35	.31	.27	.23	.19	.15	.12	.09	.07	+	+
63	.07	.09	.12	.14	.17	.20	.24	.27	.30	.32	.34	.35	.35	.35	.34	.32	.30	.27	.24	.20	.17	.14	.12	.09	.07	.05	+	+
64	.05	.07	.09	.11	.13	.15	.18	.20	.22	.24	.25	.26	.26	.26	.25	.24	.22	.20	.18	.15	.13	.11	.09	.07	.05	.04	+	+
65	.04	.05	.06	.08	.09	.11	.13	.15	.16	.17	.18	.19	.19	.19	.18	.17	.16	.15	.13	.11	.09	.08	.06	.05	.04	.03	+	+
66	.02	.03	.04	.05	.07	.08	.09	.10	.12	.12	.13	.14	.14	.14	.13	.12	.12	.10	.09	.08	.07	.05	.04	.03	.02	.02	+	+
67	.02	.02	.03	.04	.05	.05	.06	.07	.08	.09	.09	.09	.10	.09	.09	.09	.08	.07	.06	.05	.05	.04	.03	.02	.02	.01	+	+
68	.01	.01	.02	.02	.03	.04	.04	.05	.05	.06	.06	.06	.06	.06	.06	.06	.05	.05	.04	.04	.03	.02	.02	.01	.01	.01	+	+
69	+	.01	.01	.01	.02	.02	.03	.03	.03	.04	.04	.04	.04	.04	.04	.04	.03	.03	.03	.02	.02	.01	.01	.01	+	+	+	+
70	+	+	.01	.01	.01	.01	.02	.02	.02	.02	.02	.03	.03	.03	.02	.02	.02	.02	.02	.01	.01	.01	.01	+	+	+	+	+

Figure 18. Suspended sediment cloud at 120 ft deep at 2,700 sec after disposal

CONCENTRATIONS ABOVE BACKGROUND OF SIL-CLAY (VOL RATIO OF SOLIDS—MG/L OF TRACER) IN THE CLOUD 3600.00 SECONDS AFTER DUMP

120.00 FT BELOW THE WATER SURFACE

...MULTIPLY DISPLAYED VALUES BY 0.1000E-05 LEGEND... + = .LT. .01 . = .LT. .0001 0 = .LT. .000001)

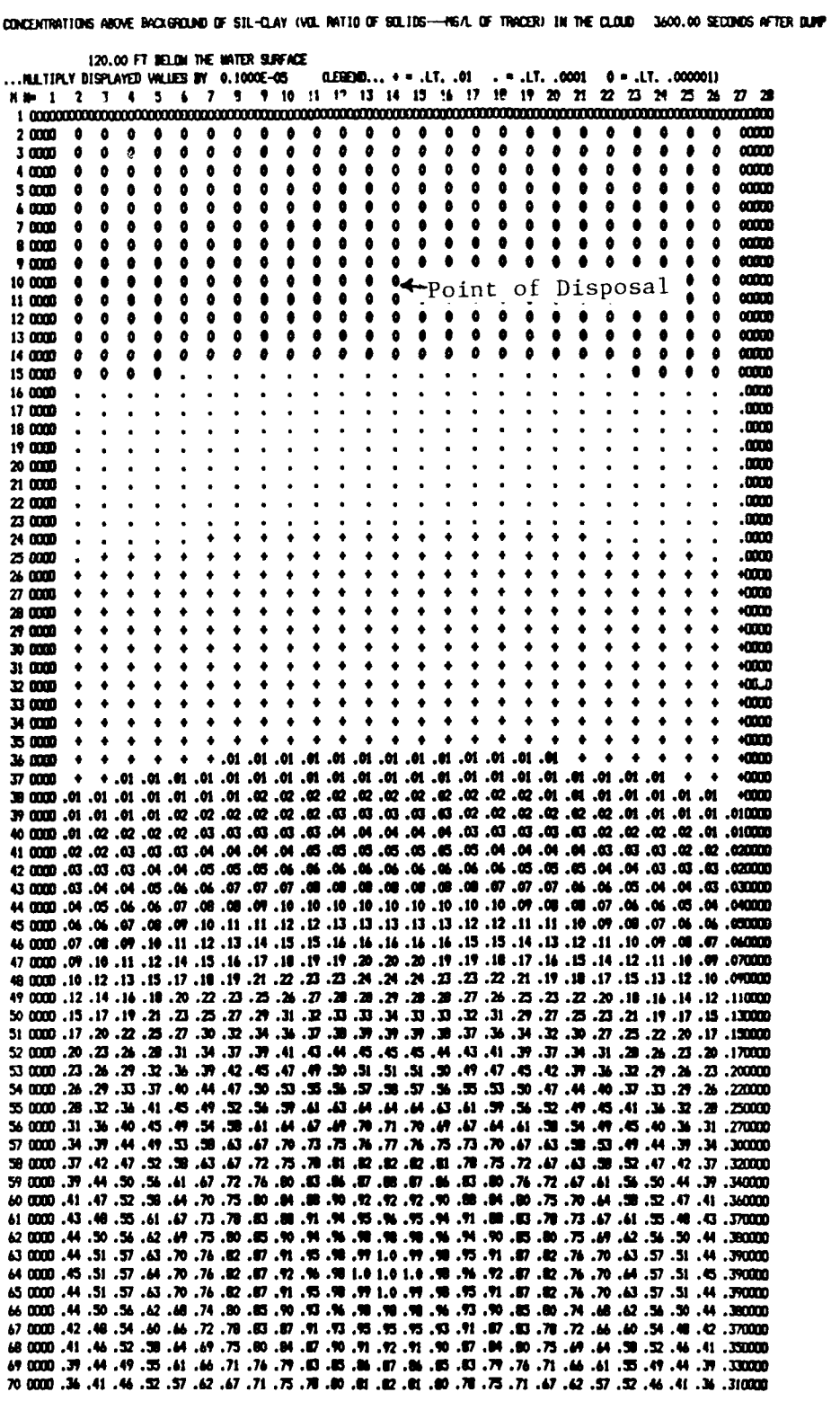

Figure 19. Suspended sediment cloud at 120 ft deep at 3,600 sec after disposal

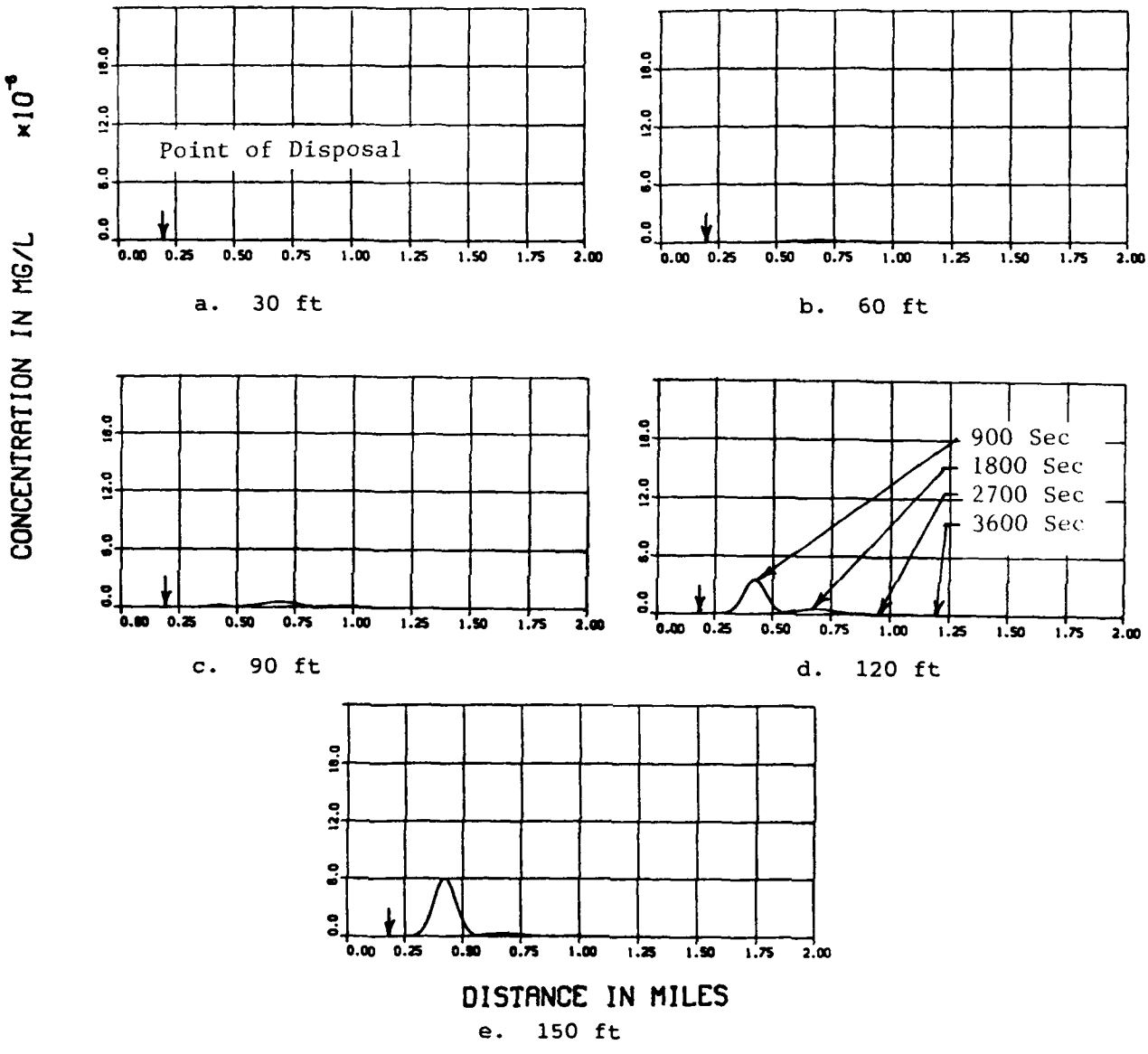

Figure 20. Sand concentration evolution relationships for fine-grained site

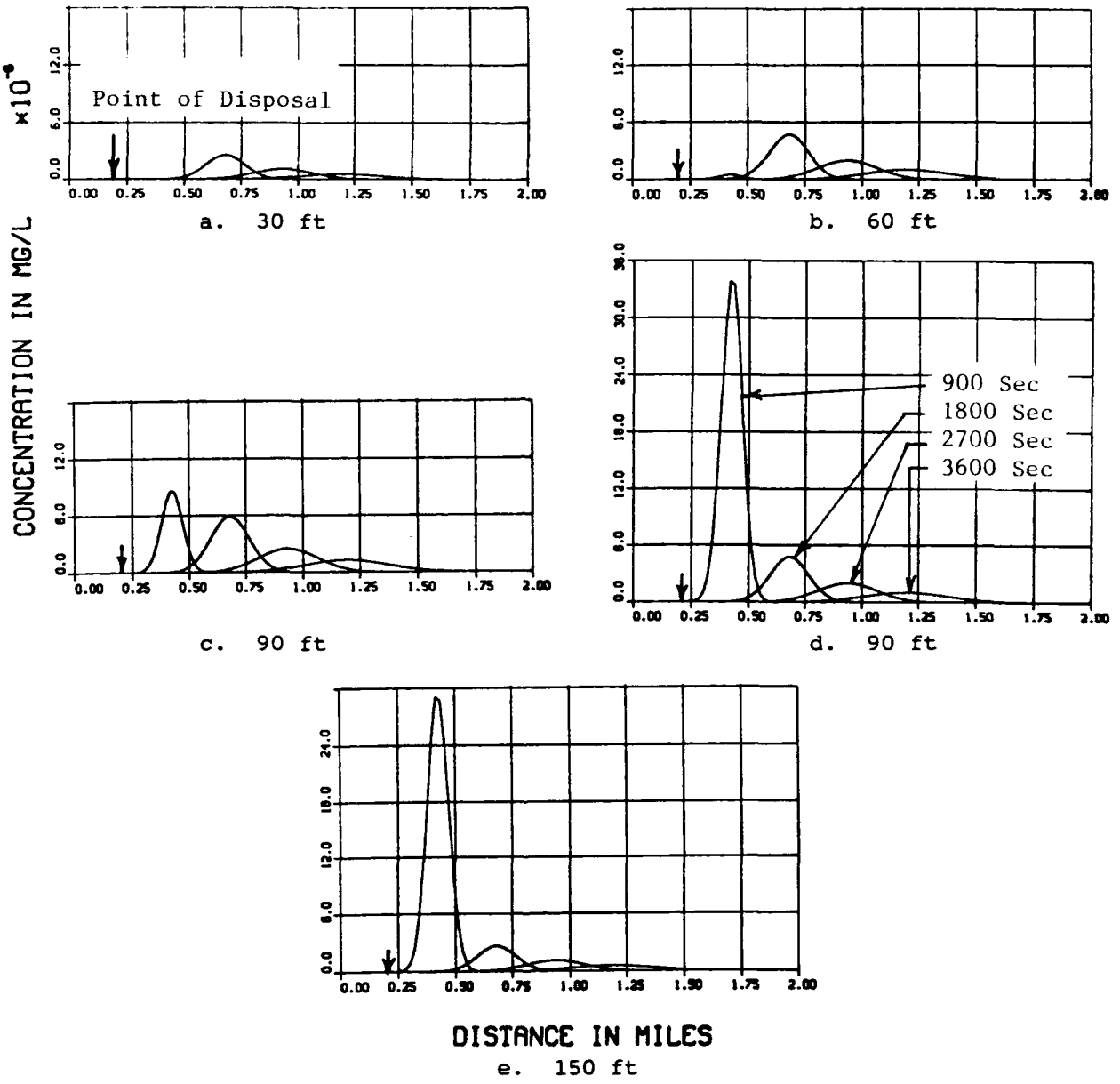

Figure 21. Silt-clay concentration evolution relationships for fine-grained site

depth is maintained for the second, third, and fourth quarter point as the cloud disperses. All results indicate a decreasing concentration in both time after disposal and distance from the release point. A summary of the sand and silt-clay concentration simulations are shown in Tables 10 and 11. In both Figures 20 and 21, the point of disposal is at grid cell 10 of Figures 16-19, corresponding to the 0.19-mile point of Figures 20 and 21.

Table 10

Summary of Computed Maximum Suspended Sand Concentration

(Concentration in mg/ℓ above ambient)

Depth	Time, sec/Approximate Distance from Disposal, Miles			
ft	900/0.25	1,800/0.51	2,700/0.76	3,600/1.02
30	4.0×10^{-13}	6.4×10^{-8}	6.3×10^{-8}	2.3×10^{-8}
60	9.0×10^{-10}	2.5×10^{-7}	1.1×10^{-7}	4.3×10^{-8}
90	1.8×10^{-7}	5.3×10^{-7}	1.4×10^{-7}	5.3×10^{-8}
120	3.5×10^{-6}	5.6×10^{-7}	1.1×10^{-7}	4.3×10^{-8}
150	6.0×10^{-6}	3.1×10^{-7}	6.4×10^{-8}	2.3×10^{-8}

Table 11

Summary of Computed Maximum Suspended Silt-Clay Concentration

(Concentration in mg/ℓ above ambient)

Depth	Time, sec/Approximate Distance from Disposal, Miles			
ft	900/0.25	1,800/0.51	2,700/0.76	3,600/1.02
30	5.7×10^{-9}	2.5×10^{-6}	1.0×10^{-6}	5.4×10^{-7}
60	4.7×10^{-7}	4.7×10^{-6}	1.9×10^{-6}	1.0×10^{-6}
90	8.6×10^{-6}	5.8×10^{-6}	2.4×10^{-6}	1.2×10^{-6}
120	3.3×10^{-5}	4.7×10^{-6}	1.9×10^{-6}	1.0×10^{-6}
150	2.9×10^{-5}	2.6×10^{-6}	1.0×10^{-6}	5.5×10^{-7}

A plot of the total sediment deposition versus distance along the axis of the disposal grid is shown in Figure 22. A three-dimensional view of the resulting disposal pattern is shown in Figure 23 with the corresponding contour plot shown in Figure 24.

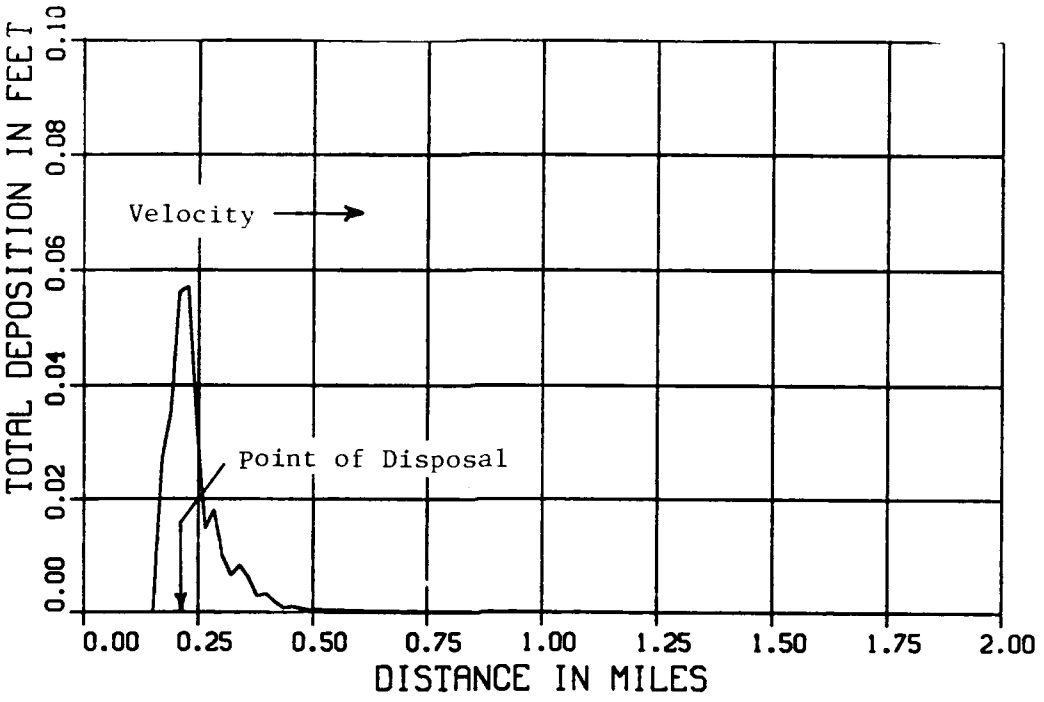

Figure 22. Total deposition pattern for fine-grained site

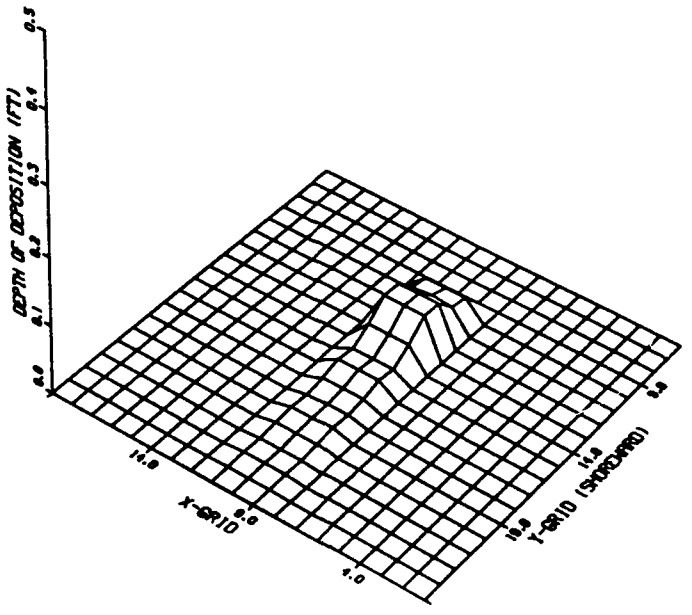

Figure 23. Three-dimensional view of fine-grained site deposition pattern

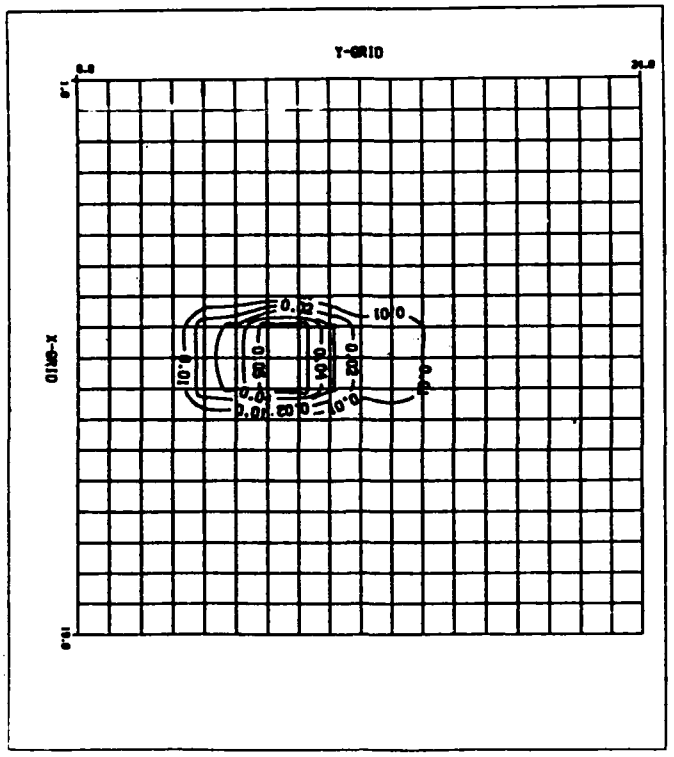

Figure 24. Contour plot of fine-grained site deposition pattern

Coarse-Grained Disposal Site Analysis

37. The single-load deposition simulation for the coarse-grained material was performed using the coefficients shown in Tables 6 and 8. Results of the simulations showed that the material descended rapidly to the ocean floor, leaving no material in suspension within the water column. Therefore, time-concentration plots comparable to Figures 20 and 21 for the fine-grained material are not available. Model results are necessarily limited to total material deposition patterns. These results are shown in the cross-sectional plot of Figure 25, the three-dimensional view of the mound of Figure 26, and the computed contour map of the site shown in Figure 27. As shown in the figures, the maximum thickness of deposition is approximately 0.23 ft, covering an approximate 400- to 500-ft-diam area. Deposition is confined to this immediate area.

38. Both DIFID analyses were based on an assumed depth-averaged velocity of 45.7 cm/sec. As shown in the prototype data analysis, this velocity represents a much higher-than-average condition. As such, the results

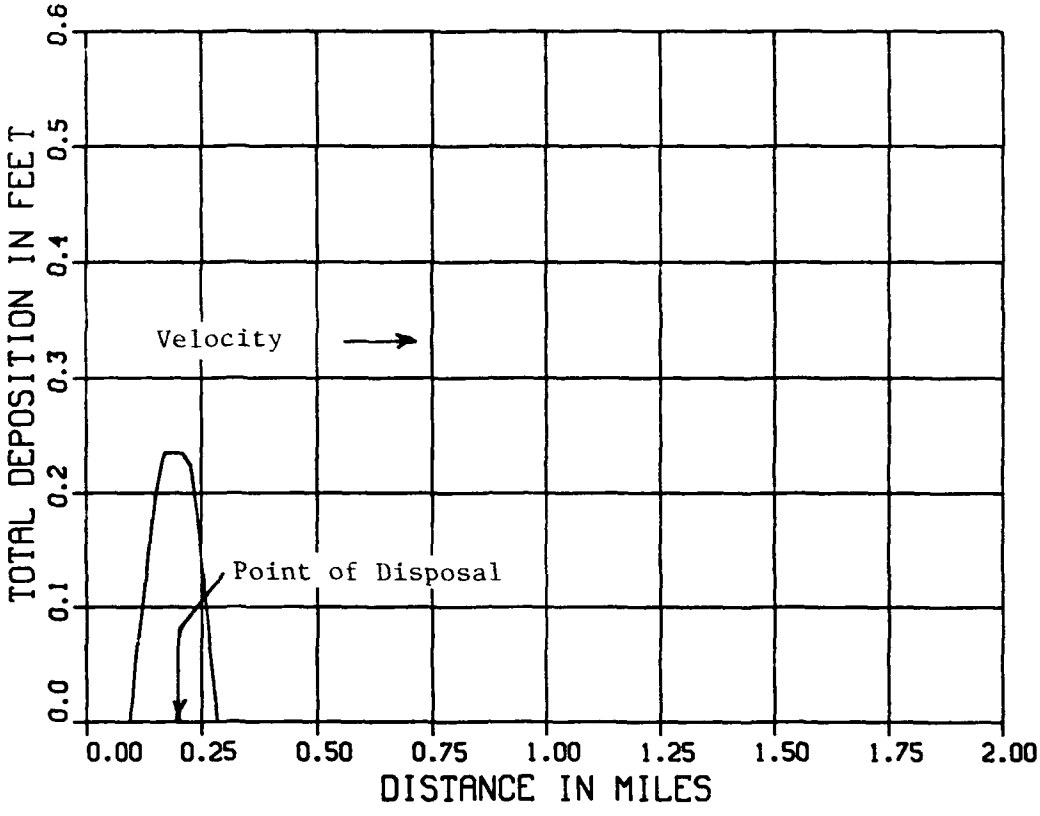

Figure 25. Total deposition pattern for coarse-grained site

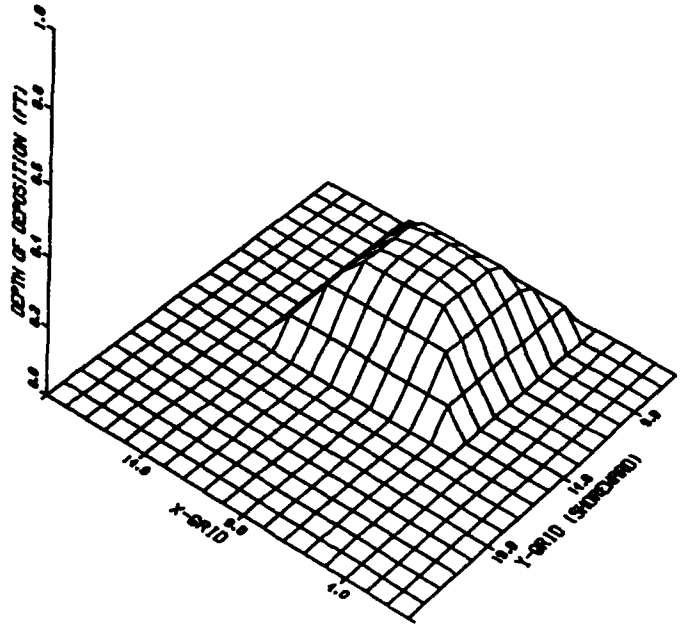

Figure 26. Three-dimensional, coarse-grained site deposition pattern

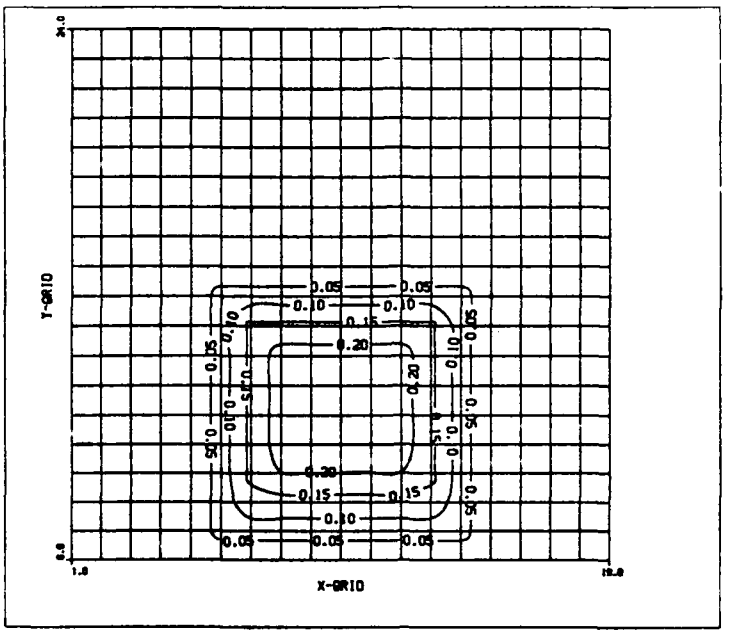

Figure 27. Contour plot of coarse-grained site deposition pattern

presented for the short-term simulation can be considered as conservative with respect to the dispersion of the suspended sediments. An analysis of the short-term analysis results will be presented following the long-term simulations described in Part IV.

PART IV: LONG-TERM MODELING

General

39. The long-term simulation phase of the site designation study investigates the behavior of a dredged material mound over time. This analysis is accomplished by developing a means of classifying disposal sites as either dispersive or nondispersive based on whether local wave and velocity fields are adequate to erode and transport significant amounts of material from the site. The local currents can be due to normal tidal action and mean flow circulation patterns or storm-related activity. Sediment transport calculations use these waves and currents to estimate mound stability as a function of the local bathymetry and sediment characteristics at both the fine- and coarse-grained sites.

40. This final phase of the site evaluation represents an extension of the short-term fate analysis of Part III in which site dispersiveness was based on the ability to effectively place material within a designated site during the disposal operation. The long-term analysis begins with the assumption that the short-term disposal operation is successful in creating a stable mound configuration. Whether the mound is dispersive or nondispersive depends on whether the local wave and current conditions are capable of resuspending and transporting significant amounts of material from the mound so that areas adjacent to the disposal site are impacted.

41. The long-term site stability analysis approach adopted for this study uses the simulated wave and current time series described in Part II to provide a quantitative estimate of the stability of the mound as a function of localized environmental conditions. The analysis approach is based on coupled hydrodynamic and sediment transport models that compute the transport of noncohesive sediment as a function of the local velocity and depth. The resulting distribution of transport is used in a sediment continuity model to compute changes in the bathymetry of the sediment mound. Bathymetry change computations are made at every 3-hr time-step. The long-term simulations of mound stability indicate whether the local wave and current regime at the disposal site are of sufficient magnitude to suspend and transport bottom sediments.

Input Data Requirement

42. The site stability methodology is dependent on the accurate prediction of sediment transport at the site under investigation. Empirical relationships for computing sediment transport as a primary function of depth-averaged water velocity, local depth, and sediment grain size were reported by Ackers and White (1973). These relationships were subsequently modified (Swart 1976) to reflect an increase in sediment transport rate when the ambient currents are accompanied by surface wave fields. This additional transport reflects the fact that wave-induced orbital velocities are capable of suspending bottom sediments, independent of the sediment put in suspension by mean currents. The total amount of sediment put into suspension by waves and currents is then transported by the ambient current field.

43. The modified Ackers-White relationships are used to compute the transport of uniformly graded noncohesive sediment in the grain diameter (D_{50} for example) range of 0.04 to 4.00 mm (White 1972). The average of the tabulated D_{50} values from the gradation curves for the coarse-grained site was computed to be 0.277 mm, with a maximum value of 0.48 mm and a minimum of 0.18 mm. Computed sediment transport versus depth-averaged velocity for a range of depths corresponding to those at the coarse-grained site are shown in Figure 28. The Phase III WIS Station 69 summary value mean wave height of 2.7 m and wave period of 10.9 sec (Jensen, Hubertz, and Payne 1989) were specified in the preparation of this family of curves.

44. Analysis of the gradation curves for the fine-grained site indicates an average D_{50} value to be 0.0384 mm, with a maximum of 0.080 mm and a minimum of 0.009 mm. Since the sediments contain approximately 25-percent noncohesive sand, the noncohesive formulation is appropriate for simulating the overall sediment transport rate (Kamphuis 1990); however, this computed grain size is slightly below the range for which the Ackers-White formulas should be applied. For example, the computed transport/velocity relationships for a 0.0384-mm sediment are shown in Figure 29. The curves predict the sediment transport magnitude to become infinitely high as the velocity approaches 2.0 ft/sec. Although the data reported in Part I do not attain this value, the inappropriateness of the theory can clearly be seen in the unrealistically high computed transport values at the higher velocities. A D_{50} value of 0.0625 was therefore selected to more realistically represent the fine-grained

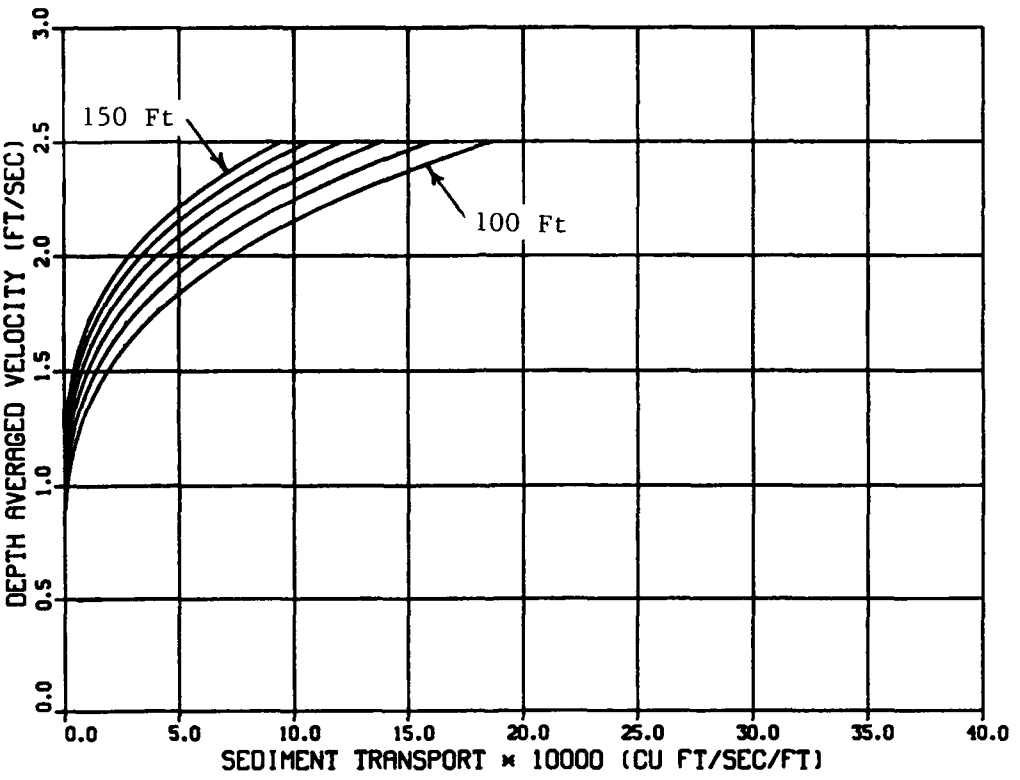

Figure 28. Sediment transport-velocity relationships for D_{50} = 0.277 mm

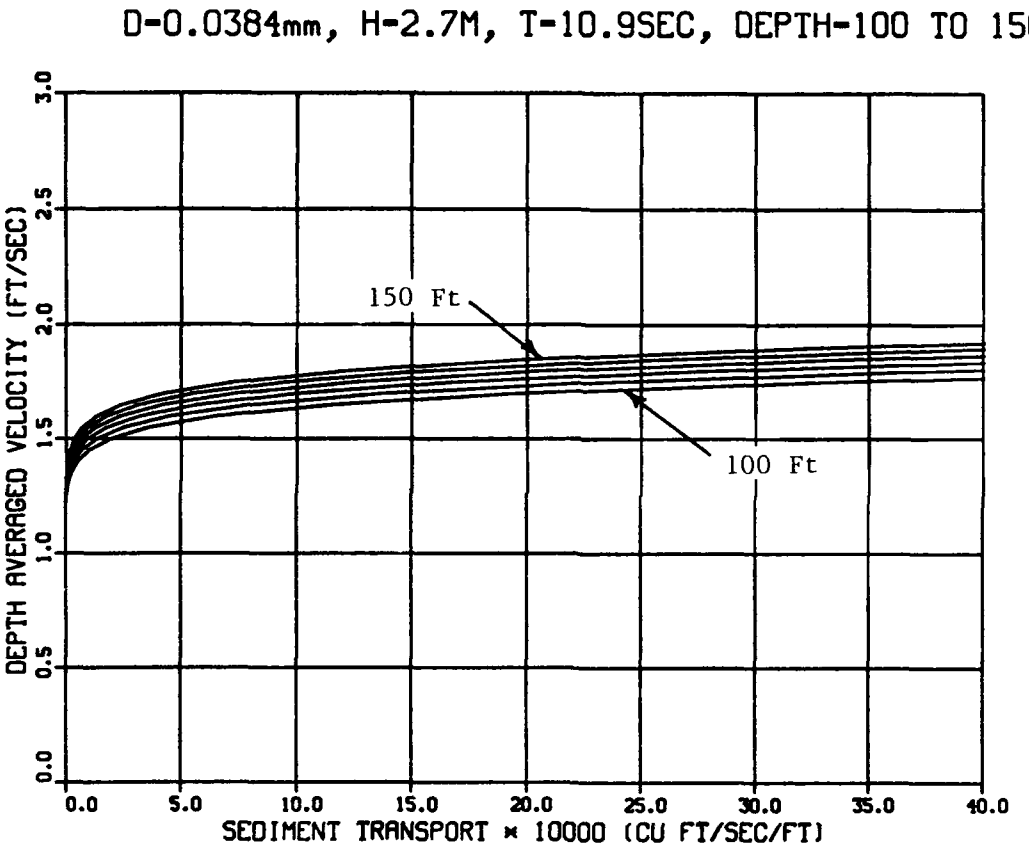

Figure 29. Sediment transport-velocity relationships for D_{50} = 0.0384 mm

site for a usable range of velocities, to include 2.0 ft/sec. The transport-velocity relationship for a 0.0625-mm sediment is shown in Figure 30.

45. The threshold velocities necessary for the initiation of sediment erosion is nearly identical in Figures 29 and 30. Since the two curves are very similar within the velocity range of interest and the specification of the 0.0625-mm sediment avoids the possibility or unrealistically large transport predictions, the use of the larger grain size to better accommodate the empirical relationship is justified. Therefore, the 0.0625-mm sediment is used for all long-term simulations pertaining to the fine-grained site.

46. The final input data requirement is that of specifying the geometric configuration of the sediment mound. The proposed fall 1990 dredging operation would dispose of 415,000 cu yd of sand in Cell E5 of Quadrant 2 (Figure 1). This approximate volume of material was selected as the target volume for the test mound. An approximate mound height was determined from the bathymetric surveys of the SF-3 disposal area denoted in Figure 1. A

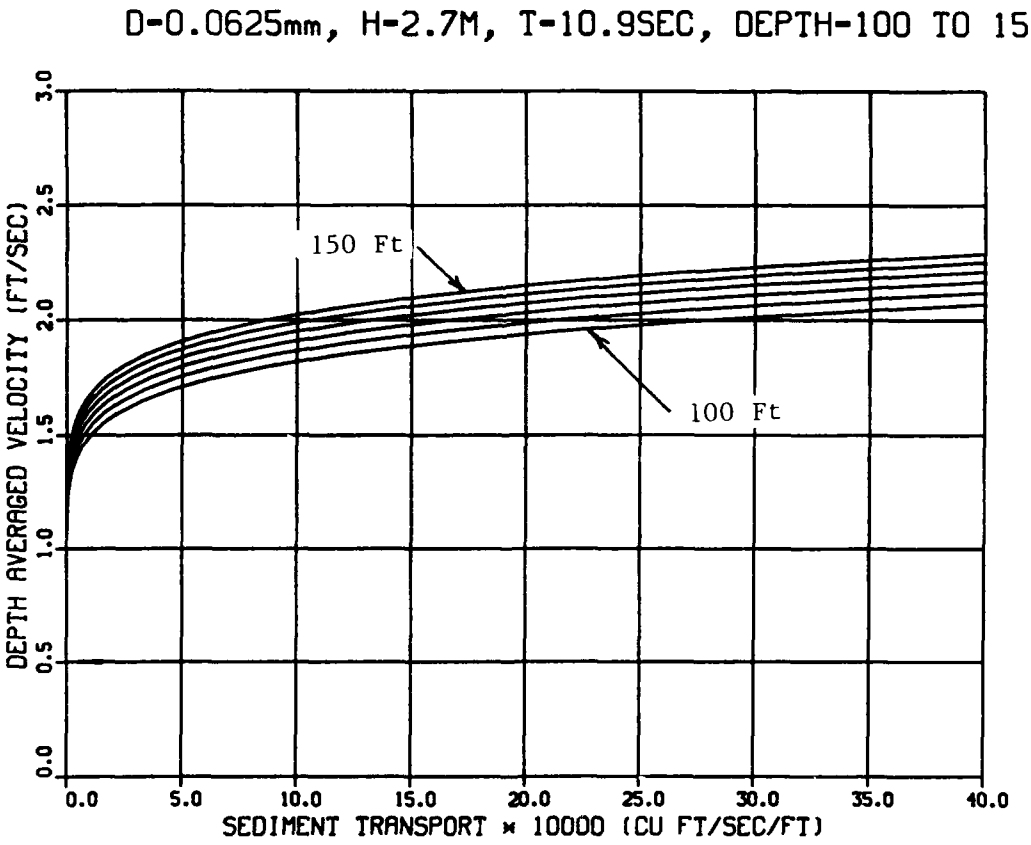

Figure 30. Sediment transport-velocity relationships for D_{50} = 0.0625 mm

predisposal survey of the site was collected in September 1984 with subsequent surveys in June 1985, May 1987, and April 1988. These data indicate well-defined disposal features covering areas of 1,000 to 1,500 ft in diameter. The features contain multiple mounds with an average total height above the undisturbed bottom of 15 to 20 ft. A truncated pyramid with a height of 16 ft, 1,100-ft square base, and side slopes of 1:25 was selected as the test mound configuration for the long-term modeling effort. The computed volume of the mound is 409,000 cu yd, approximately that of the proposed fall 1990 disposal operation. A three-dimensional perspective view and contour map of the test mound are shown in Figures 31 and 32.

Long-Term Model Simulations

47. The long-term analysis described in the following section uses wave and velocity time series to compute the time evolution of the shape of the mound. A quantitative assessment of mound stability is made by computing the location of the centroid of the mound along the central mound axis for each computational time-step of the simulation. These computations are made by balancing the summation of moments at each computational grid. Simulation results are also presented in the form of postsimulation perspective and contour plots as well as time evolution plots of the changing cross-sectional profile along the axis of the mound.

48. The stability analysis is made by estimating mound response to long periods of exposure to the simulated WIS wave field and synthesized tidal series developed in Part II. In addition to this normal condition simulation, a storm-event analysis was performed in an attempt to investigate single-event-related erosion of the test mound. The filtered velocity data were examined to determine a typical duration of high-intensity storm activity. The result was the selection of an 8-day event, a period which approximates that shown in days 10-18 of Period 2 or days 226-234 of Period 4. A simulated V component constituent of the velocity field with this period and an amplitude of 60 cm/sec was combined with the computed astronomical constituents shown in Table 4. The resulting 8-day time series is shown in Figure 33.

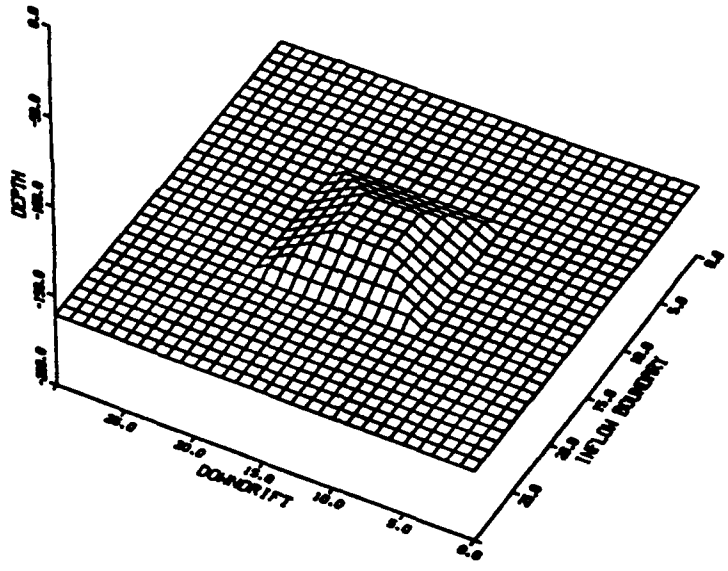

Figure 31. Idealized disposal mound perspective view

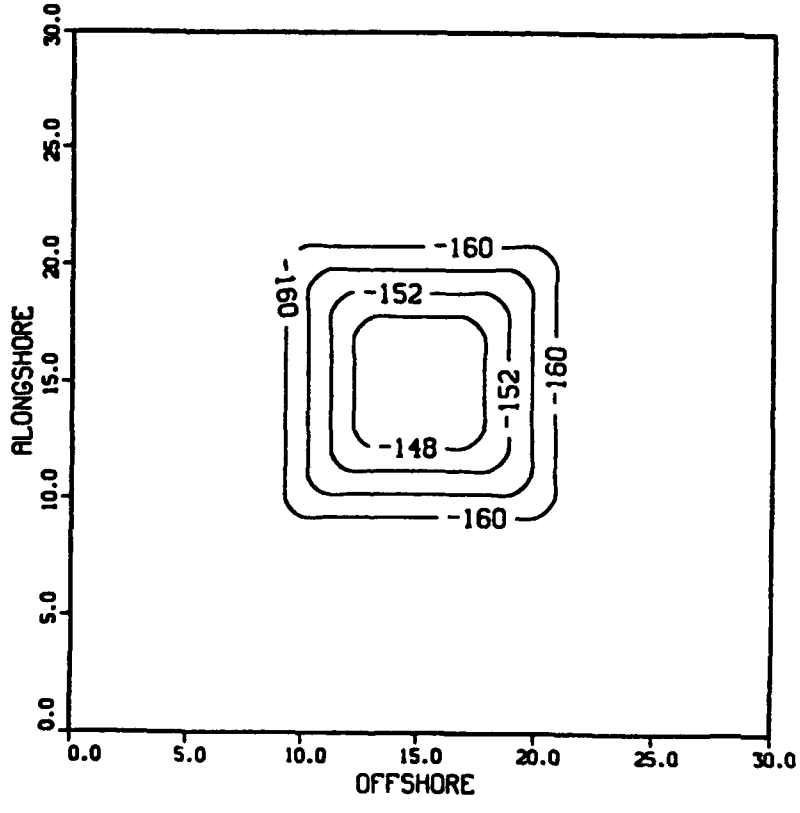

Figure 32. Idealized disposal mound contour map

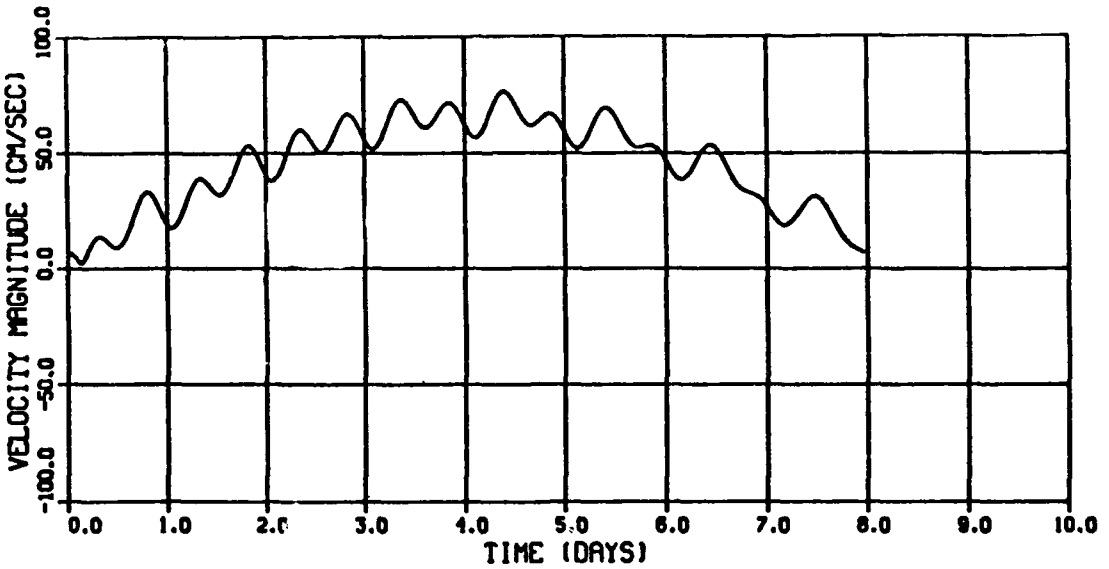

a. Velocity magnitude

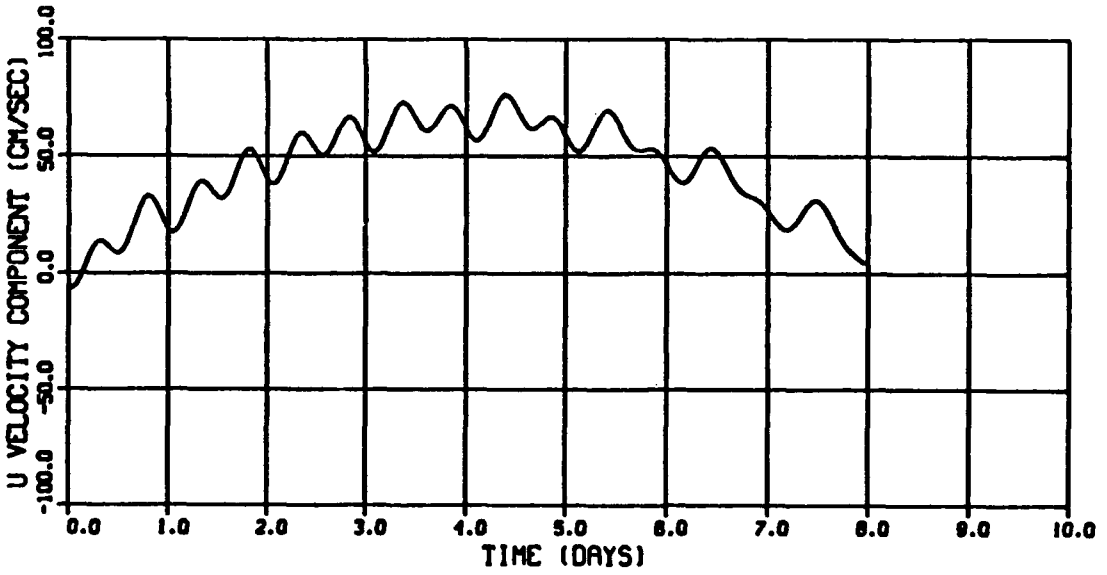

b. Velocity component

Figure 33. Simulated storm surge time series (Continued)

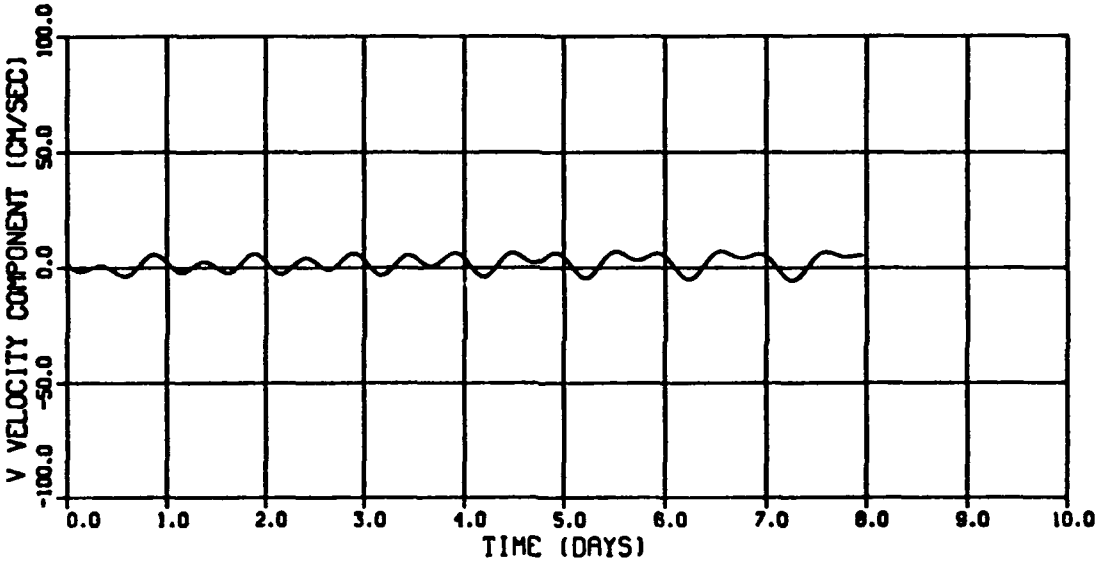

c. Velocity component

Figure 33. (Concluded)

Fine-Grained Disposal Site Analysis

49. The long-term boundary conditions of Part II were subjected to the test mound configuration described previously. The mean depth of flow was specified as 55 m, and the mound was assumed to consist of noncohesive sediment with an effective diameter of 0.0625 mm. Results of the simulations indicate that sediment movement is initiated only during periods of spring tide and/or during storm events when the depth-averaged velocities may exceed approximately 1.5 ft/sec. Since the velocities are generally below this value and only reach peak values of approximately 1.6 ft/sec, the computations showed very little net movement of the mound centroid. In fact, due to the slow and predictable migration rate, simulations were limited to 96 days during which time two full cycles of the 48-day, low-frequency current are experienced at the mound. Computed net movement of the mound during the entire simulation was only 0.31 ft. In view of the repetitive nature of velocity field shown in Figure 14 and the fact that the imposed wave field corresponds to the high-energy winter period beginning 1 January of the simulated year, longer simulations were not necessary. Plots of the postsimulation contour map of the mound and the computed cross-sectional evolution of the mound axis are shown in Figures 34 and 35. As shown, no perceptible net change in mound configuration is shown, although sediment movement is indicated during peak current events.

50. The simulation of the 8-day high intensity event for the fine-grained mound resulted in a 32.3-ft movement of the centroid, with slight erosion indicated in front of the mound and deposition on the leeward crest and face. The contour map and cross-sectional profile migration plots are shown in Figures 36 and 37. These results indicate that definite movement of the mound occurs during extreme events; however, the velocities necessary for this movement are not common. For example, peak velocity magnitudes shown in Figure 33 are not shown in the middepth prototype data for Periods 2 and 3. The simulated storm, therefore, represents a severe event; however, the computed erosion is not severe.

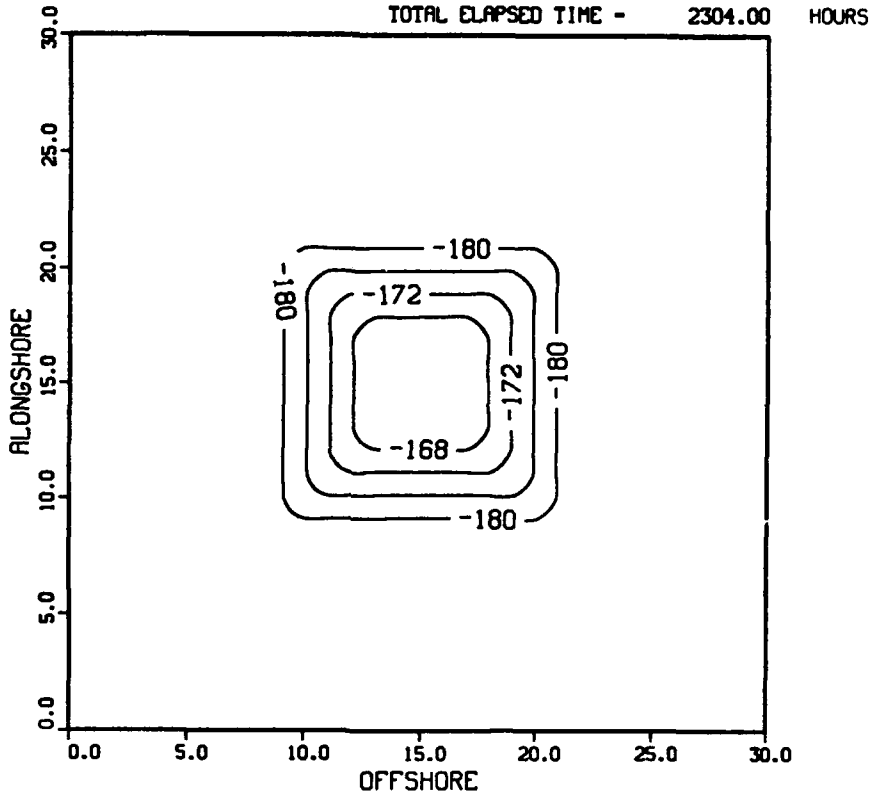

Figure 34. Long-term simulation contour of fine-grained site

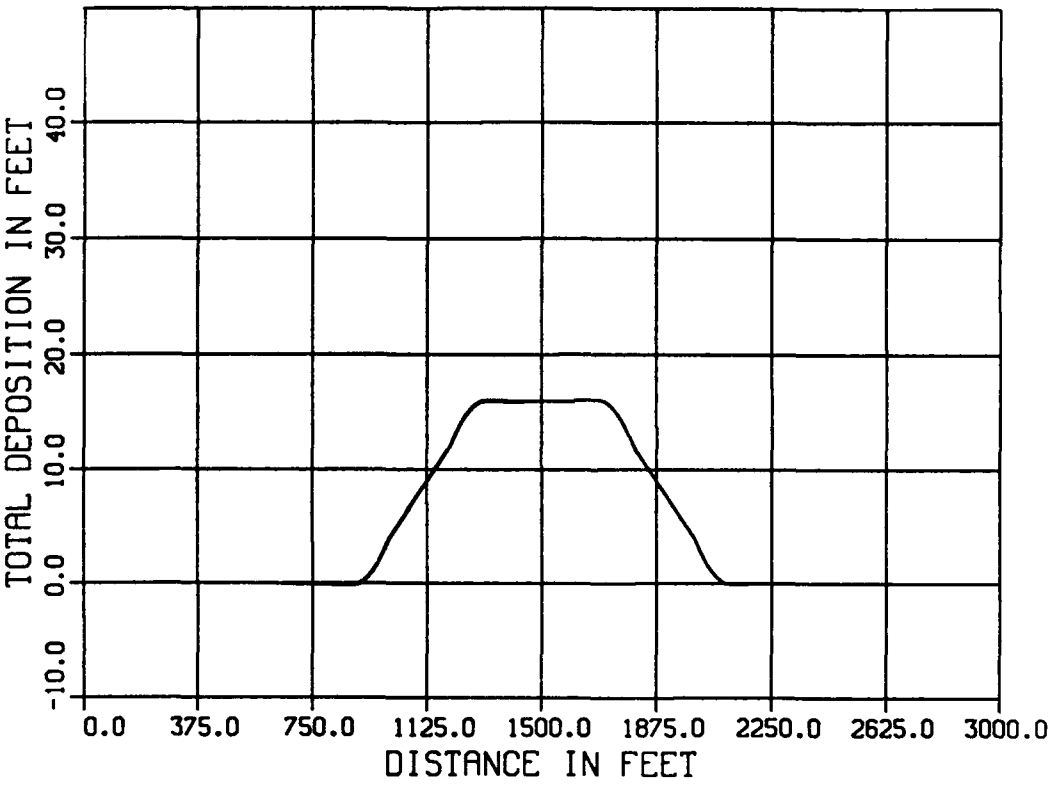

Figure 35. Long-term simulation mound axis migration history for fine-grained site

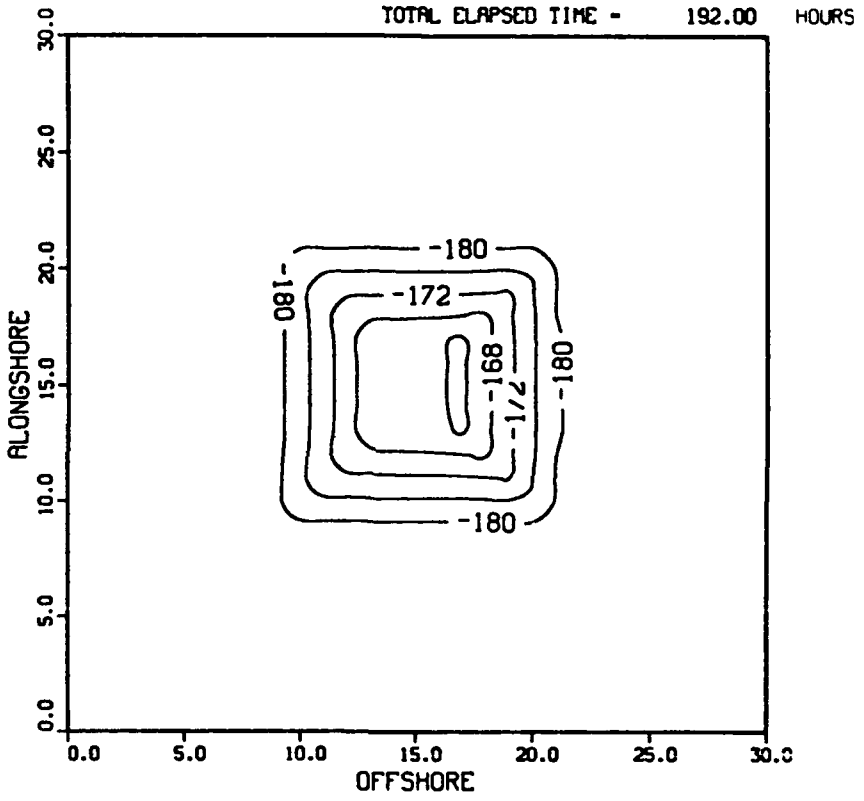

Figure 36. Storm event simulation contour of fine-grained site

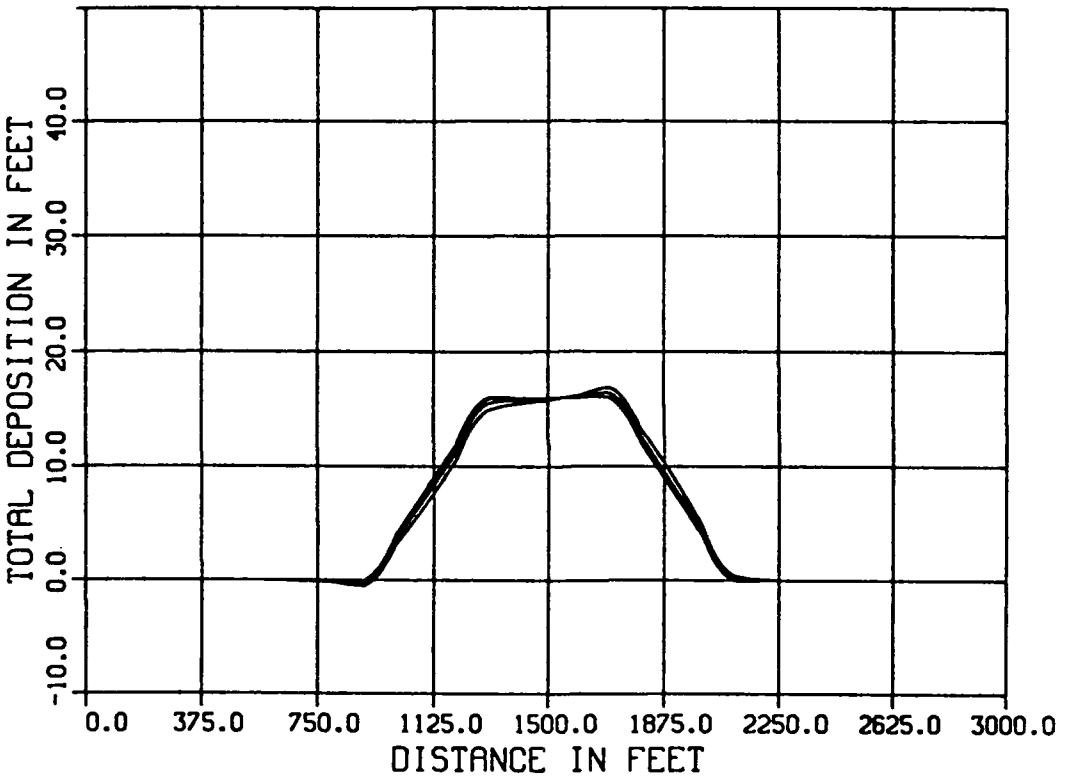

Figure 37. Storm event simulation mound axis migration history for fine-grained site

Coarse-Grained Disposal Site Analysis

51. Long-term simulations for the coarse-grained disposal site are based on identical boundary conditions used for the 55-m site analysis. Simulation results were similar to those of the fine-grained simulations in that the velocities are near the threshold value necessary for sediment movement. The 96-day simulation predicted only a 0.37-ft net migration of the mound. As in the fine-grained site simulations, sediment is transported only during peak flow periods, and these periods represent only a small percentage of the flow. The similarity of results is due to a balancing of greater depths and lower wave-induced orbital velocities at the fine-grained site versus reduced depths and elevated orbital velocities at the coarse-grained site. The storm surge simulation results indicate little net movement of the coarse material, with a total centroid migration distance computation of only 3.1 ft. As in the fine-grained site, coarse material is transported during high-energy periods; however, the net effect is small since the long-term average currents are small, below 5.0 cm/sec.

PART V: CONCLUSIONS

Fine-Grained Site

52. The short-term dispersion analysis of the disposal site for fine-grained materials was based on the results of the DIFID model. The sediments to be disposed at the site were specified to be composed of 75-percent silt-clay and 25-percent fine sand. The dispersion computations were performed for a 1-hr simulation. Results are reported in the form of the spatial and temporal distribution of the suspended sediment cloud through the water column as well as the total sediment deposition pattern on the ocean floor.

53. Suspended sediment computations were reported separately for the sand and silt-clay components of the sediment. Results of the computations show that the maximum concentration of suspended sand in the water column 1 hr after disposal is approximately 5×10^{-8} mg/ℓ or 0.00005 parts per billion (ppb) above ambient concentration levels. This concentration corresponds to approximately 1 mile from the disposal site. The corresponding concentration of silt/clay in suspension is approximately 1×10^{-6} mg/ℓ (0.001 ppb). These results indicate that the material rapidly disperses following its release from the dredge. The computed deposition pattern indicates that maximum depths of approximately 0.06 ft occur approximately 300 ft from the release point and that essentially all material is contained within a 0.30-mile radius of the disposal point. The minimal impact outside the immediate disposal area is due to the low ambient currents in the vicinity of the disposal site.

54. The long-term analysis of site stability was based on both a 96-day simulated time series of wave and tide data and an 8-day simulated storm surge hydrograph. Results of the 96-day simulation indicate that movement of material occurs only during periods of large current activity. Analysis of the prototype data indicates that currents required for this movement occur at a frequency of approximately 20 to 30 days. However, these large currents do not occur in a consistent direction. In fact, the long-term mean depth-averaged currents are on the order of less than 5.0 cm/sec. As such, the computed net migration of the mound was only 0.31 ft. This figure does not imply that sediment does not move, but that the net movement, considering ebb and flood as well as spring and neap tides, is essentially zero.

55. A storm hydrograph (half sine wave) was defined as an 8-day event in which the maximum depth-averaged velocities approached 2.5 ft/sec. These

magnitudes are greater than any observed in the 348 days of middepth prototype data (Periods 3 and 4). The simulated storm represents a severe event; however, the computed movement of the mound was only on the order of 30 ft. This amount of mound erosion and deformation is small compared with the intensity of the storm required to produce a peak depth-averaged velocity of 2.5 ft/sec in 180 ft of water.

Coarse-Grained Site

56. The short-term dispersion analysis for the coarse-grained disposal site is based on a sediment distribution of 93-percent sand and 7-percent silt/clay. Due to the large percentage of sand and the corresponding rapid descent of the material, dispersion computations were performed only for 400 sec. Results of the suspended sediment concentration distribution indicate that all sediment was deposited within the first 100 sec following disposal and that no material remained in suspension. The total sediment deposition pattern is symmetric with the centroid located approximately 150 ft from the point of disposal. The computed mound covered an approximate 600-ft-diam area with 0.2 ft of material. The negligible impact outside the immediate disposal area is due to both the low ambient currents and the high percentage of sand contained in the load.

57. The long-term site stability analysis was also based on a 96-day simulated wave and tide record and an 8-day storm surge hydrograph. Results for the 96-day simulation were similar to those at the fine-grained site. Ambient currents transport sediment only during periods of high wave and current intensity, and these periods occur only at frequencies on the order of 20 to 30 days. When these currents are combined with the residual flow of only approximately 5 cm/sec, the maximum excursion of the mound was computed to be only 0.4 ft. The identical storm defined for the fine-grained site produced a mound movement of only approximately 3 ft.

Concluding Remarks

58. Conclusions of the study indicate that both proposed disposal sites are basically nondispersive. This conclusion is based on two approaches of analysis. Short-term simulations of the disposal operation indicate that sediments are deposited on the bottom rapidly, leaving very little or no

sediment in suspension for subsequent transport into sensitive areas. A long-term simulation of sediment mound stability shows that, although sediment at either location can be moved short distances during peak current periods, the net long-term effect of local waves and currents on the mound is negligible. It would appear, therefore, that either site will remain in place following disposal.

REFERENCES

Ackers, P., and White, R. W. 1973. "Sediment Transport: New Approach and Analysis," Journal of the Hydraulics Division, American Society of Civil Engineers, Vol 99, No. HY11, pp 2041-2060.

Borgman, L. E., and Scheffner, N. W. 1991. "The Simulation of Time Sequences of Wave Height, Period, and Direction," Technical Report DRP-91-2, US Army Engineer Waterways Experiment Station, Vicksburg, MS.

Brandsma, M. G., and Divoky, D. J. 1976. "Development of Model for Prediction of Short-Term Fate of Dredged Material Discharged in the Estuarine Environment," Contract Report D-76-5, US Army Engineer Waterways Experiment Station, Vicksburg, MS.

Burington, R. S., and May, D. C. 1958. Handbook of Probability and Statistics with Tables, Handbook Publishers, Inc., Sandusky, OH.

Ebersole, B. A., Cialone, M. A., and Prater, M. D. 1986. "Regional Coastal Processes Numerical Modeling System; Report 1, RCPWAVE - A Linear Wave Propagation Model for Engineering Use," Technical Report CERC-86-4, US Army Engineer Waterways Experiment Station, Vicksburg, MS.

Jensen, R. E., Hubertz, J. M., and Payne, J. B. 1989. "Pacific Coast Hindcast Phase III North Wave Information," WIS Report 17, US Army Engineer Waterways Experiment Station, Vicksburg, MS.

Johnson, B. H. "User's Guide for Models of Dredged Material Disposal in Open Water" (in preparation), US Army Engineer Waterways Experiment Station, Vicksburg, MS.

Johnson, B. H., and Holliday, B. W. 1978. "Evaluation and Calibration of the TETRA TECH Dredged Material Disposal Models Based on Field Data," Technical Report D-78-47, US Army Engineer Waterways Experiment Station, Vicksburg, MS.

Johnson, B. J., Trawle, M. J., and Adamec, S. A. 1988. "Dredged Material Disposal Modeling in Puget Sound," Journal of Waterways, Port, Coastal, and Engineering, American Society Civil Engineers, Vol 114, No. 6, pp 700-713.

Kamphuis, J. W. 1990. "Influence of Sand or Gravel on the Erosion of Cohesive Sediment," Journal of Hydraulic Research, Vol 28, pp 43-53.

Minerals Management Service. 1989. "The Northern California Coastal Circulation Study: Results of the Pilot Program," OCS Study MMS-89-0008, US Department of the Interior, Washington, DC.

Scheffner, N. W. "Disposal Site Evaluation for the New York Bight" (in preparation), US Army Engineer Waterways Experiment Station, Vicksburg, MS.

Scheffner, N. W., and Swain, A. "Evaluation of the Dispersive Characteristics of the Miami and Fort Pierce Dredged Material Disposal Sites" (in preparation), US Army Engineer Waterways Experiment Station, Vicksburg, MS.

Swart, D. H. 1976. "Predictive Equations Regarding Coastal Transports," Proceedings of the 15th Coastal Engineering Conference, Honolulu, Hawaii.

Trawle, M. J., and Johnson, B. H. 1986. "Alcatraz Disposal Site Investigation," Miscellaneous Paper HL-86-1, US Army Engineer Waterways Experiment Station, Vicksburg, MS.

White, W. R. 1972. "Sediment Transport in Channels: A General Function," Wallingford Hydraulics Research Station, INT 104, Wallingford, UK.

APPENDIX A
RAW AND FILTERED VELOCITY DATA FROM MINERALS MANAGEMENT SERVICE GAGES E60 AND E90

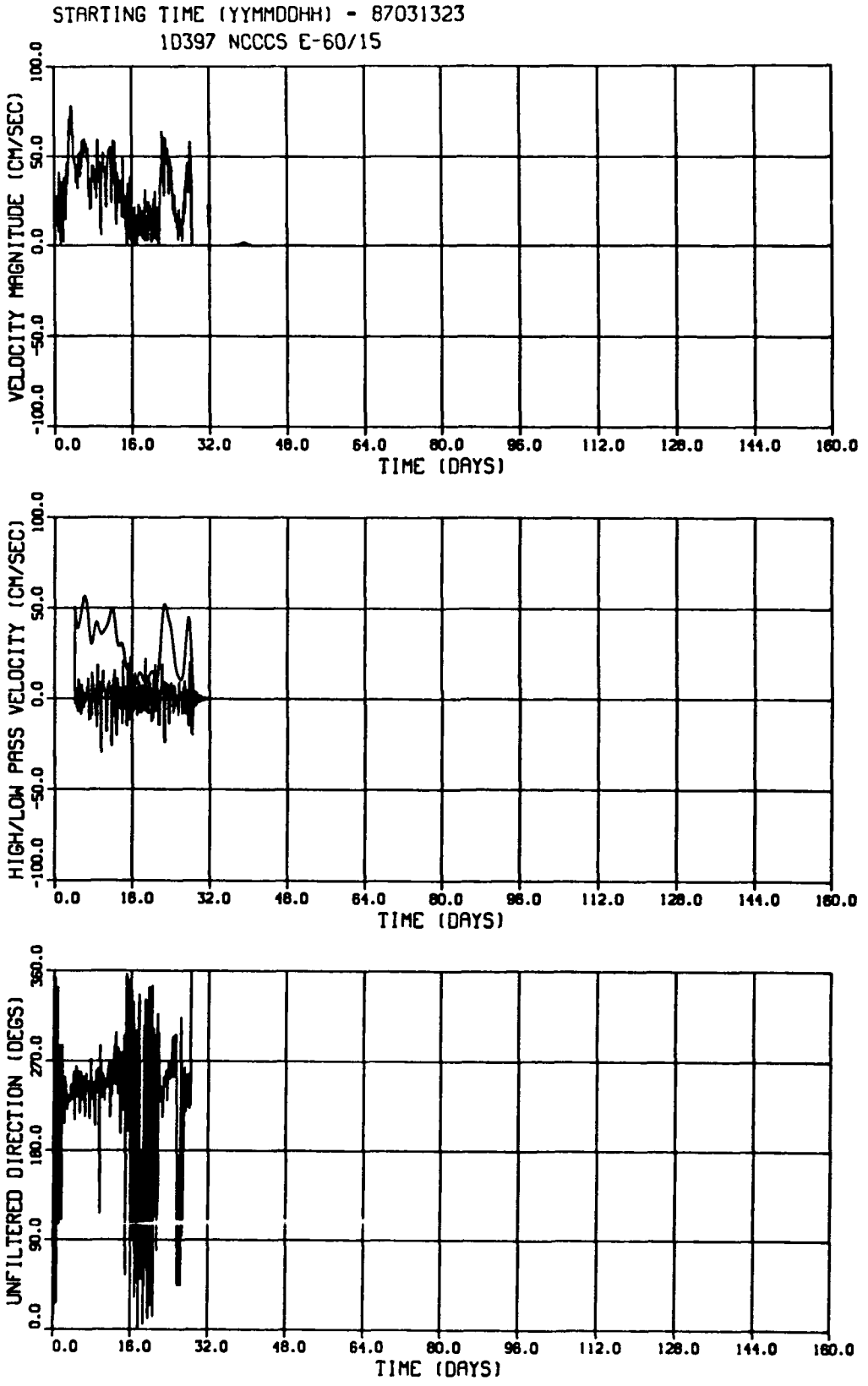

Figure A1. Meter E60/15 current data - Period 1

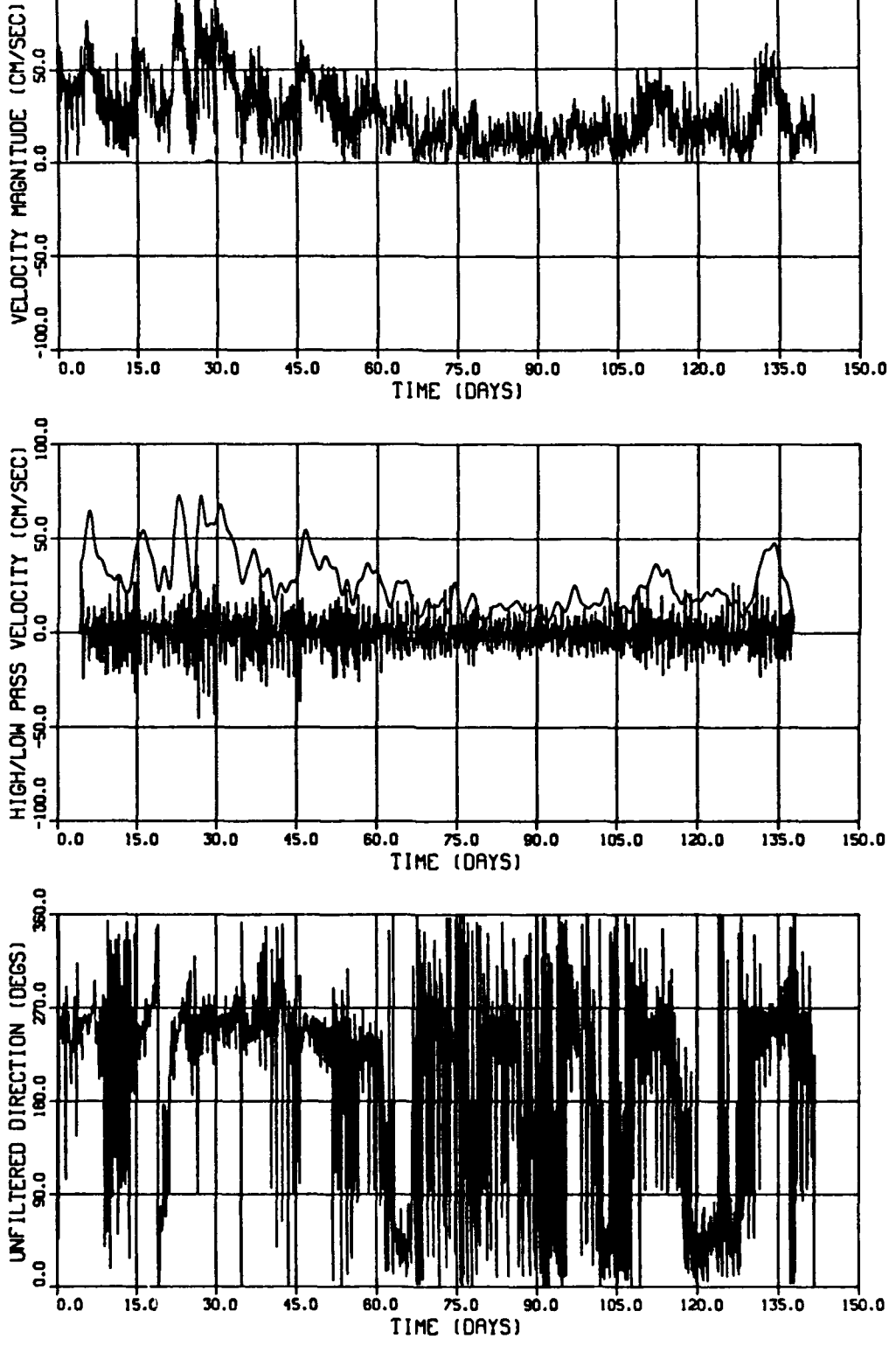

Figure A2. Meter E90/15 current data - Period 1

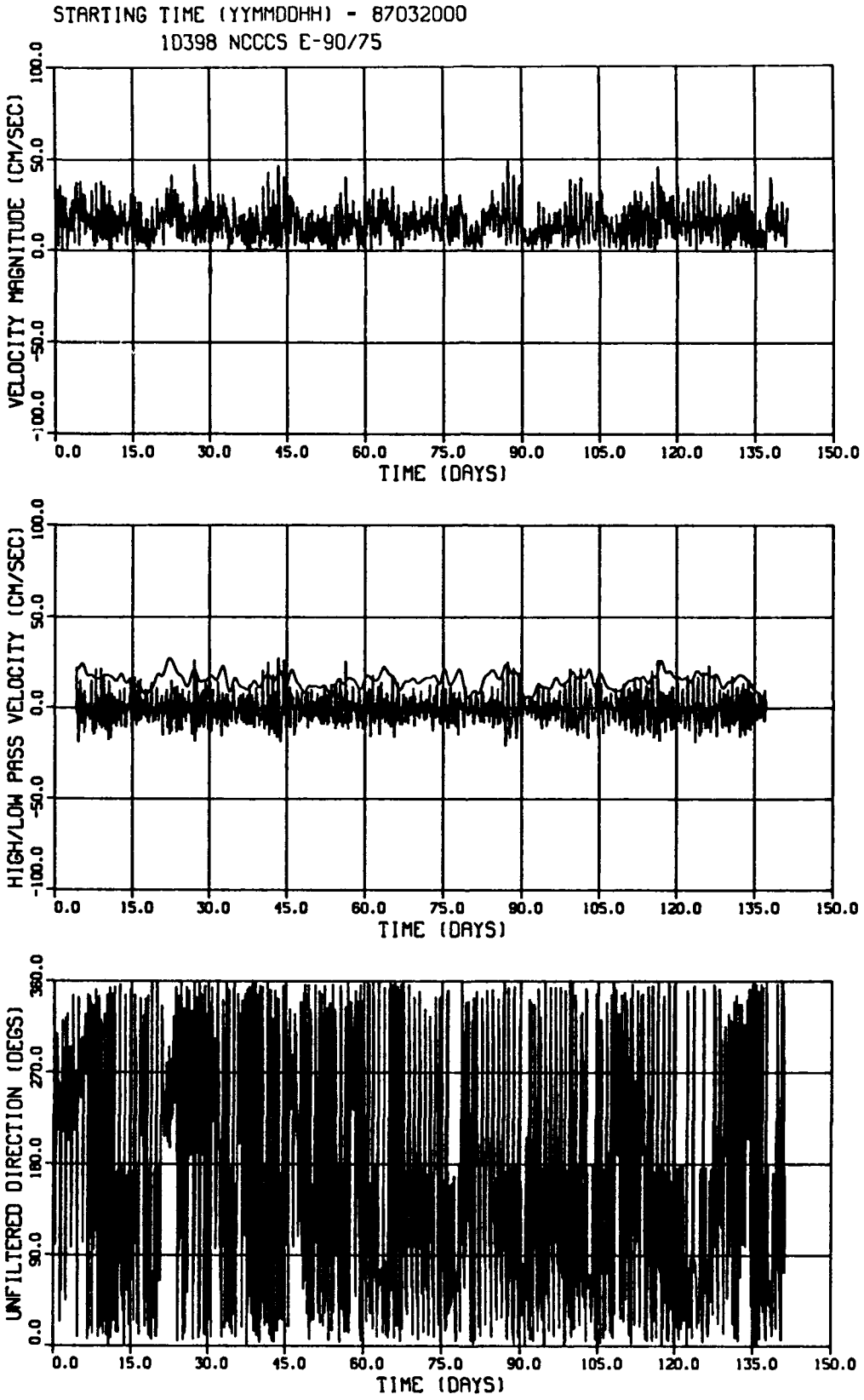

Figure A3. Meter E90/75 current data - Period 1

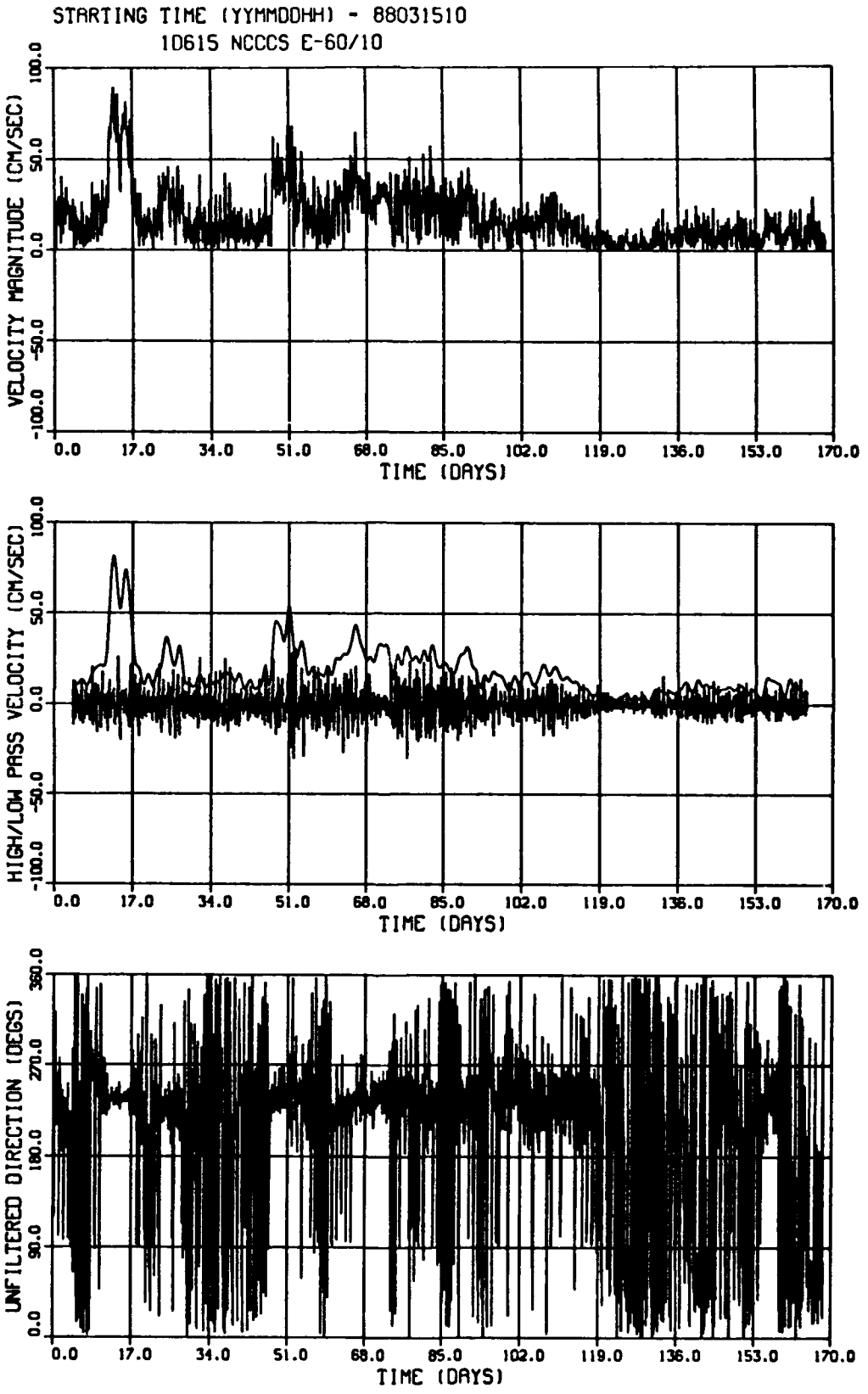

Figure A4. Meter E60/10 current data - Period 2

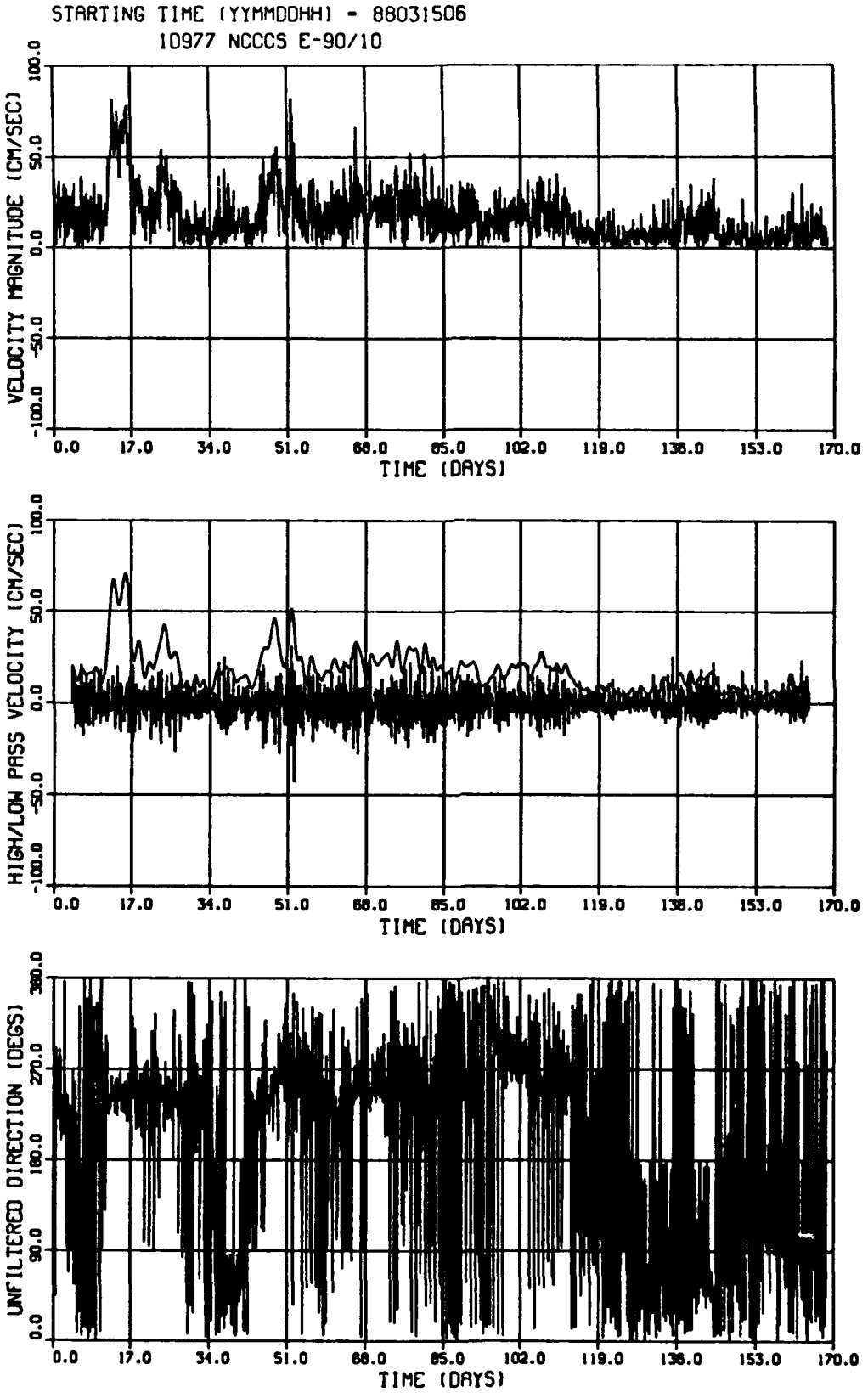

Figure A5. Meter E90/10 current data - Period 2

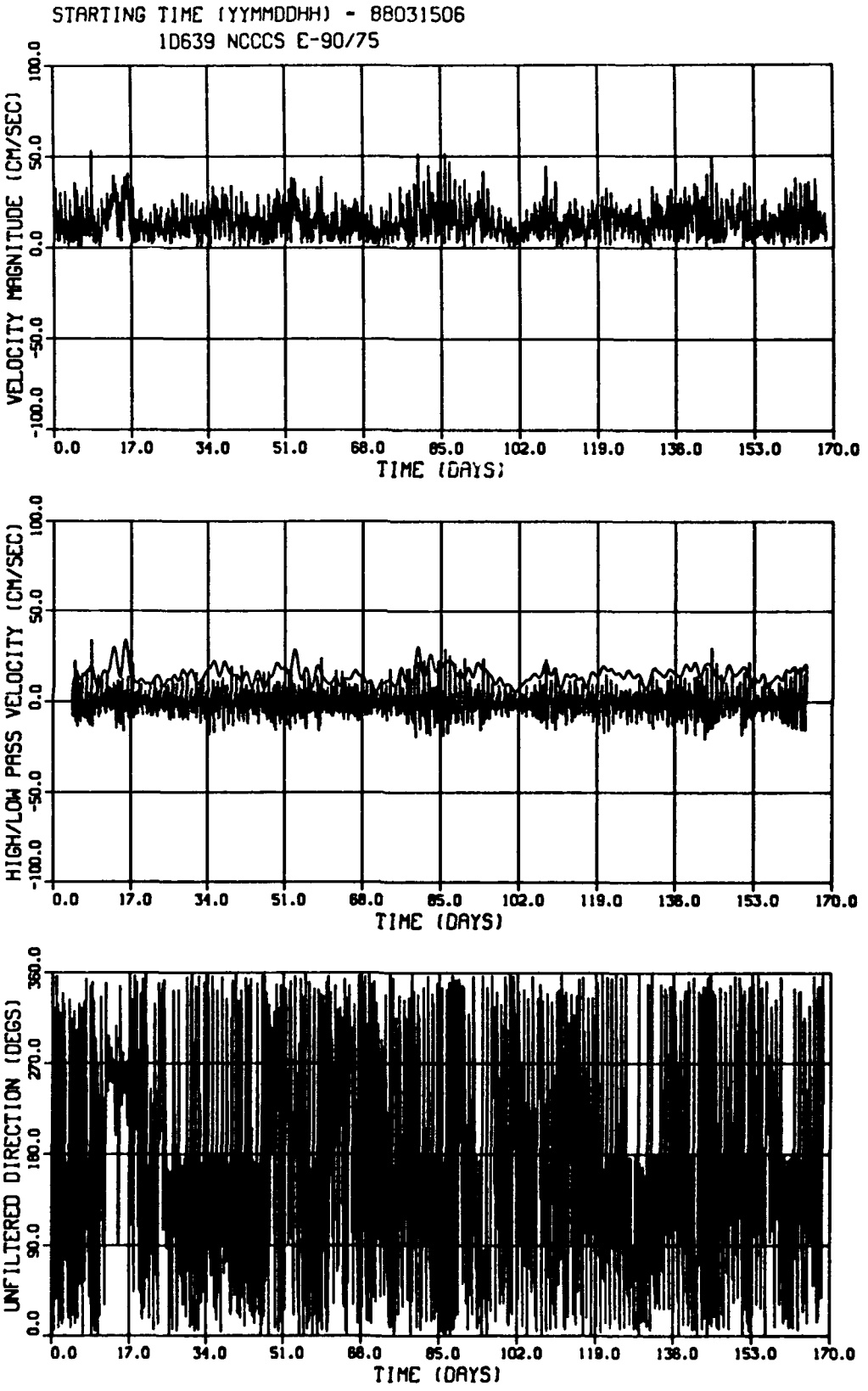

Figure A6. Meter E90/75 current data - Period 2

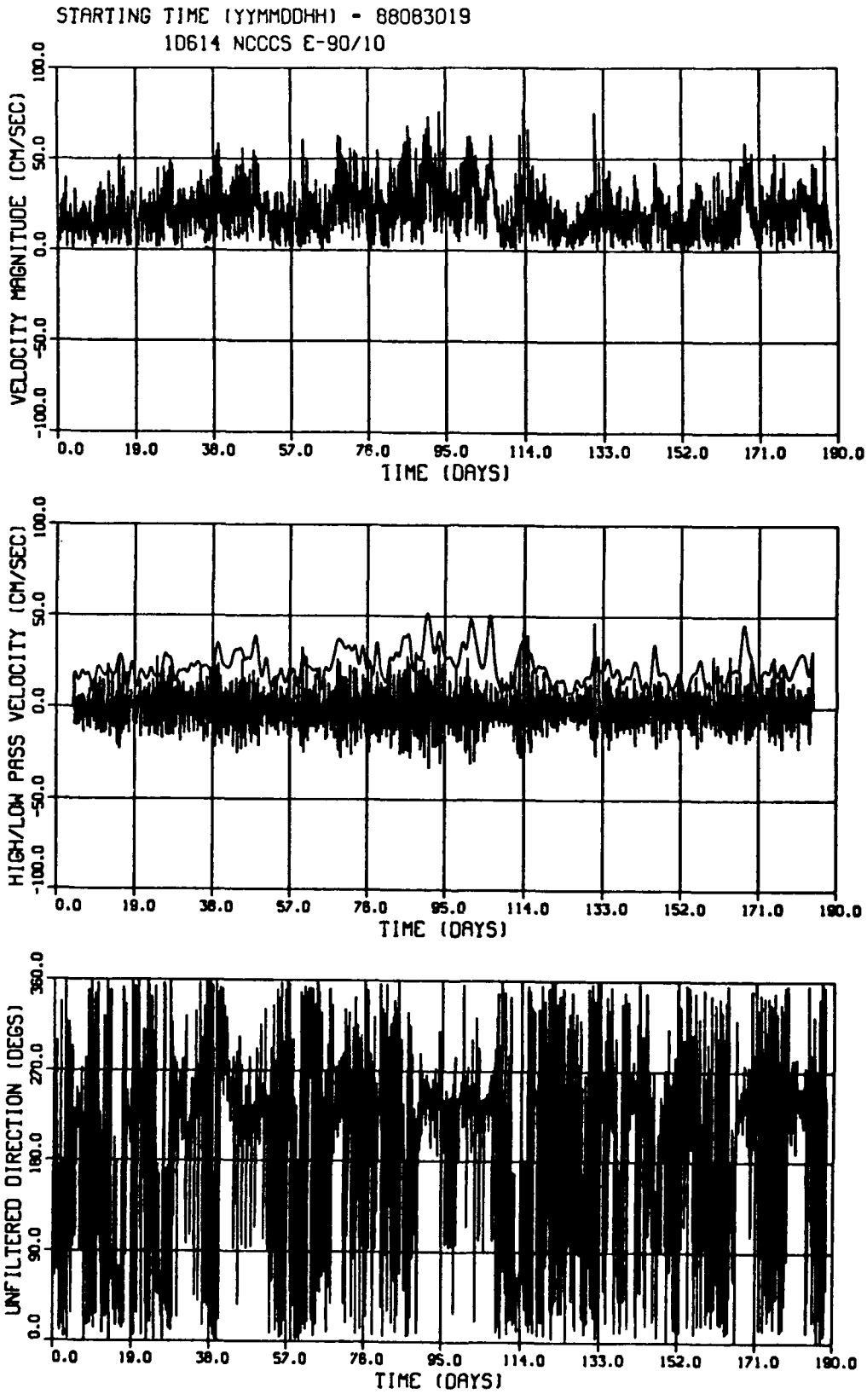

Figure A7. Meter E90/10 current data - Period 3

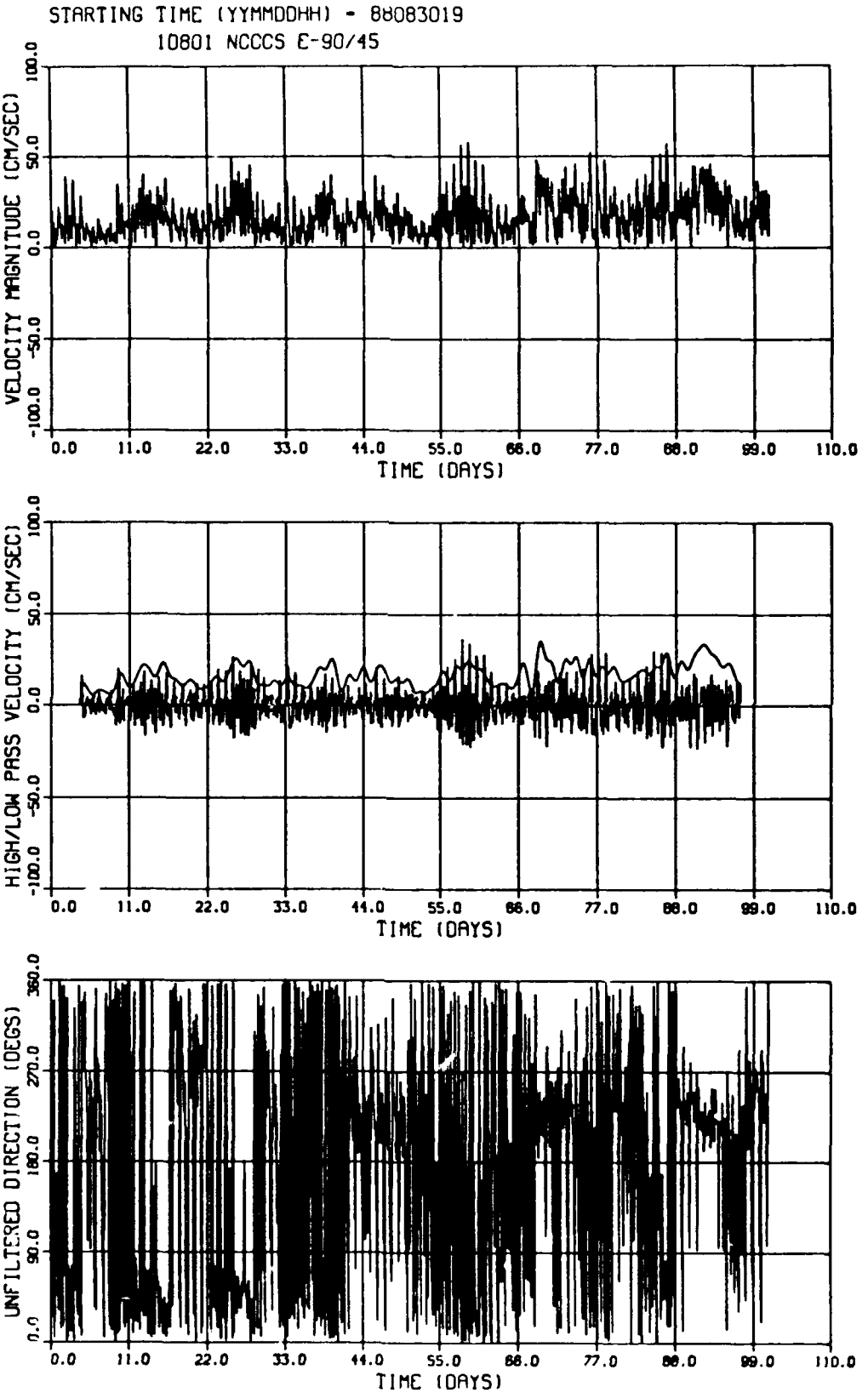

Figure A8. Meter E90/45 current data - Period 1

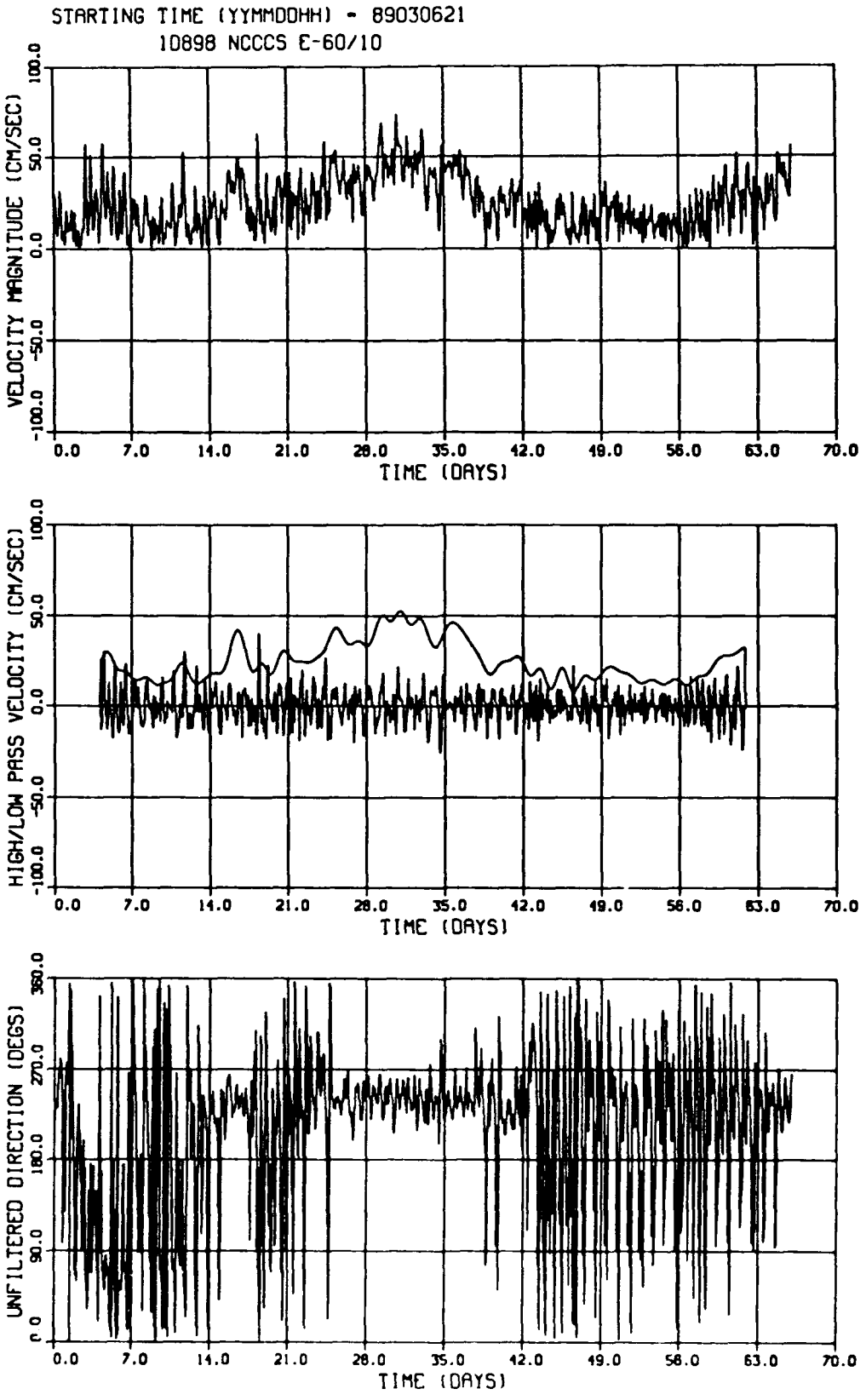

Figure A9. Meter E60/10 current data - Period 1

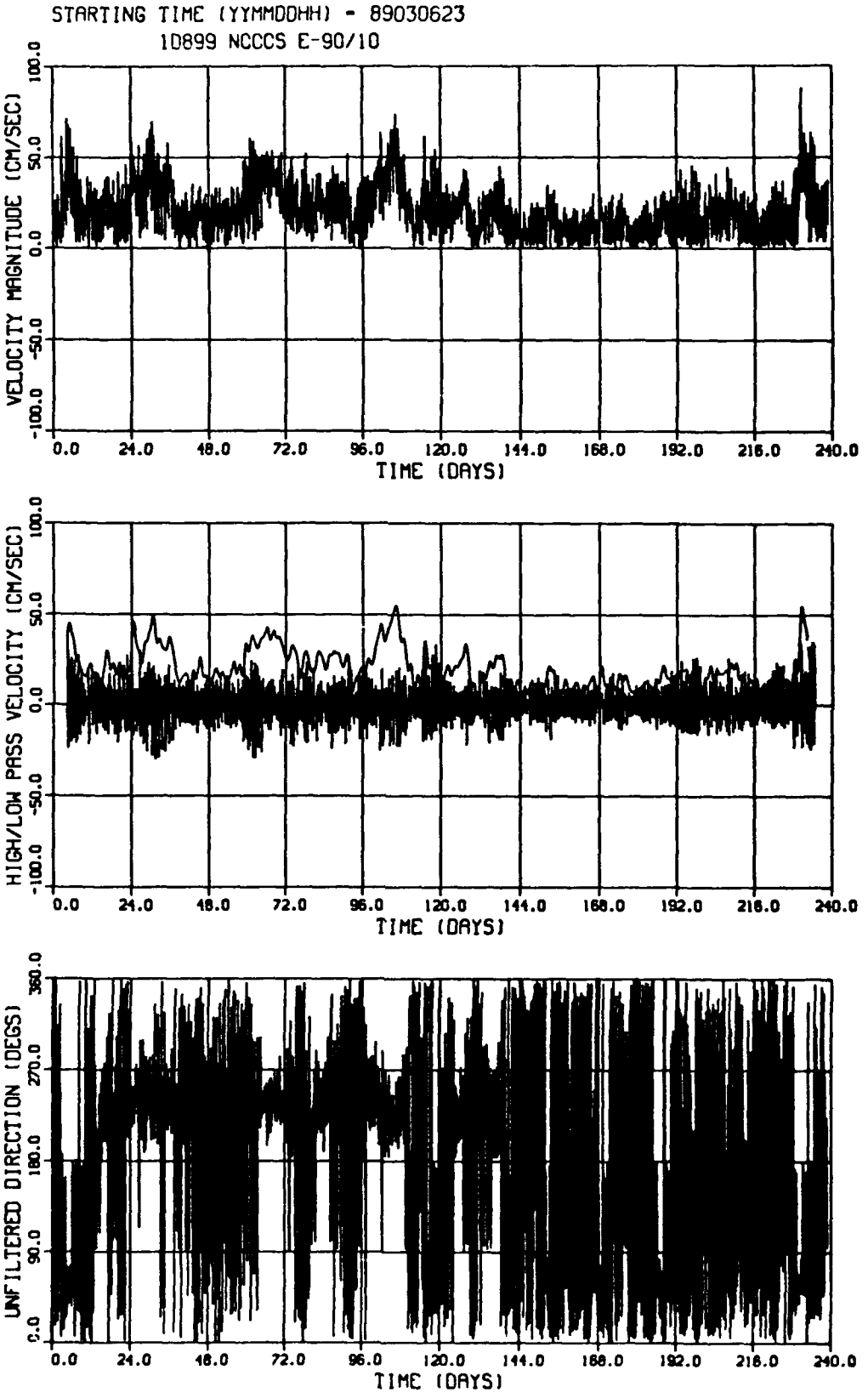

Figure A10. Meter E90/10 current data - Period 4

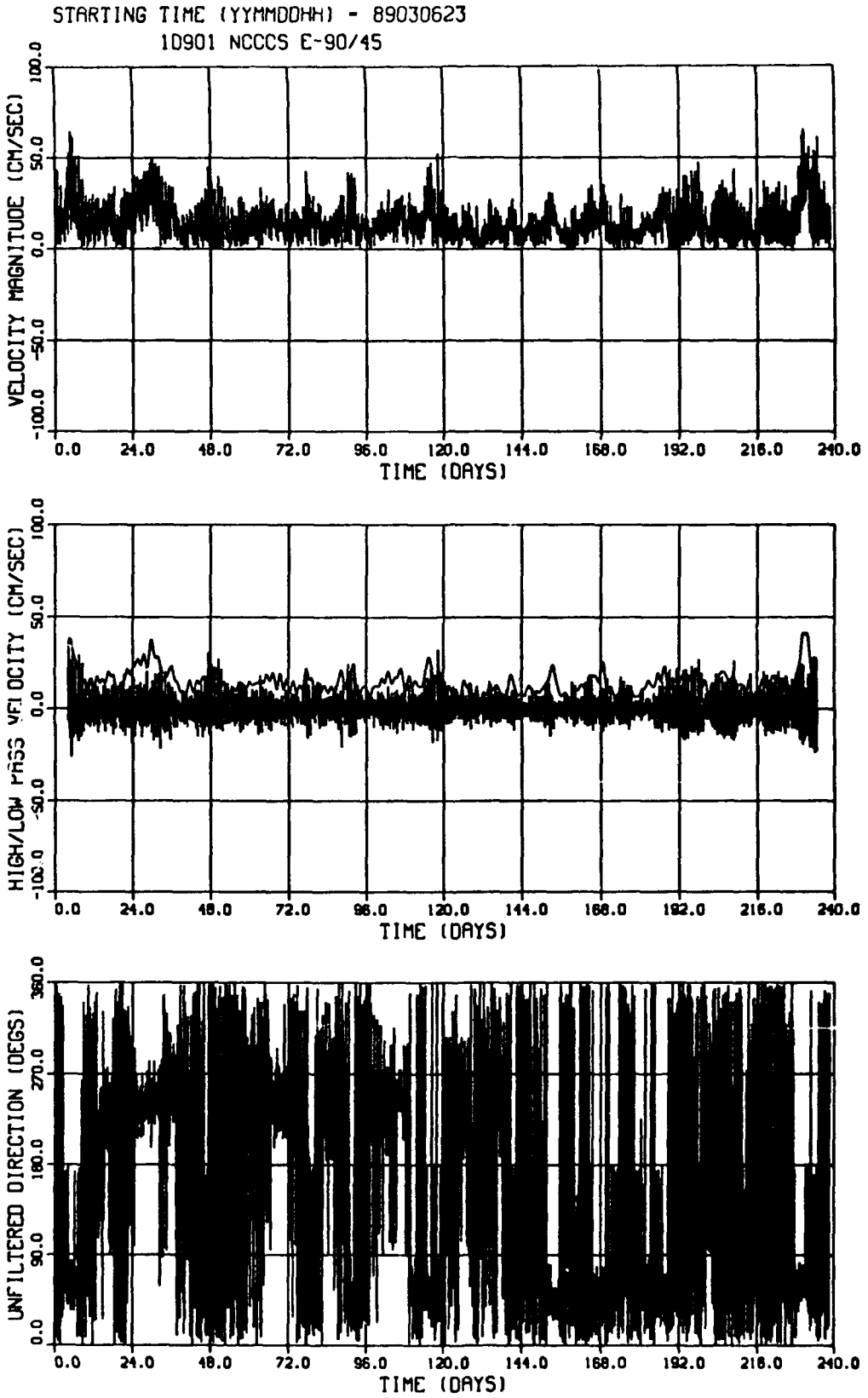

Figure A11. Meter E90/45 current data - Period 4

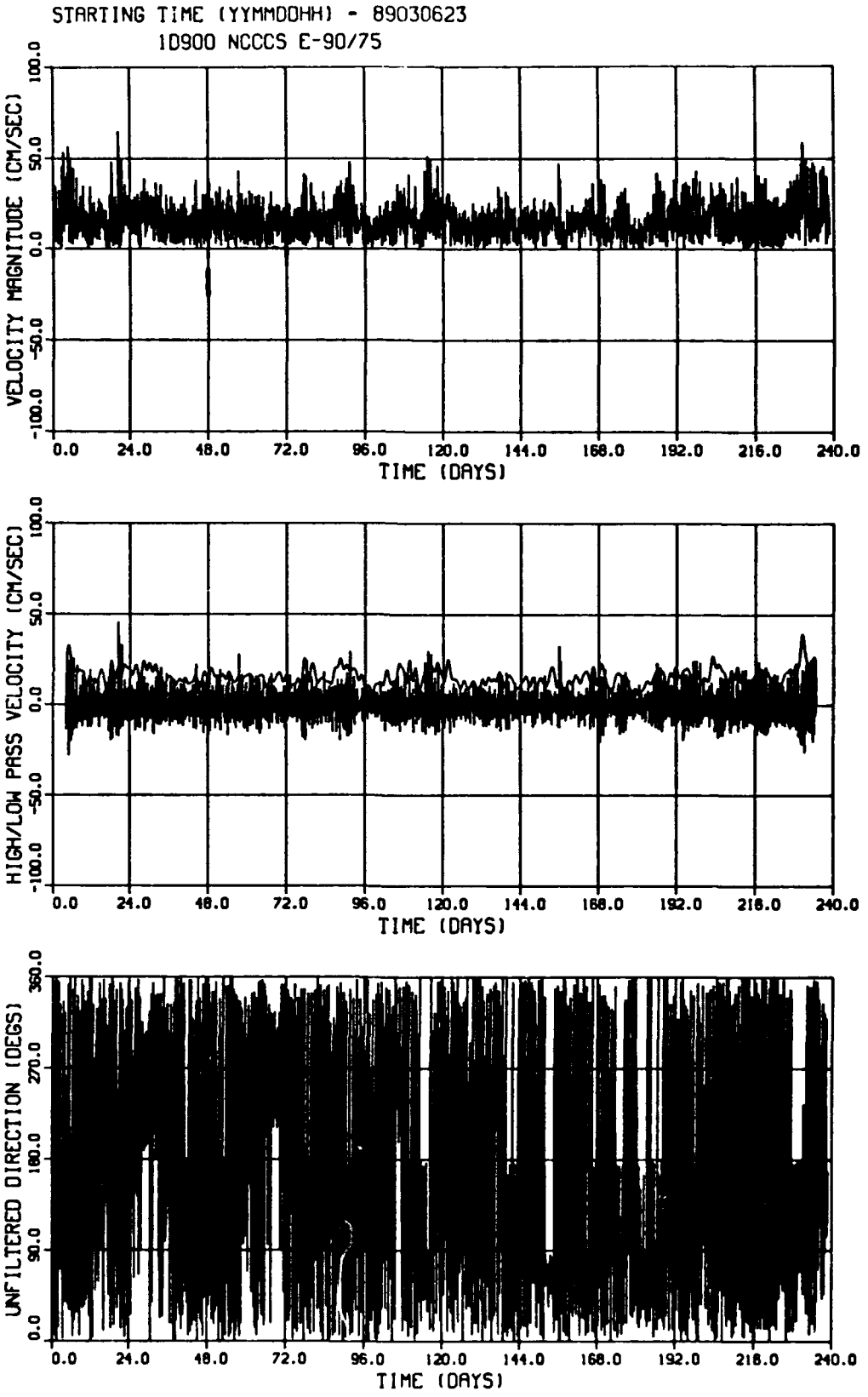

Figure A12. Meter E90/75 current data - Period 4

Waterways Experiment Station Cataloging-in-Publication Data

Scheffner, Norman W.
Dispersion analysis of Humboldt Bay, California, interim offshore disposal site / by Norman W. Scheffner, Coastal Engineering Research Center ; prepared for US Army Engineer District, San Francisco and Department of the Army, US Army Corps of Engineers.
84 p. : ill. ; 28 cm. — (Miscellaneous paper ; DRP-92-1)
Includes bibliographic references.
1. Dredging — California — Humboldt Bay — Environmental aspects. 2. Sediment transport. 3. Spoil banks — California — Humboldt Bay. 4. Dredging spoil — California — Humboldt Bay. I. Title. II. United States. Army. Corps of Engineers. San Francisco District. III. United States. Army. Corps of Engineers. IV. Coastal Engineering Research Center (U.S.) V. US Army Engineer Waterways Experiment Station. VI. Series: Miscellaneous paper (US Army Engineer Waterways Experiment Station) ; DRP-92-1.
TA7 W34m no.DRP-92-1

SUPPLEMENTARY

INFORMATION

DEPARTMENT OF THE ARMY
WATERWAYS EXPERIMENT STATION, CORPS OF ENGINEERS
3909 HALLS FERRY ROAD
VICKSBURG, MISSISSIPPI 39180-6199

REPLY TO
ATTENTION OF

CEWES-CR-O

21 December 1992

Errata Sheet

No. 1

DISPERSION ANALYSIS OF HUMBOLDT BAY,
CALIFORNIA, INTERIM OFFSHORE DISPOSAL SITE

Miscellaneous Paper DRP-92-1

June 1992

On pages 43, 44, 45, and 65 (or any page with reference to), concentrations of suspended sediment are erroneously reported in mg/ℓ. The reported values are actually nondimensional ratios of volume of solids to volume of solution. To convert these reported values to units of mg/ℓ, multiply by 2.6 (density, p. 37) $\times 10^{6}$. For example, the value of 5×10^{-8} mg/ℓ reported on p. 65 should read 1.3×10^{-1} mg/ℓ.